

UNIVERSITY OF TWENTE.

Faculty of Science & Technology,
MSc Biomedical Engineering

Effect of background optogenetic input on memory formation of cultured networks

Nikolaos Kikirikis
M.Sc. Thesis
September 2022

Supervisors:

prof dr. ir. M.J.A.M. van Putten, (Michel)
dr. ir. Joost le Feber
dr. ir. T. Heida (Ciska)
PhD candidate Martina Lamberti

Clinical Neurophysiology group Group
Faculty of Science & Technology,
University of Twente
P.O. Box 217
7500 AE Enschede
The Netherlands

Abstract

Up to now, it is not clear why systems consolidation arises mainly during slow wave sleep (SWS) and what are the underlying mechanisms of this phenomenon. An important difference between SWS and awake state is the low afferent input that is observed during SWS. Low or high afferent input has been correlated with variations in activity patterns and network excitability of cortical neurons. At low levels of afferent input, cultures exhibit burst dominated activity patterns which replicate slow oscillations (SO) observed during SWS. Therefore, cultures are able to consolidate (the so called) memory traces induced by electrical stimulation. In this study we administered high afferent background input on cortical cultures by means of optogenetic stimulation and we examined the effect on memory trace formation. Interestingly, repeated electrical stimulation on AAV-transduced cortical cultures did not lead to memory trace formation. When high levels of background input are present, excitability of the network remains unchanged and inability to induce memory trace formation further persists. We hypothesize that AAV transduction may be responsible for this phenomenon by reducing network excitability.

Contents

Abstract	iii
List of acronyms	vii
1 Introduction	1
1.1 Neuronal signal transduction	1
1.2 Synaptic plasticity	3
1.2.1 Short-term synaptic plasticity	3
1.2.2 Long-term synaptic plasticity	4
1.3 Optogenetic stimulation	4
1.4 In-vitro neuronal networks	5
1.4.1 Activity patterns	6
1.4.2 Connectivity	6
1.4.3 Excitability	7
1.5 Memory formation and consolidation	8
1.5.1 In-vivo	8
1.5.2 In-vitro	9
1.6 Aim of this study	9
2 Methods	11
2.1 Cell culturing	11
2.2 Data acquisition	12
2.3 Experimental design	14
2.3.1 Optogenetic stimulation experiments	14
2.3.2 Control memory experiments	16
2.3.3 Background input memory experiments	16
2.4 Data analysis	17
2.4.1 Raster plots	17
2.4.2 Mean firing rate	18
2.4.3 Bursting frequency	18
2.4.4 Conditional firing probabilities	18
2.4.5 Euclidean distances (ED)	20

2.4.6	Single pulse response (SPR)	20
2.4.7	Average network response	21
2.4.8	Area under the curve of the mean post-stimulus time histogram	22
3	Results	23
3.1	Optogenetic stimulation experiments	23
3.1.1	Overview	23
3.1.2	Effect of different stimulation frequencies on activity	24
3.1.3	Effect of different optogenetic stimulation frequencies on network excitability	25
3.2	Control & background input memory experiments	26
3.2.1	Overview	26
3.2.2	Temporal development of efficacy of electrical stimulation	26
3.2.3	Effect of 5 Hz background optogenetic stimulation on activity patterns during spontaneous activity recordings and stimulation periods.	27
3.2.4	Effect of random, background optogenetic stimulation on memory trace formation and consolidation	28
3.2.5	Effect of random, background optogenetic stimulation on network excitability	30
4	Discussion	31
4.1	Effect of different light stimulation frequencies on activity & excitability	31
4.2	Background optogenetic input at 5 Hz did not alter activity patterns	33
4.3	Network excitability during spontaneous activity recordings remain unchanged in response to background input	34
4.4	Repeated electrical stimulation could not elicit memory trace formation in virally transfected cultures expressing ChR2.	35
4.5	Efficacy of electrical stimulation	36
5	Conclusions	37
6	Study limitations and future perspectives	39
	References	41
	Appendices	

List of acronyms

CNS	Central Nervous System
AP	Action Potential
LTP	Long-Term Potentiation
LTD	Long-Term Depression
ChR2	ChannelRhodopsin-2
AAV	Adeno-Associated Virus
MEA	MicroElectrode Array
AD	Alzheimer's Disease
SO	Slow Oscillation
NB	Network Burst
TTX	TetroTodoXin
STDP	Spike Timing-Dependent Plasticity
EEG	ElectroEncephaloGram
PEI	PolyEthylenImine
DIV	Days In-Vitro
ISI	Inter-Stimulus Interval
BF	Bursting Frequency
CFP	Conditional Firing Probability
SPR	Single Pulse Response
ED	Euclidean Distance
PSTH	Post-Stimulus Time Histogram

AUC	Area Under the Curve
SEM	Standard Error of Mean
SWS	Slow-Wave-Sleep

Introduction

1.1 Neuronal signal transduction

Neurons are the building blocks of the human central nervous system (CNS) which is comprised of over 100 billion neurons (Walinga and Stangor, 2014). An illustration of the basic compartments of a neuron can be found in Figure 1.1. Primary function of these cells is to receive and pass information through the brain and nervous system via electrochemical signals that coordinate actions and sensory information (Woodruff, 2022). Signal transduction between neurons takes place through electrical signals called action potentials or chemical cues released at synapses called neurotransmitters. In general, an action potential (AP) is the transmembrane voltage change that occurs in excitable cells like neurons, endocrine, and muscle cells (Betts et al., 2013). For a neuron, an AP is reflected as a rapid rise and fall of the transmembrane voltage known as membrane potential (Ritchie and Rogart, 1977). Neurons work in an “all-or-nothing” way which means that higher amplitudes of stimulus will not generate larger amplitudes of APs (Sasaki et al., 2011). Membrane potential arises from ionic concentration gradients and the fact that the cell membrane is semipermeable to selec-

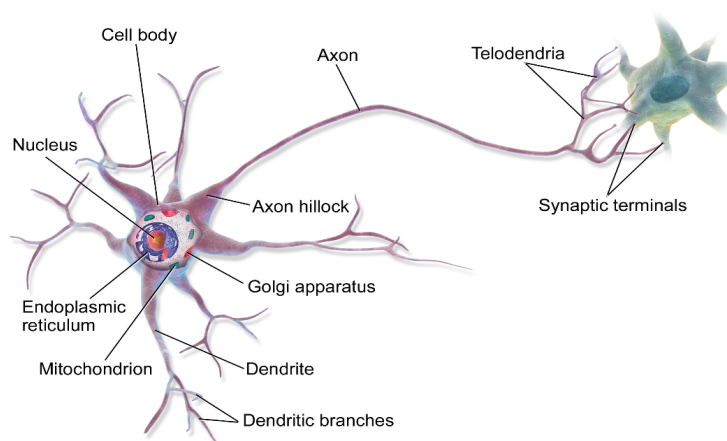


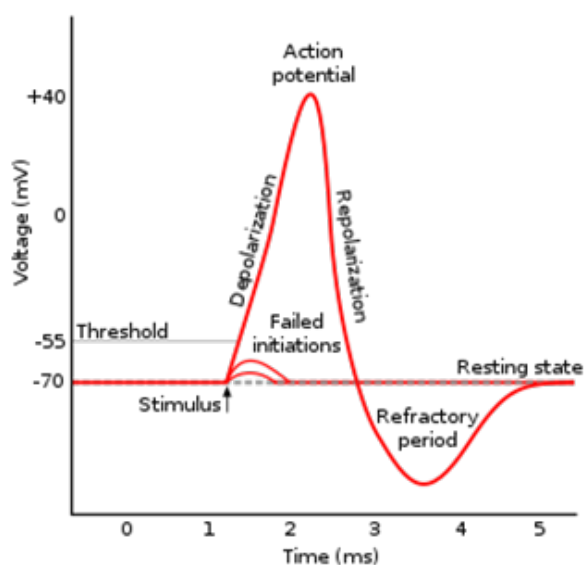
Figure 1.1 Schematic of neuronal structure (Blausen, 2022)

tive ions through passive ion channels, voltage-gated channels, and ion pumps. The generation of an AP can be divided into three main sections: the depolarization, the repolarization, and the refractory period (Sasaki et al., 2011). Neurons' transmembrane resting potential ranges from -60 to -70 mV and by altering the relative membrane permeability to specific ions, a rapid (1-2 ms) depolarization of the membrane occurs at around +50 mV followed by repolarization and a refractory period where membrane potential at first undershoots and then returns to its resting state (Betts et al., 2013; van Putten, 2020); Figure 1.2(A).

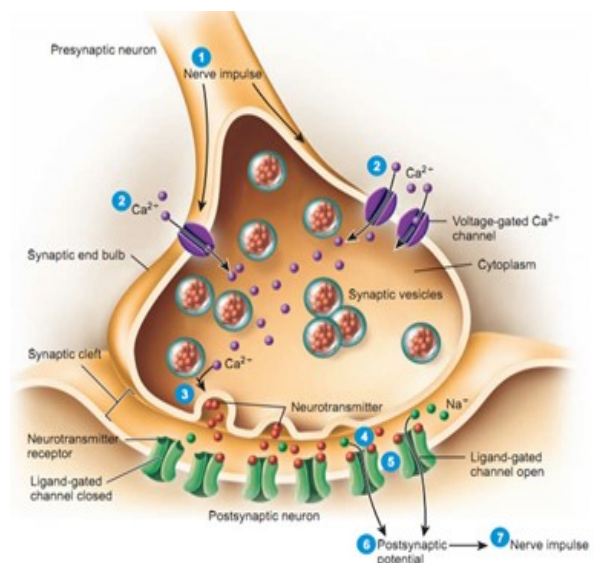
Synapses (Greek for conjunction) are defined as microscopic gaps where the terminal buttons of one neuron are in close apposition with the receptors of another. In many synapses, the signal-passing neuron (presynaptic neuron) transfers the information from its axon to the dendrites or soma of the target neuron (post-synaptic neuron) (Perea et al., 2009). This transfer of information through a synapse is called synaptic transmission and can be divided into two categories:

1) Electrical synaptic transmission, where the plasma membranes of the two cells are connected through gap junctions which allow the flow of ions from one cell to the other hence the passive transmission of action potentials. Electrical synapses, allow for a fast, bi-directional transfer of information and are also involved in the synchronized activity of neuronal groups (e.g. synchronized activity in the hypothalamus)(Purves and Williams, 2001).

2) Chemical synaptic transmission (Fig 1.2(B)), is the process where chemical cues (neurotransmitters) from the cell membrane of the pre-synaptic neuron are diffused and up taken from the receptors of a post-synaptic neuron or other cells. A chemical



(A) Generation of an action potential (fil)



(B) Illustration of chemical synaptic transmission (Kizirian, 2022)

Figure 1.2 Signal transduction processes in neuronal communication

synapse enables slow and unidirectional signal transduction and is sensitive to fatigue, pH changes, and hypoxia (Purves and Williams, 2001).

1.2 Synaptic plasticity

The ability of the neuron to regulate the efficacy and strength of synaptic transmission at existing synapses through activity-dependent mechanisms is defined as synaptic plasticity (Mateos-Aparicio and Rodríguez-Moreno, 2019). This mechanism is suggested to be linked with memory trace formation of short-term experiences and plays a key role in early brain development (Citri and Malenka, 2008). Multiple mechanisms are associated with synaptic plasticity, although earlier work has proven using computer modeling that both short-term and long-term plasticity mechanisms are involved in memory consolidation.

1.2.1 Short-term synaptic plasticity

Short-term synaptic plasticity can be elicited by transient activity bursts that cause aggregation of calcium ions in the pre-synaptic neuron which in turn modulate the probability of neurotransmitter release (Citri and Malenka, 2008). Short-term plasticity has a duration that ranges from milliseconds to minutes and is suggested to play a crucial role in short-term memory. Stimulation patterns that trigger short-term synaptic plasticity are paired-pulse stimulation and repetitive high-frequency stimulation (Zucker et al., 2002).

Two stimuli with short inter-stimulus interval can lead to paired-pulse facilitation or depression according to the response that the first stimuli elicited (Katz, 1968). Paired-pulse depression can emerge by an interstimulus interval of less than 20 ms that elicits shortage of the release-ready pool neurotransmitter vesicles from the first stimulus due to high probability of transmitter release. On the contrary, paired-pulse facilitation stems from an interstimulus interval of 20 to 500 ms that increases calcium ion concentration in the pre-synaptic neuron, where probability neurotransmitter release from the first stimulus is relatively low and has a tendency to increase from the second stimulus (Dobrunz and Stevens, 1997).

Repetitive high-frequency stimulation or tetanic stimulation delivers extended stimulation trains (200 ms – 5 sec) at a frequency ranging from 10–200 Hz. This kind of stimulation pattern can induce both short-term or long-term plasticity according to the stimulation frequency (Bliss and Lømo, 1973). This notion can be validated considering that the effects of tetanic stimulation are longer compared to paired-pulse stimulation, lasting from seconds to minutes. Synaptic depression arises from neurotransmitter depletion while facilitation from augmentation in neurotransmitter release

([Dobrunz and Stevens, 1997](#)).

1.2.2 Long-term synaptic plasticity

Two fundamental forms of long-term synaptic plasticity are long-term potentiation (LTP) and long-term depression (LTD) whose effects on synaptic connectivity strength can last from minutes to several hours ([Bin Ibrahim et al., 2022](#)). Both mechanisms of long-term synaptic plasticity are closely linked with cognitive tasks such as learning and memory ([Bi and Poo, 1998](#)). A potential mechanism that induces LTP and LTD is spike-timing-dependent plasticity (STDP) ([Bin Ibrahim et al., 2022](#)). STDP acts on glutamatergic synapses and is exhibited in different neuronal circuits of the brain. If the presynaptic action potential preceded the excitatory postsynaptic potential (EPSP) then synaptic strength is increased and time-dependent LTP (t-LTP) is induced. On the other hand, if the EPSP preceded the pre-synaptic potential then the efficacy of connection is decreased and we observe a time-dependent LTD (t-LTD) ([Bi and Poo, 1998](#)). The maximal latency between the two action potentials for STPD to happen should be around 20 msec where smaller latencies result in more prominent connectivity strength variations ([Fröhlich, 2016b](#)).

An additional way to induce changes at a synaptic level is through homeostatic plasticity. One of the mechanisms that comprise this phenomenon is called “synaptic scaling” which includes calibration of the strength of synaptic connections in response to prolonged activity changes. For instance, a prolonged increase in neuronal firing will cause a net decrease in excitatory synaptic weights while prolonged exposure to decreased activity will result in a net increase in these weights. Compared to LTP and LTD homeostatic plasticity is thought to span on a longer timescale and correlate with the development of neural networks ([Tien and Kerschensteiner, 2018](#)). This kind of plasticity is also assumed to play a key role in maintaining an activity balance and its disruption is suggested to be involved in neurodegenerative diseases such as epilepsy ([Lignani et al., 2020](#)).

1.3 Optogenetic stimulation

Karl Deisseroth et al. were the first to exhibit genetic manipulation and optical methods as means of triggering action potentials in neurons [Boyden et al. \(2005\)](#). Optogenetics involves genetically engineered cells expressing light-sensitive proteins on their membrane, called opsins. With this method, one can acquire control of neural activity by increasing or decreasing neuronal excitability with millisecond precision. Excitation is achieved via the expression of opsins called channelrhodopsins (e.g. ChR2) while inhibition through halorhodopsins (e.g. NpHR) ([Tian et al., 2021](#)). In this study,

we aim to activate neuronal targets through Channelrhodopsin-2 (ChR2). ChR2 is a nonspecific blue light-sensitive ion channel with a 7-transmembrane protein structure. While optically activated, ChR2 goes through a conformational change in its structure allowing for ion transportation inside and outside the target cell, creating a photocurrent. Driving force of ion transfer is a concentration and charge gradient therefore photocurrent amplitude can be affected by the pH or medium composition. As a result, light stimulation can trigger neuronal spikes if the depolarization threshold is reached (Bertucci et al., 2019). ChR2 carrying plasmid is transduced into target cells through viral vectors with the most popular being the Adeno Associated Virus (AAV). In this way expression differences of ChR2 arise from cell to cell which influences the reliability of spike generation. For instance, cells with low ChR2 expression can only reach subthreshold activation without spike induction (Schoenenberger et al., 2011). For this cause, variants of ChR2 have been engineered like H134R mutant which is also used in our project. This mutation allows for an increase in the magnitude of photocurrents compared to wild-type ChR2 resulting in more robust spiking (Nagel et al., 2005). In the current project, we used an AAV that combines ChR2 and fluorescent proteins in a single plasmid, allowing for co-expression. In that way, we are able to monitor transduction efficacy in the culture as well as individual neuron expression levels (Schoenenberger et al., 2011). Hence, optogenetics comprises a tool that offers cell-specific targeting and high temporal resolution therefore in many cases is preferred over electrical stimulation or pharmacological manipulation (Tian et al., 2021).

1.4 In-vitro neuronal networks

Cellular neural networks display activity patterns (spontaneous activity) that are strongly connected with dynamic network properties such as connectivity and excitability (Tibau and Soriano, 2018). Micro-electrode arrays (MEAs) comprise a tool to assess network dynamics by allowing simultaneous and high spatiotemporal signal detection (Cabrera-Garcia et al., 2021). Neuronal tissue is not easily accessible and in-vivo experiments are difficult to perform. However, culturing of neuronal networks on MEAs provides the user with an in vitro model with relatively high experimental freedom, including simultaneous electrophysiological recording from many neurons, the possibility to construct distinct network architectures, and electrical, pharmacological, or optogenetic stimulation [30]. Cultured networks on MEAs provide a robust template for studying network dynamics, which may be exploited to study the underlying mechanisms of cognition and pathophysiological conditions like epilepsy, stroke, and Alzheimer's disease (AD) (Cabrera-Garcia et al., 2021; Pelkonen et al., 2021).

1.4.1 Activity patterns

Slow oscillation (SO) dominates activity patterns in the cortex during slow-wave sleep. SO includes transition between active and silent phases of neural activity with a frequency of 1 Hz. A simplified model can be found in cortical in-vitro cultures, which typically exhibit network bursts. These bursts have been shown to disappear when cultures receive more regular input, and have been suggested to be associated with low afferent input (D'Andola et al., 2019; Saberi-Moghadam et al., 2018). In the first week in-vitro, cortical cultures start firing action potentials, and activity persists for the lifetime of the culture. After one week in culture, networks begin to display bursting behavior which gradually increases until the 3rd week when bursts are dominating the activity patterns (Wagenaar et al., 2005b). Cebrera et. al (Cabrera-Garcia et al., 2021) found that cortical cultures during development from the 1st to the 3rd week in-vitro exhibited an increase in mean firing rate (MFR) and bursting frequency. Network burst (NB) suppression with tetrodotoxin (TTX) hampered network formation (Corner et al., 2002), suggesting that synchronized activity plays a role in network development and maturation.

NBs can also be elicited artificially through electrical stimulation. It has been illustrated that stimulation evoked NBs resemble the spontaneously generated ones arising from endogenous activity patterns, independently from the stimulation source (Pasquale et al., 2017). Except for network development, network bursting is hypothesized to have other functional roles (Zeldenrust et al., 2018):

- 1) Bursting can assist in reliable information transfer through synapses.
- 2) Bursts constitute an additional means of communication in parallel with single spikes.
- 3) Network bursts have a greater impact on target cells than single spikes and can prepare their targets for the incoming of a specific input.
- 4) Bursting enables synaptic plasticity modulation, thus it is engaged with cognitive mechanisms like memory.

1.4.2 Connectivity

Connectivity can be distinguished into three types: structural, functional, and effective connectivity. Structural connectivity contains the anatomical connections that couple neuronal elements. Functional connectivity is referred to the statistical dependencies between activity in different units while effective connectivity is defined as the direct causal interactions between neuronal elements (Sun et al., 2020).

In the case of in-vitro neuronal networks cultured on MEAs connectivity is assessed through functional connectivity estimation using statistical correlation methods or mutual information (Sun et al., 2020) or maximum entropy models (Lamberti et al., 2022). During the 1st week, in-vitro neurons become structurally connected forming a neu-

ronal network. Consequently, connectivity changes may be observed during temporal development of the network by creating new synaptic connections. Absence of external input makes the network highly excitable (strong excitatory connections), which leads to bursting activity through recurrent excitatory structural connections (Wagenaar et al., 2005b). Activity can have minor fluctuations around a fixed activity pattern which corresponds to a connectivity motif. Activity and connectivity mutually affect each other. The observation that both are stable on time scales of hours to days suggests that endogenous activity patterns (spontaneous activity patterns) and connectivity are in balance. Networks without afferent input are able to maintain this stability, with occurring activity patterns supporting current connectivity. It is believed that the key mechanism involved in maintaining this stability is STDP once during bursting activity several spikes are generated in the time window where STDP takes place (le Feber et al., 2015). However, a significant shift in activity can drive the network to re-arrange its connections and obtain a new activity-connectivity balance by synaptic strength modulation in response to stimulation. It has been shown that tetanic or low-frequency electrical stimulation is able to induce connectivity changes (le Feber et al., 2007; Le Feber et al., 2010). Another study shows that a decrease in the strength of functional connections reduces synchronous firing patterns, supporting further an interplay between activity and connectivity (Le Feber et al., 2014).

1.4.3 Excitability

In cortical cultured networks, it has been shown that the lack of sensory input and the existence of recurrent excitatory connections lead to hyper-excitable networks exhibiting oscillatory firing in spontaneous activity patterns (Le Feber et al., 2014), and that regular input by electrical stimulation is able to transform burst dominated activity patterns back to more dispersed firing (Wagenaar et al., 2005b). These network bursts seem to temporarily reduce network excitability for second-long periods after each network burst. It is suggested that the possible mechanism for this phenomenon is activity-dependent synaptic depression due to neurotransmitter depletion in the readily releasable vesicle pool of synapses, commonly referred to as Short-Term Depression (STD). Consequently, stronger and longer-lasting bursts can lead to greater synaptic depression (lower excitability) and longer time intervals for the synapses to recover and reoccurrence of spontaneous fluctuations that may again include network bursts (Baltz and Voigt, 2015). This hypothesis can be further supported by a study done by (Opitz et al., 2002) where they showed a positive correlation between burst duration and the time interval of a preceding burst.

In principle, network excitability can be characterized as the ease of inducing a network response when a stimulus is applied (Baltz and Voigt, 2015) or the average response of a network to a spike in one of the neurons in the network. Neurons demon-

strate an abundance of stimulus-response patterns which serve as an indication of network excitability (Gal et al., 2010). Efficacy, length, and delay of stimulus-response are linked with occurring activity patterns, demonstrating an activity-excitability dependence (Weihberger et al., 2013). Several studies observed burst suppression and excitability reduction by directly applying excitatory pharmacological agents to cortical cultures (Baltz and Voigt, 2015; Dias et al., 2021; Le Feber et al., 2014). Thus, activity patterns can be modulated by altering the excitability of a network and vice versa.

1.5 Memory formation and consolidation

Memory is an important feature that helps animals to store and retrieve former knowledge and experiences and adapt behavior in order to survive. Briefly, memory is a process where information is first encoded, then consolidated and stored in order to be retrievable in the future. Encoding involves the writing of information in the brain. Consolidation is the process of strengthening and stabilization of information for long-term periods. Storage of memory requires persistent modulations of the brain for preserving the information. Finally, retrieval of information involves the reactivation of stored information which allows behavioral adaptation to the environment (Ortega-de San Luis and Ryan, 2022). However, in this section, we will focus mostly on the encoding and consolidation part as observed in humans in-vivo and in animal models in-vitro.

1.5.1 In-vivo

Encoding and storage of memories are suggested to take place in functionally connected assemblies whose connection strength is modified during learning, known as engrams (Zhang et al., 2020). Regarding memory consolidation, there are two mechanisms that occur sequentially known as cellular and systems consolidation. The former refers to cellular modifications taking place at individual neuronal synapses in order for the memory trace to stabilize while the latter indicates a dynamic interplay between brain compartments (Wang et al., 2010). In general, memory consolidation is thought to be linked with slow oscillations (SO) during slow-wave sleep which offers augmented memory and cognitive performance (D'Andola et al., 2019).

There is one dominant theory of how memory consolidation takes place in the brain during slow-wave sleep. At first, a filtering process through synaptic modification of the hippocampal system chooses which memory traces are going to persist. Next, the memories that “survived” this process are replayed to the cortex where information can now be stored. Memory traces are replayed during slow-wave sleep through sharp-wave ripples. These ripples can regulate plasticity in neuronal populations of the hippocampus or interact with thalamocortical synchronized activity, called sleep spindles, that modify synaptic connections in the neocortex (Axmacher et al., 2006;

[Nadel et al., 2012](#)). This interplay between the neocortex and hippocampus is an example of systems consolidation that results in memory traces that can last from days to weeks ([Wang et al., 2010](#)).

1.5.2 In-vitro

Whereas memory consolidation is associated with oscillatory behavior as observed during slow-wave sleep, cortical cultures have been proposed as a slow-wave sleep model due to the exhibition of oscillatory synchronous firing patterns (network bursts). In sufficiently developed cortical cultures network bursts occur under a frequency which approximates the frequency of δ -waves (0.1 – 4 Hz) detected by EEG during slow-wave sleep ([Zhang et al., 2020](#)). Earlier work showed that repeated stimulation of cortical networks leads to the formation and consolidation of memory traces that persist for at least several hours, even if meanwhile other memory traces are formed ([Wagenaar et al., 2005b](#)). Another study supports that low-frequency electrical stimulation is able to induce connectivity changes whose magnitude is sensitive to the stimulation protocol applied ([Le Feber et al., 2010](#)).

1.6 Aim of this study

It is an open question why memory consolidation occurs mainly during slow wave sleep, and what is the role of oscillatory activity and network excitability in this process. One important difference between the awake state and slow wave sleep is the cholinergic tone in the cortex, which is high when awake, but very low during slow wave sleep ([Gais et al., 2003](#)). Recent work showed that oscillatory patterns, as well as memory consolidation were facilitated by a low cholinergic tone, possibly through cholinergic modulation of network excitability ([Dias et al., 2021](#)). Another important difference between the awake state and slow wave sleep, that may also affect network excitability, is the presence or absence of afferent input. Goal of this project is to monitor the effect of random background input on oscillatory firing, network excitability and memory consolidation in cultured ChR-2 transduced cortical networks. Taking into account the aforementioned we assume that cortical cultures with low afferent input exhibiting network bursts will be able to consolidate memory traces once they simulate the behavior of the cortex during slow-wave sleep. At first, we investigate the response of cultures in different stimulation frequencies in terms of activity and network excitability. Next, we examine whether transduced cultures are able to form memory traces in response to repeated electrical stimulation. Finally, by introducing random, background optogenetic input we observe the effect on memory trace formation and network properties (activity / excitability). We hypothesize that in conditions with high

afferent input (background optogenetic stimulation) network excitability will decrease and memory trace formation will be impaired.

Methods

2.1 Cell culturing

Cortical cells were obtained from rat pups that were decapitated at day 1 post-natal in compliance with Dutch and European laws and guidelines regarding animal research. Cells were dissociated by trypsin treatment and trituration which resulted in a cell suspension of around 1000 cells/ μ l. These included excitatory and inhibitory neurons, as confirmed by electrophysiological [le Feber et al. \(2016\)](#) and immunohistochemical experiments [Le Feber et al. \(2018\)](#). Glial cells and especially astrocytes were also present in the culture once they have shown to enhance neuronal function and viability [Bélanger and Magistretti \(2022\)](#). The presence of glial cells was validated through immunofluorescence staining of GFAP protein found at the glial cytoskeleton as shown in 2.1. Next, cells were plated on the glass surface of a Multi-Electrode Array (MEA) depicted in 2.2(A) [Kussauer et al. \(2019\)](#), acquired from Multi Channel Systems (MCS), Reutlingen, Germany; that were precoated with polyethyleneimine (PEI) for optimal cell adhesion. The day after plating, cells were transfected with 15 μ l of Adeno Associated Virus (AAV) that carried the gene expressing ChannelRhodopsin-2 (ChR-2) fused with mCherry driven by the CaMKII α promoter which targets only the excitatory

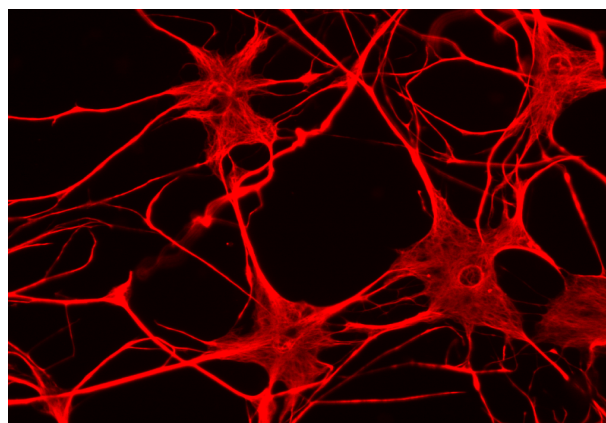


Figure 2.1 Validating the presence of astrocytes by immunofluorescence staining of GFAP

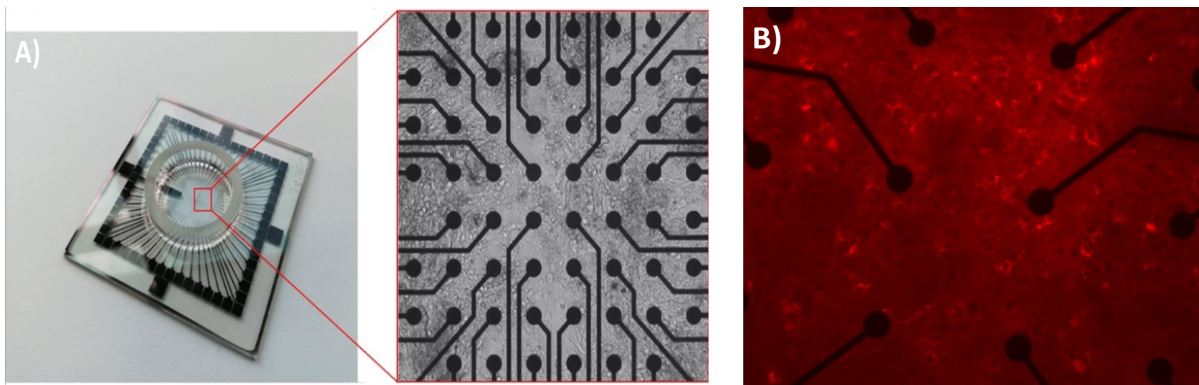


Figure 2.2 A) Illustration of a flat MEA with the circular chamber, glued at the center. At higher magnification, the 60 titanium-nitride electrode grid is apparent. B) Example of a cultured MEA with rat cortical neurons co-expressing ChR-2 and mCherry fluorescent protein.

neurons. The initial volume of virus with a physical titre of $1.31 \cdot 10^{13}$ GC ml⁻¹ was diluted 100 times in DBPS. Successfully transfected excitatory cells are illustrated in Fig.2.2(B). These cells were able to express ChR-2 on their surface, enabling activation by shedding blue light Fröhlich (2016a). Culturing of the cells took place in a circular chamber glued on the center of the MEA with inner diameter $d = 20$ mm. The center of the chamber contains 60 titanium nitride electrodes ($30 \mu\text{m}$ diameter, $200 \mu\text{m}$ pitch) which allow to record electrical signals or stimulate electrically. The chamber was filled with $700 \mu\text{l}$ of R12 medium Romijn et al. (1984). Cultures were stored in an incubator at $36 \text{ }^\circ\text{C}$, 5% of CO_2 and high humidity conditions. The experiments took place in a custom-made Faraday cage to minimize artifacts emerging from interfering electromagnetic noise. After one week of culturing, spontaneous action potential discharges start to appear and network bursts are increasing in duration and frequency, reaching their maximum during the third week in vitro, followed by large scale synaptic pruning and reaching a state that is generally considered as ‘mature networks’ after ~ 21 days, described in Van Pelt et al. (2004). Experiments were conducted 25 ± 7 days after plating (DIV 18-32) so that synchronous network firing discharges were dominating spontaneous activity.

2.2 Data acquisition

Data acquisition was done in measuring setup located outside of the incubator. The entire setup was covered by Plexiglass cage which was continuously perfused with a gas mixture of 21% O_2 , and 5% CO_2 at a constant rate of 2 liter/min in order to maintain stable environmental conditions for experiments. A computer regulated two mass flow controllers through a custom-made LabVIEW script. The gases before ending up in the cage were moisturized with deionized water through two bubblers. During

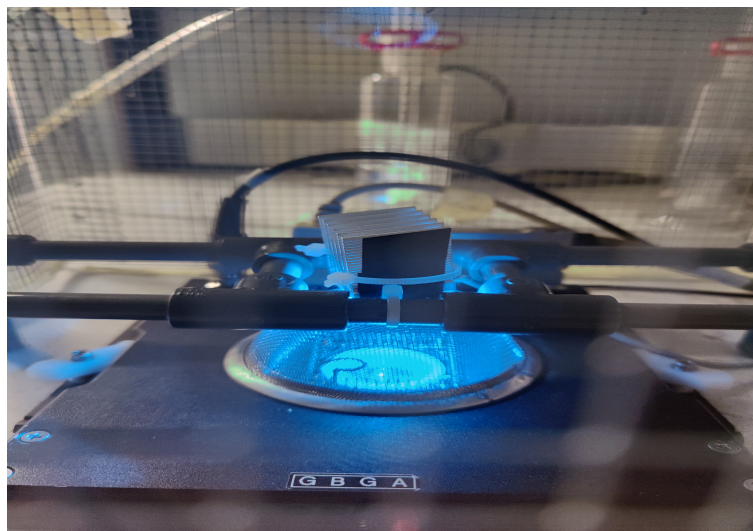


Figure 2.3 Cortical culture inside the recording setup which is stimulated with blue light pulses.

experiments, the culture chamber was tightly sealed with a PDMS ring bearing a water-retaining but CO_2 and O_2 permeable membrane (ALA Scientific), to halt evaporation of the medium and prevent infections from its surroundings. While in the recording setup, MEAs were kept at a constant temperature of 36°C through a heating plate connected to a PID controller.

The recording setup was able to acquire signals from 59 MEA channels (one channel served as reference) with a sampling frequency of 16 kHz and noise levels ranging generally from $3\text{--}7 \mu\text{V}_{\text{RMS}}$. Data acquisition was carried out from a custom-made LabVIEW software which executed amplification (1000x) and band-pass filtering (0.1 – 6 kHz). The software was also capable of controlling electrical and light stimulation as well as illustrating a real-time raster plot and post-stimulus-time-histogram (PSTH). For chronic electrical and light stimulation the automation of the stimulation protocol was essential therefore the existing LabVIEW application was modified. Specifically, post-modification the program was capable of changing between stimulation electrodes automatically and allow the user to apply electrical stimulation together with light stimulation at varying frequencies. These changes were critical for conducting the desired experiments. An instance of the recording setup can be found in Fig 2.3.

Spike detection was executed in compliance with the rule that each detected signal should be at least 5.5 times higher than the estimated root-mean-square noise level. The noise levels were adapted during the recording for each electrode following an adaptive noise estimation algorithm. If the signal exceeded the detection threshold, a timestamp, the electrode number, a 6 ms waveform, and the estimated noise level at that electrode were stored. Furthermore, if electrical or optogenetic stimulation was applied, the timestamps of each stimulus were also saved. All stored candidate spikes underwent an off-line artifact detection as done in [Wagenaar et al. \(2005a\)](#). For a candidate spike to be valid it needs to conform to the following rules:

- no other peaks with equal or higher amplitude were recorded within a 1 ms around the main peak of the waveform.
- no other peaks with the same polarity and more than 90% of the amplitude of the candidate spike existed within a 0.3 ms window around the peak.
- no other peaks with the same polarity and more than 50% of the amplitude of the candidate spike existed within a 1 ms window around the peak.
- no more than one peak should exist at the exact same timestamp.
- there should not be a peak whose width is smaller than 3/16 ms at 50% of the original peak.

2.3 Experimental design

We divided the project into three sets of experiments. In the first set, we aimed to determine the effect of different optogenetic stimulation frequencies on network activity and excitability. We will refer to this set as “optogenetic stimulation experiments”. Based on these results we defined the optimal stimulation frequency to apply in our next set of experiments. In the second set, we replicated part of the experiments done by [Dias et al. \(2021\)](#) where cultures are subjected to electric stimulation to identify the underlying mechanisms of memory consolidation; from now on, this set will be mentioned as “control memory experiments”. The last set of experiments is the combination of electric and optogenetic stimulation which explores the effect of random background optogenetic input on the consolidation of memory; this last set will be referred as “background input memory experiments”.

In principle, we set some exclusion criteria which were evaluated post-analysis in order to enhance robustness and reliability of our findings. Overall, we excluded from the analysis cultures that had recorded less than 2^{15} spikes per spontaneous activity recording or did not respond to electrical stimulation or the number of active electrodes was < 15 . As active electrodes we consider the ones that recorded at least 250 spikes at the time of analysis.

2.3.1 Optogenetic stimulation experiments

In this set of experiments, we tested different light stimulation frequencies to inspect network responses to random background optogenetic stimulation and determine which stimulation frequency will be applied to the *background input memory experiments*. Optogenetic stimulation was conducted via a LED, positioned at the center above the culture (wide-field), capable of illuminating with 450 nm of light (blue) with varying pulse width and intensity (maximal intensity 2.44 W/m^2). To achieve random background input, the interstimulus intervals (ISIs) were generated from a pseudorandom number

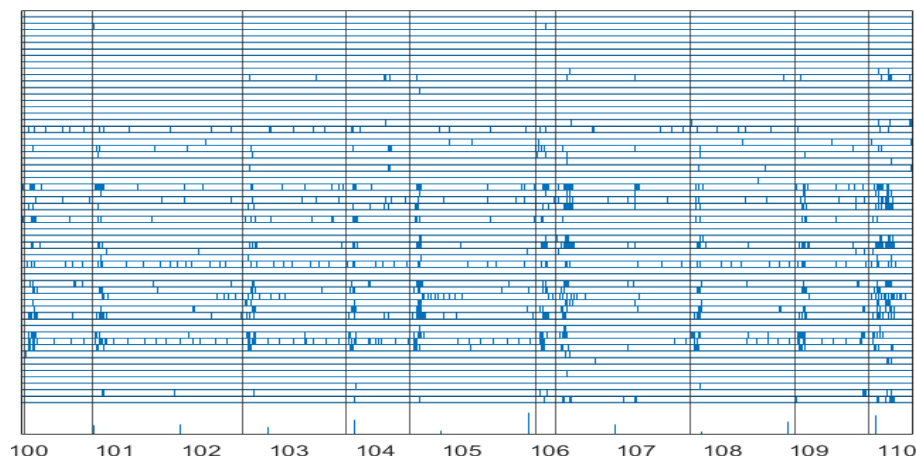


Figure 2.4 Sample raster plot of 10 seconds which shows the activity of a culture at 1 Hz optogenetic stimulation. It is evident that due to wide-field light stimulation after each light pulse (vertical black lines), follows a global burst which validates the responsiveness to light stimulation.

generator following a uniform distribution and by setting the minimum and maximum of the distribution we were able to achieve different mean stimulation frequencies (namely 0.1, 0.2, 0.5, 1, 2 and 5 Hz). Before starting the experiment, responsiveness to light stimulation was tested in all cultures by checking the real-time raster plot illustrated in the LabVIEW application. Since stimulation performed in a wide-field fashion we expected synchronous activation of transfected neurons thus a culture was responsive if a global burst in the raster plot was evident as seen in Figure 2.4.

Next, we investigated which are the minimum values of pulse duration and light inten-

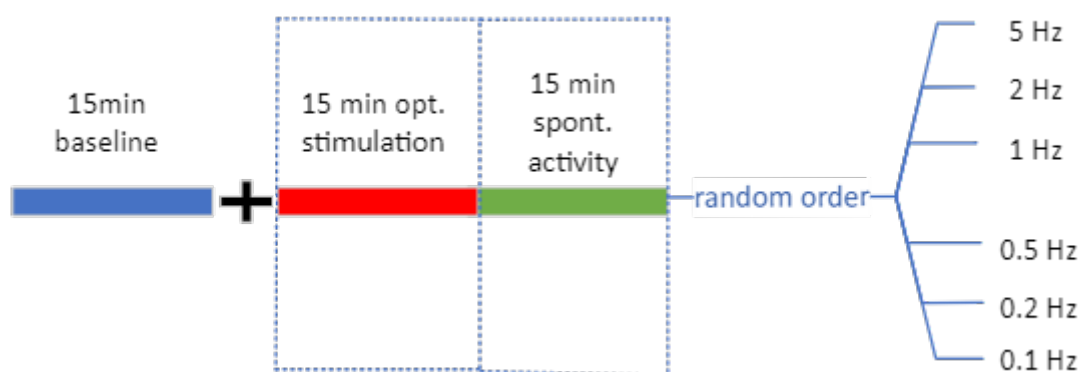


Figure 2.5 Schematic representation of optogenetic stimulation experiments. Prior to experimental protocol a 15 min baseline was recorded. Experimental protocol (dotted rectangular) was repeated for every stimulation frequency. The sequence of the mean stimulation frequencies applied was randomized.

sity that triggered a clear response and used these in the experimental protocol. Prior to experimental protocol we recorded a 15 min baseline recording. Experimental protocol consisted of 15 min of optogenetic stimulation at a specified frequency followed

by a 15min of spontaneous activity recording. This protocol was repeated for each stimulation frequency, in a random sequence as illustrated in Figure 2.5.

2.3.2 Control memory experiments

These experiments, aimed to assess whether cultures were able to consolidate memory traces while electrically stimulated at two pre-selected electrodes. All cultures were stimulated with low frequency ($f = 0.2$ Hz) and $200 \mu\text{s}$ wide biphasic rectangular current pulses (negative phase first). To determine which electrodes were suitable for stimulation and what amplitude to use, we first probed all electrodes in pseudorandom order at three different amplitudes (12, 24 and $36 \mu\text{A}$). We selected two stimulation electrodes and a stimulation amplitude that induced a clear stimulus response between 20–100 ms latencies. Prior to experimental protocol we recorded 1 hour of baseline activity. Experimental protocol consisted of five stimulation periods of 10 minutes for the first stimulation electrode, each followed by an hour of spontaneous activity recording. Then, this protocol was repeated for the second stimulation electrode, and finally repeated again for the first stimulation electrode. An outline of the experimental protocol which lasted in total 18.5 hours is illustrated in Figure 3.5.

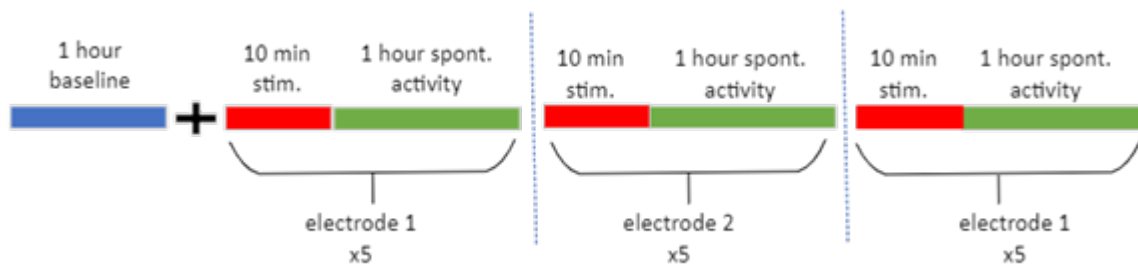


Figure 2.6 Schematic representation of control memory experiments. Prior to experimental protocol a 1 hour baseline was recorded. Experimental protocol consisted of a 10 min stimulation with biphasic current pulses ($200 \mu\text{s}$ wide) at 0.2 Hz, followed by 1 hour of spontaneous activity recording. This paradigm was repeated 5 times for each stimulation electrode. The same protocol was used also in background input memory experiments with the only difference that during electrical stimulation, optogenetic stimulation at 5 Hz was also applied.

2.3.3 Background input memory experiments

Background input memory experiments aimed to unravel the effects of random optogenetic background stimulation in the consolidation of memory traces. In this case, we will apply the same protocol as described under control memory experiments, but now with additional random optogenetic stimulation during the electrical stimulation period. The light stimulation frequency that had the most robust effect on network's excitability as emerged from *optogenetic stimulation experiments* was utilized.

2.4 Data analysis

The signals recorded stem from single or multi-unit activity since one electrode could be in contact with more than one neuron, thus we are going to refer to the activity of one electrode rather than a neuron. We used various metrics to examine network activity we plotted raster plots, calculated the mean firing rate (MFR) and bursting frequency (BF). Excitability was assessed by computing the mean single pulse response (SPR) strengths during spontaneous activity recordings while during optogenetic stimulation excitability was estimated by evaluating the average network response to light stimulation. Functional connections were explored by conditional firing probabilities (CFPs) and changes in functional connectivity by Euclidean Distances (ED). Finally, effectiveness of electrical stimulation was determined by computing the area under the curve of the mean post-stimulus time histogram (PSTH).

Analysis and calculation of all readouts was done in MATLAB 2020a while averaging between experiments performed using Microsoft Excel 365. Designing of graphs was done by Origin 2019b and all results are shown as mean values while error bars indicate the standard error of the mean (SEM). Statistical treatment was done using IBM SPSS statistics 28 with a significance level of $\alpha = 5\%$. Prior to statistical comparison all data sets were tested for normality and equality of variances using Shapiro-Wilk's test and Levene's test, respectively. If data were normally distributed a one-way or two-way repeated measures ANOVA was applied. In case of non-normally distributed data we utilized the non-parametric equivalents which are a Kruskal-Wallis test and a Mann-Whitney U test. In the event of a statistically significant result from the aforementioned tests a post-hoc test was applied. In normal data a repeated measures ANOVA pairwise comparison was made while in non-normal data a Wilcoxon signed-rank test. Due to multiple pairwise comparisons we needed to adjust manually the resulted p-values by applying a Holm-Bonferroni correction.

2.4.1 Raster plots

Raster plots are graphical representations of the spikes recorded at each electrode with respect to time. On the y-axis, channel numbers are shown (0-59), where x-axis shows the time. Each recorded spike is indicated by a "tick" in the corresponding channel. The recording software displays a real-time raster plot to monitor activity and firing patterns of culture while experimenting, or it can be recreated in MATLAB from stored data.

2.4.2 Mean firing rate

The mean firing rate was calculated as described in [Bologna et al. \(2010\)](#). First, the mean firing rate of each active electrode was calculated by dividing the total number of spikes per active electrode to the total time of the recording. Then, we averaged between firing rates of all active electrodes and ended up with the mean firing rate (MFR) of the culture which provided us with the number of spikes per second per electrode (spikes/sec/electrode). This metric is used to quantify activity of the neuronal culture.

2.4.3 Bursting frequency

To evaluate the effect of light stimulation on activity patterns of networks we developed an algorithm able to monitor the frequency that synchronous firing occurred during spontaneous activity recordings and stimulation periods. From now on, we will refer to this behavior as network bursts. At first, we divided the long-term recording into data blocks of 2^{15} elements. We chose to divide data into chunks of a pre-determined number of spikes rather than a constant duration to avoid activity fluctuations between chunks. All chunks were analyzed individually and an average bursting frequency (BF) was estimated for each one of them. Many algorithms have been designed to identify network bursts, but there is no generally accepted definition of network burst, and all algorithms use certain assumptions [Välkki et al. \(2017\)](#). Our algorithm detected a network burst whenever more than 60% of all active electrodes are recording at least one spike in a time interval of 100 ms. In addition, a detection is considered valid only if there is not another burst detected in a specified exclusion range before the detected burst. When optogenetic stimulation is not included in the experiment, exclusion range is fixed to 0.5 sec. Otherwise, the exclusion range is adaptive and follows the minimum of the uniform distribution used for stimulating optogenetically as mentioned in section 2.3.1. The algorithm provided us with an array containing the burst timestamps and the total number of bursts from which we could calculate the bursting frequency of the culture if we divided it by the time of the recording. To evaluate the accuracy of the algorithm, we visually inspected raster plots and checked for false positive detections. In general, the algorithm was more accurate in spontaneous activity recordings compared to light stimulation. Especially at high frequencies the probability of having false-positive detections increased. However, this method provided us with a good estimate of occurring bursting patterns.

2.4.4 Conditional firing probabilities

In order to quantify functional connectivity between pairs of active electrodes, we utilized a cross-correlation related measure called conditional firing probabilities (CFPs)

le Feber et al. (2007) . For evaluating the effect of stimulation in cultures we applied this measure in baseline and spontaneous activity recordings which were divided into data blocks with a fixed amount of recorded spikes (2^{15}). The block size was chosen in a way to provide us with a sufficiently high number of data blocks to enable statistical analysis of the results. In each data block, the CFP curve of every active pair of electrodes was calculated. We define as conditional firing probability ($CFP_{i,j}[\tau]$) the probability that an electrode j recorded a spike within a latency = 500 ms (in time bins of 0.5 ms) after a spike was recorded at electrode i at $t = 0$. More precisely, $CFP_{i,j}[\tau]$ is realized as the number of spikes recorded at electrode i , followed by an action potential at electrode j with delay τ ($N_{followi,j}[\tau]$), divided by the total number of spikes recorded at electrode i (N_i):

$$CFP_{i,j}[\tau] = \frac{N_{followi,j}}{N_i} \quad (2.1)$$

From the above analysis a CFP curve for every combination of active electrodes derived and a four-parameter equation was fitted (Figure 2.7):

$$CFP_{i,j,fit}[\tau] = \frac{M_{i,j}}{1 + \left(\frac{\tau - T_{i,j}}{w_{i,j}}\right)^2} + offset_{i,j} \quad (2.2)$$

The fitted function gives estimates of $M_{i,j}$ which corresponds to the maximum magnitude above offset and interpreted as the strength of a connection; $T_{i,j}$ which is the latency (ms) where the fitted equation reaches its maximal value; $w_{i,j}$ is translated as the width at 80% of the maximum amplitude above offset and regulates the shape of the curve and $offset_{i,j}$ that is interpreted as uncorrelated spontaneous activity. For a pair of electrodes to be functionally connected a set of criteria should be met: 1) $M_{i,j}$ should be at least twice the value of the $offset_{i,j}$; 2) $T_{i,j}$ should not be less than 250

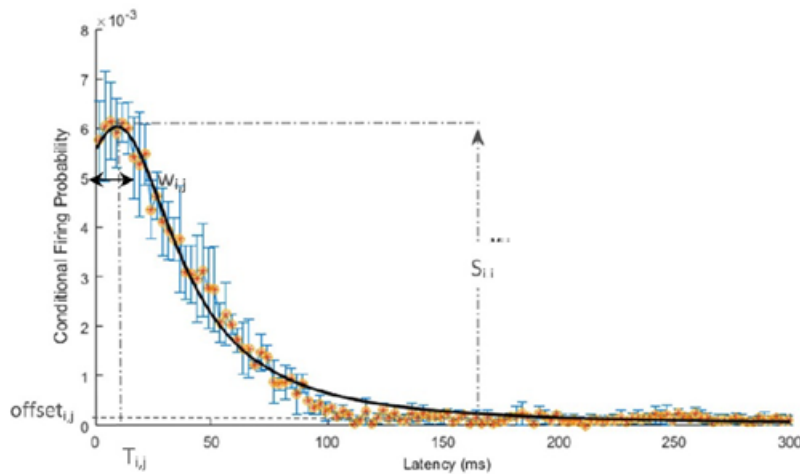


Figure 2.7 Conditional firing probability (CFP) graph illustrating the fitted function (black line) and the parameters of equation 2.2.

ms; 3) $w_{i,j}$ should not exceed the 250 ms limit and 4) $w_{i,j}$ had to be larger than 10 ms to prevent fitting to a single outlying.

This analysis was conducted for all pairs of active electrodes resulting in 60x60 matrices, one for each parameter of the fitted function. If one of the criteria was not met or one of the electrodes was not considered active then a zero value was assigned. For our project, the matrix M containing the strength of all functional connections was relevant and used to determine changes in the strength of functionally connected electrodes as described later on, in the Euclidean distances section.

2.4.5 Euclidean distances (ED)

The connectivity matrices (M) obtained from CFP analysis, enabled us to monitor how connectivity strength evolves throughout the course of the experiment. To determine the degree of variation in the strength of the connections induced from each stimulation electrode we calculated the Euclidean distances (ED_0) between connectivity matrices obtained from spontaneous activity recordings at time t and time t_0 as expressed in (8):

$$ED_0(t) = \sqrt{\sum_{i=1}^n \sum_{j=1}^m [M_{i,j}(t) - M_{i,j}(t_0)]^2} \quad , t > t_0 \quad (2.3)$$

As t_0 was utilized a baseline recording, which was the last 1-hour spontaneous activity recorded before the first stimulation period at each electrode. For instance, to evaluate connectivity changes induced from the first stimulation electrode, t_0 will be the baseline recorded prior to the experimental protocol but for assessing changes in the second stimulation electrode as t_0 will now serve the fifth spontaneous activity recording from the first electrode. In the analysis, only non-zero elements of the connectivity matrices are taken into account. After calculating ED_0 between all possible pairs of connectivity matrices using equation 2.3, the resulting values are averaged for each 1 hour of spontaneous activity and normalized to the mean connection strength of the recording used as t_0 . The values resulting from ED_0 analysis were compared to $ED_{baseline}$ which is the averaged and normalized Euclidean distances between data blocks of the recorded spikes series which served as baseline recordings. The normalization factor arose from the mean connection strength of all baseline recording data blocks.

2.4.6 Single pulse response (SPR)

The degree in which neurons are connected is strongly correlated linearly with the excitability of the network [Le Feber et al. \(2014\)](#). However, using CFPs we are not able to directly quantify excitability because CFP strongly depends on the dynamic state

of the network. More precisely, if the activity of the network is dominated by network bursts it is more probable that electrode i will record more than one spikes in the time interval of the analysis (500 ms). This phenomenon leads to an overestimation of CFP values. Therefore, in order to have a cleaner measure of network excitability we used Single Pulse Response (SPR) analysis which significantly reduced this overestimation as described in [Le Feber et al. \(2014\)](#). SPR is the average response recorded at electrode j to a single spike at electrode i ($\text{SPR}_{i,j}$). SPR analysis is applied only to spontaneous activity recordings. Again long-term recordings are divided into blocks of 2^{15} action potentials, which are analyzed as CFP, with the only difference that we deconvolve the autocorrelation of electrode i from $\text{CFP}_{i,j}$. The end product is again a connectivity matrix (S) for each block of data which contains estimates of the SPR strengths between functionally connected pairs of electrodes. Network excitability is estimated by averaging the values from SPR connectivity matrices of each spontaneous activity recording. Before averaging across cultures, excitability was normalized to baseline network excitability. This analysis is employed to unravel any after-effects of background stimulation on network excitability.

2.4.7 Average network response

Typically, stimulus responses are quantified by the area under the curve of post-stimulus time histograms (PSTHs), but this was not possible for the higher stimulation frequencies, as multiple light pulses overlapped with the period of analysis [Takahashi et al. \(2012\)](#). To quantify the excitability of the network during optogenetic stimulation we counted the number of spikes recorded 100 msec after cessation of each light pulse, and then averaged to the total number of light pulses (N) at that stimulation period. This metric corresponds to the average network response to light stimulation which is defined as:

$$\text{Average network response} = \frac{\sum_{i=1}^N R_i(t_i + p + 100 \text{ ms})}{N} \quad (2.4)$$

Where t_i is the timestamp of a light pulse, p the duration of light pulse and R_i the number of spikes counted at that interval. In case the analysis interval overlapped with the timestamp of the next light pulse, that stimulation was not taken into account because the spike count was “polluted” with the direct light activation occurred from the following pulse. This occurred mostly at the highest stimulation frequency (5 Hz). This metric exhibits the average network response to optogenetic stimulation and can be considered as an estimate of excitability during light stimulation.

2.4.8 Area under the curve of the mean post-stimulus time histogram

A post-stimulus time histogram (PSTH) was constructed per electrical stimulation period to evaluate the mean effectiveness of stimulation throughout the experiment. We counted the average number of spikes in 5ms bins in the interval 300 ms before and 300 ms after the stimulus. The effectiveness of stimulation was quantified by the area under the curve (AUC) of the mean PSTH. Electrical stimulation directly activates a subset of neurons in the near vicinity of the stimulation electrode, or with an axon in this area. These neurons, in turn can activate other neurons in the network. This latter phase referred as network response, depends on synaptic propagation, and typically has latencies between 15 and 300 ms [73] as illustrated in Figure 2.8. To obtain a clear outcome of effectiveness of electrical stimulation, we extracted the uncorrelated background firing as estimated from the 300 msec period prior to stimulus onset by calculating the AUC in this epoch ($AUC_{background}$) and subtracted it from the computed area during stimulation (AUC_{stim}). If the resulting value was 0 in any of the stimulation periods it means that the culture was not responding to electrical stimulation which is a good reason to exclude it from the analysis.

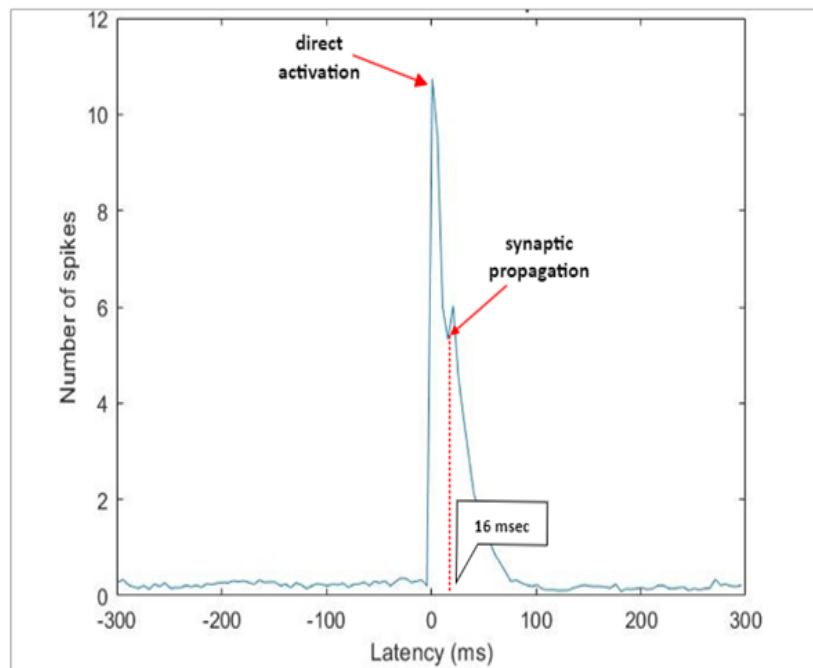


Figure 2.8 Post stimulus time histogram (PSTH) exhibiting the difference between direct activation and synaptic propagation; spikes are counted in 5 ms bins. Typically, network response has a latency of 300 ms (AUC_{stim}) and involves the direct activation (latency ~ 15 ms) and synaptic propagation. Direct activation is excluded from the spike counts as we are solely interested in synaptic propagation of the stimulus. Negative latencies display the spontaneous activity before stimulus onset ($AUC_{background}$).

Results

3.1 Optogenetic stimulation experiments

3.1.1 Overview

In this set of experiments random, background optogenetic stimulation was administered at different mean stimulation frequencies ranging from 0.1 to 5 Hz. In total 15 cultures were used from which three were excluded because of insufficient number of active electrodes (< 15). An overview of all experiments including the ones that met the exclusion criteria can be found in Appendix A. The frequency that spawned the most apparent changes in network excitability will be used as background stimulation in *background input memory experiments*.

First experiments had a maximum stimulation frequency of 1 Hz, higher frequencies were added in later experiments. The table below summarizes the number of experiments that have been conducted for every stimulation frequency.

Table 3.1: Sample size (n) for each stimulation frequency

Stimulation frequency (Hz)	0.1 Hz	0.2 Hz	0.5 Hz	1 Hz	2 Hz	5 Hz
Sample size (n)	8	12	12	12	8	4

Stimulation for 15 min at different frequencies was applied to reveal the direct effects of stimulation while the 15 min recording of spontaneous activity right after stimulation was applied to unveil possible after-effects.

3.1.2 Effect of different stimulation frequencies on activity

Figure 3.1 illustrates the relationship between the normalized MFR as calculated during stimulation and spontaneous activity recordings for every stimulation frequency. We evaluated the effect of light stimulation on mean firing rate (MFR) for each stimulation frequency by comparing the MFR between stimulation periods and the baseline recorded prior to experimental protocol Fig 3.1(A). MFR tended to increase with stimulation frequency during periods of optogenetic stimulation, but not significantly (repeated measures ANOVA, $p > 0.77$). MFR during spontaneous activity recordings did not differ significantly from baseline values (repeated measures ANOVA $p > 0.61$). In Figure 3.1(B) we observed that optogenetic stimulation robustly affected bursting patterns during stimulation periods. Bursting frequency (BF) increased with stimulation frequency and became significantly different from baseline values at stimulation frequencies ranging from 0.2 to 1 Hz (Kruskal-Wallis, $p < 0.015$). Stimulation frequencies > 1 Hz revealed a reduction in BF values which is not significant in relation to the peak at 1 Hz (Kruskal-Wallis, $p > 0.76$). In contrast, BF values during spontaneous activity recordings (green line) seemed to remain unchanged compared to baseline (repeated measures ANOVA, $p > 0.66$).

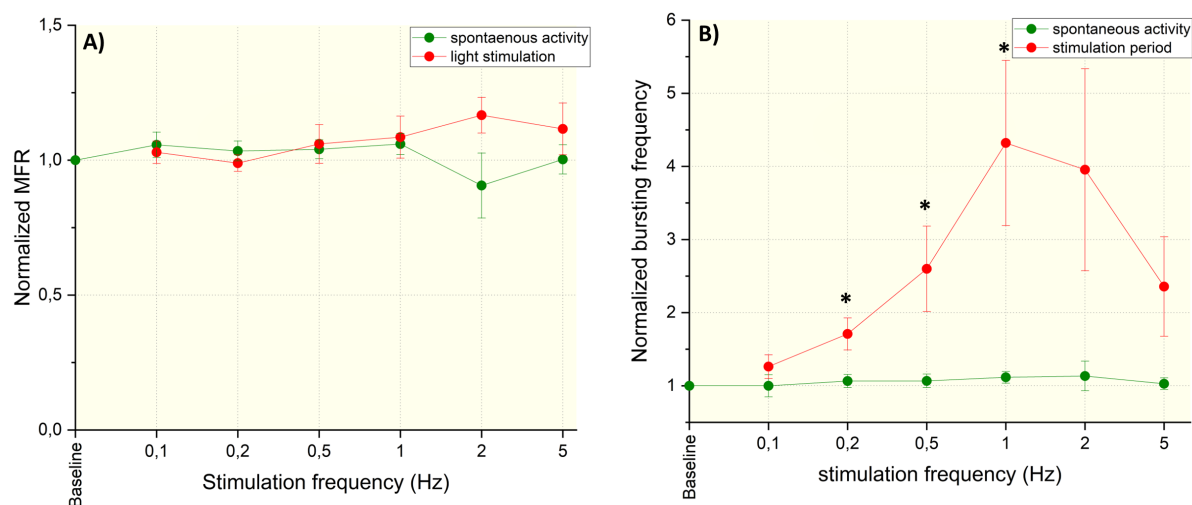


Figure 3.1 Mean firing rate (MFR) and bursting frequency (BF) for each stimulation frequency during stimulation periods (red line) and spontaneous activity recordings (green line); all values are normalized to baseline to allow comparison between experiments. A) MFR during light stimulation was not significantly different from baseline neither during stimulation periods nor spontaneous activity recordings. B) BF during light stimulation was significantly different at frequencies ranging from 0.2 to 1 Hz while during spontaneous activity recordings there were no significant changes in bursting patterns; * indicates significant changes from baseline (post-hoc Wilcoxon signed-rank test with Holm-Bonferroni correction) and error bars indicate the SEM.

3.1.3 Effect of different optogenetic stimulation frequencies on network excitability

To study possible after-effects and direct consequences of different light stimulation frequencies on network excitability we calculated the mean SPR strengths during spontaneous activity recordings (Fig. 3.2(A)) and we quantified the average network response during light stimulation (Fig 3.2(B)), respectively. Higher stimulation frequencies tended to lower network excitability in the period after stimulation, but effects were not significant (repeated measures ANOVA, $p > 0.492$).

Average network response to optogenetic stimulation as calculated by equation 2.4 exhibited a considerable decline with increasing stimulation frequency. This decrease became significant for frequencies ≥ 0.5 Hz (repeated measures ANOVA, $p < 0.002$). For this analysis a file with all the stimulation timestamps was required, which was not retrievable in four of the experiments, reducing the maximum sample size for this metric to $n=8$. From these findings we observe that during light stimulation with 5 Hz, network excitability showed the most prominent reduction therefore we choose to apply this frequency in *background input memory experiments*.

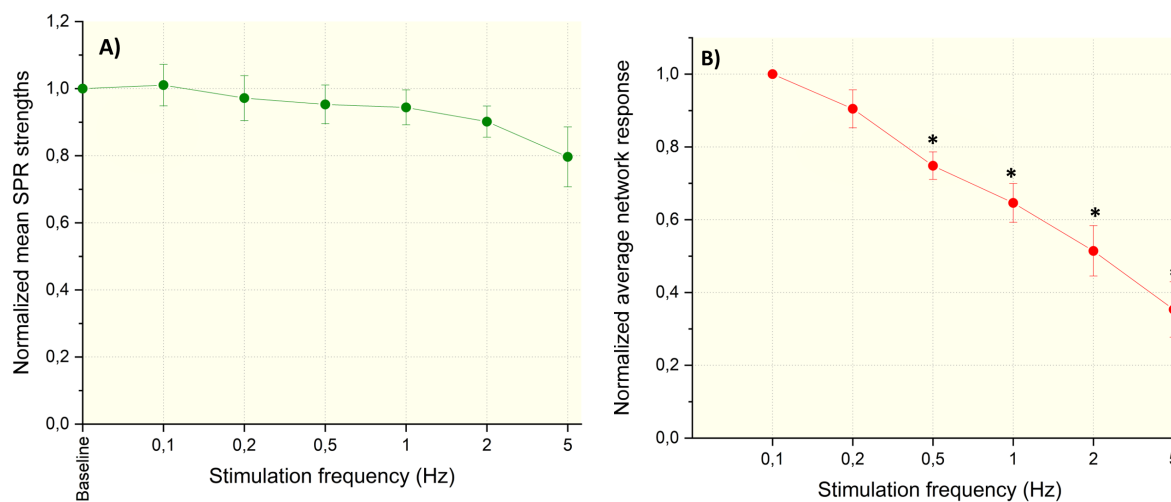


Figure 3.2 Effect of different optogenetic stimulation frequencies on network excitability. A) Normalized SPR strengths during spontaneous activity recordings. Data were normalized to baseline SPR strength values. All frequencies tested showed no significant alterations in excitability compared to baseline values. B) Normalized average network response as an estimate of network excitability during stimulation periods. Data were normalized to the values of the average network response of the lowest stimulation frequency. Stimulation frequencies ≥ 0.5 Hz revealed a significant reduction in average network response; * indicates significant changes between baseline and different stimulation frequencies (post-hoc Wilcoxon signed-rank test with Holm-Bonferroni correction, $p < 0.44$) and error bars indicate SEM.

3.2 Control & background input memory experiments

3.2.1 Overview

Control memory experiments were conducted to assess if virally transduced cultures, expressing ChR-2 are able to form memory traces. In these experiments, we used 18 cultures where 10 of them were excluded post-analysis due to failure of stimulating effectively through electrical stimulation (see Appendix A).

In *background input memory experiments* we administered random, background light pulses with a mean frequency of 5 Hz in parallel with the electrical stimulation periods as described in Methods section. We used 9 cultures from which 1 was excluded due to failure of stimulating effectively with electrical pulses (see Appendix A). We evaluated the effects of optogenetic stimulation on activity, excitability and memory trace formation.

3.2.2 Temporal development of efficacy of electrical stimulation

Figure 3.3 depicts the temporal evolution of the normalized area under the curve (AUC) of the mean post-stimulus time histogram (PSTH) due to electrical stimulation averaged between experiments. AUC values from *control memory experiments* remained stable with no significant changes compared to the AUC at the first stimulation period (repeated measures ANOVA, $p > 0.55$). The same pattern is observed also in the AUC values of *background input memory experiments* which increased slightly but not significantly (repeated measures ANOVA, $p > 0.27$). Comparison of AUC values between control and background input experiment showed no considerable difference

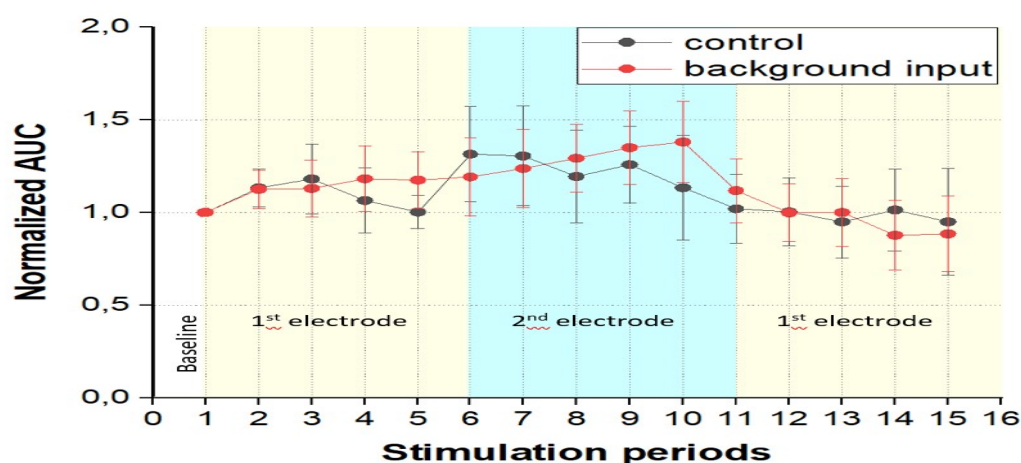


Figure 3.3 Normalized AUC of the mean PSTH during control and background input experiments. As normalization factor served the AUC from the 1st stimulation period. Effectiveness of electrical stimulation and remained unchanged throughout the duration of the experiments in both control and background input experiments; error bars indicate the SEM.

(two-way repeated measures ANOVA, $p > 0.9$).

3.2.3 Effect of 5 Hz background optogenetic stimulation on activity patterns during spontaneous activity recordings and stimulation periods.

Activity of the network is assessed by means of firing rate and bursting frequency. We compared these metrics during spontaneous activity recordings to investigate possible after-effects and during stimulation periods to study the direct response to 5 Hz background light stimulation.

Figure 3.4(A) shows the MFR evolution of control (black line) and background input experiments (red line) during the 1-hour spontaneous activity recordings. MFR values during spontaneous activities did not change significantly from baseline neither in control (repeated measures ANOVA, $p > 0.59$) nor background input memory experiments (repeated measures ANOVA, $p > 0.44$). Comparison between the two groups yielded no statistically significant difference (two-way repeated measures ANOVA, $p > 0.3$).

Figure 3.4(B) illustrates the MFR temporal evolution of control and background input memory experiments during the 10-minute stimulation periods. MFR values during stimulation periods did not change significantly from baseline in both control (repeated measures ANOVA, $p > 0.12$) and background input memory experiments baseline (repeated measures ANOVA, $p > 0.06$). Comparison between the two set of experiments showed no significant differences (two-way repeated measures ANOVA, $p > 0.54$).

In Figure 3.4(C) we assess the frequency of network bursts as occurred in control and background input experiments during spontaneous activity recordings. BF during spontaneous activity recordings did not significantly change from baseline values during the course of control (repeated measures ANOVA, $p > 0.37$) and background input memory experiments (Kruskal-Wallis, $p > 0.79$).

Figure 3.4(D) illustrates the evaluated BF for control and background input memory experiments during periods of stimulation. In control experiments, BF during stimulation periods did not differ significantly from baseline values (repeated measures ANOVA, $p > 0.06$). Similarly, in experiments where background input was administered BF values did not differ significantly from baseline (Kruskal-Wallis, $p > 0.53$). Comparison between BF values of control and background input experiments showed no significant difference between them (Mann-Whitney U test, $p > 0.72$).

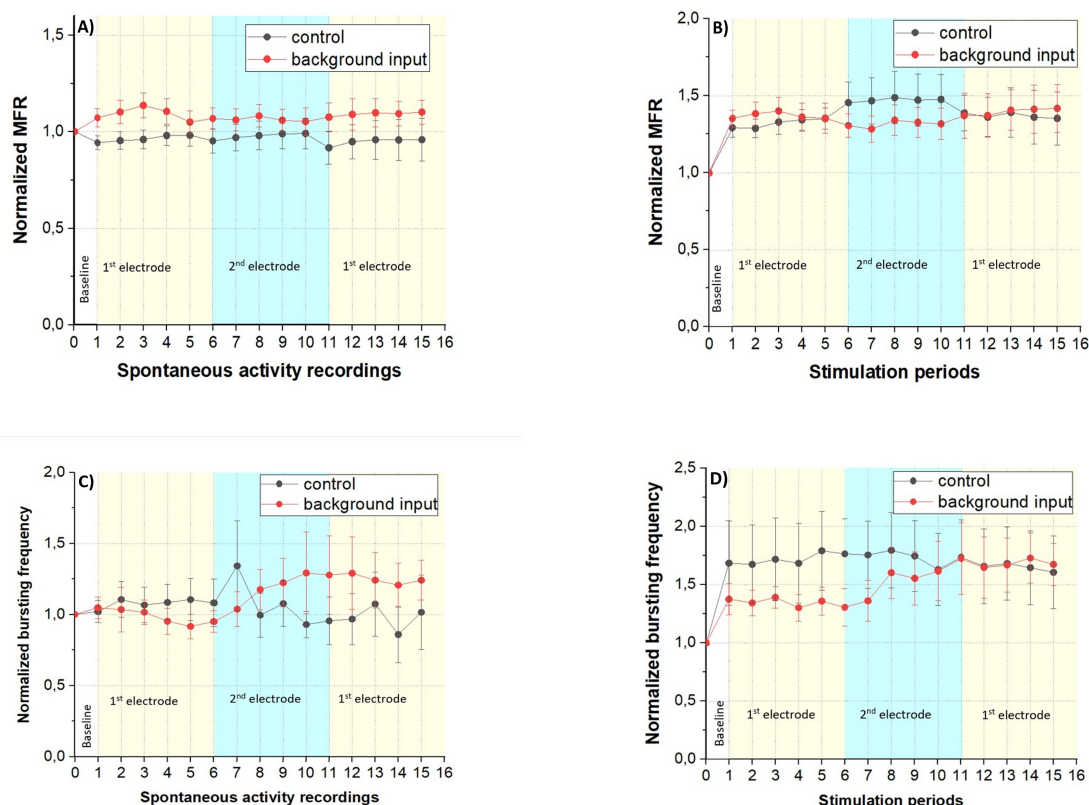


Figure 3.4 Background optogenetic stimulation at 5 Hz did not alter MFR (top graphs) or BF (bottom graphs) during spontaneous activity recordings and stimulation periods. A) Normalized MFR values of control (black line) and background input (red line) memory experiments during spontaneous activity recordings. MFR did not change significantly from baseline values in control experiments during the course of the experiment. Administration of background input failed to induce any after effects and MFR values were maintained around baseline. Comparison between the two set of experiments showed no significant difference. B) Normalized MFR values of control and background input memory experiments during stimulation periods. MFR in control and background input experiments did not change significantly from baseline values. Comparison between the two set of experiments showed no significant difference C) Normalized BF values of control and background input memory experiments during spontaneous activity recordings. BF did not alter significantly from baseline values neither in control nor background input memory experiments. The two set of experiments are statistically different in terms of distributions but not medians. D) Normalized BF of control and background input experiments during periods of stimulation. BF did not differ significantly from baseline values, in both control and background input memory experiments. Comparison between the two set of experiments showed no significant difference. All values were normalized to baseline values and error bars indicate SEM.

3.2.4 Effect of random, background optogenetic stimulation on memory trace formation and consolidation

Functional connectivity was assessed by conditional firing probability (CFP) analysis which was conducted only in periods of spontaneous activity. From this analysis con-

nectivity matrices were obtained containing the connection strength of each pair of active electrodes. Connectivity changes were computed by calculating the Euclidean distance (ED) between connectivity matrices. A significant change in connectivity followed by no further change compared to mean baseline connectivity ($ED_{baseline}$) indicates a memory trace formation. To assess the degree of changes in connectivity inferred by each stimulation electrode we computed the ED between connectivity matrices of the baseline recording and 1-hour spontaneous activity recordings (ED_0). Figure 3.5(A) shows the normalized ED_0 for control experiments while figure 3.5(B) illustrates the normalized ED_0 for background input experiments. In control experiments, stimulation with the 1st electrode exhibited an increase in normalized ED_0 but not in a significant degree compared to

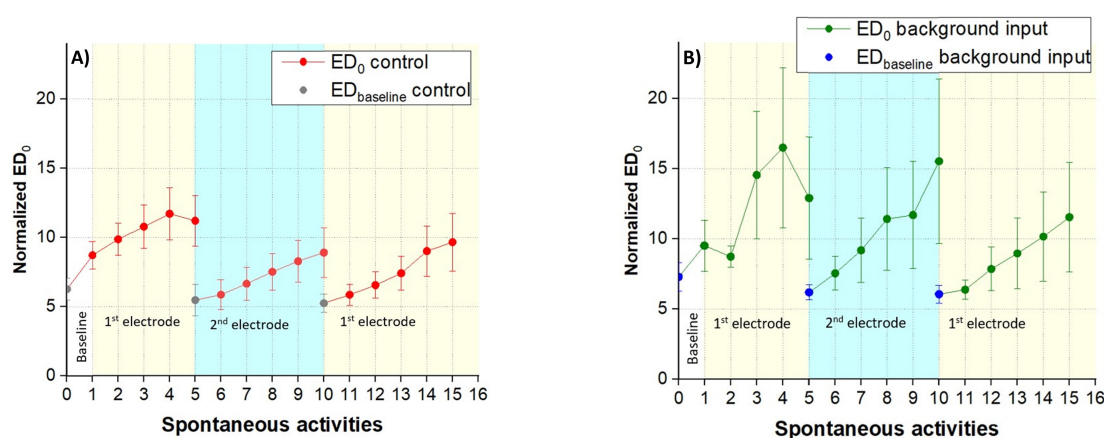


Figure 3.5 Normalized Euclidean distances between baseline and 1-hour spontaneous activities (ED_0) for control and background input experiments; white area corresponds to the 1st baseline recording prior to experimental protocol. A) Normalized ED_0 throughout the course of control experiments. Electrical stimulation did not infer significant connectivity changes. Stimulation with the 1st electrode (yellow area) and the 2nd electrode (blue area) did not reveal any memory trace formation, once connectivity changes were statistically insignificant (Wilcoxon signed-rank test with Holm Bonferroni correction). B) Normalized ED_0 throughout the course of background input experiments. Electrical stimulation combined with random, background optogenetic stimulation with mean frequency at 5 Hz did not show any significant connectivity changes. Stimulation with the 1st electrode (yellow area) and the 2nd electrode (blue area) did not reveal any memory trace formation, once connectivity changes were statistically insignificant; error bars indicate SEM.

$ED_{baseline}[0]$ (Kruskal-Wallis, $p > 0.072$). The first stimulation period yielded a larger connectivity change than subsequent stimulation periods. Switching to the 2nd stimulation electrode, again there was no significant connectivity changes compared to $ED_{baseline}[5]$ that could presume a memory trace formation (Kruskal-Wallis test, $p > 0.211$). In a similar way, stimulation with the 1st electrode for the second time did not induce any significant differences in connectivity compared with $ED_{baseline}[10]$ (Kruskal-

Wallis test, $p > 0.282$).

In background input experiments, a similar pattern is observed with the 1st stimulation electrode being incapable of forming a memory trace hence, inducing any significant connectivity changes (Kruskal-Wallis test, $p > 0.229$). Stimulation with the 2nd electrode again did not induce any significant changes in connectivity (Kruskal-Wallis test, $p > 0.115$). Switching back to the 1st stimulation electrode revealed insignificant connectivity changes (Kruskal-Wallis test, $p > 0.444$). Generally, the error bars in background input experiments are considerably larger than control experiments.

3.2.5 Effect of random, background optogenetic stimulation on network excitability

To unveil any possible effects arising from random, background optogenetic stimulation on network excitability we compared the calculated mean SPR strengths of control and background input experiments. Figure 3.6 illustrates the normalized SPR strengths as calculated in each 1-hour spontaneous activity recording for control and background input experiments. In control cultures, SPR values remained close to baseline over the entire course of the experiment and did not showed any significant difference from baseline values (Kruskal-Wallis test, $p > 0.98$). In cultures where optogenetic background input was administered, there is an upward trend in SPR values which is not significant from baseline (Friedman test, $p > 0.99$). In addition, comparison between SPR values of control and background input revealed no statistically significant differences (Mann-Whitney U test, $p > 0.151$).

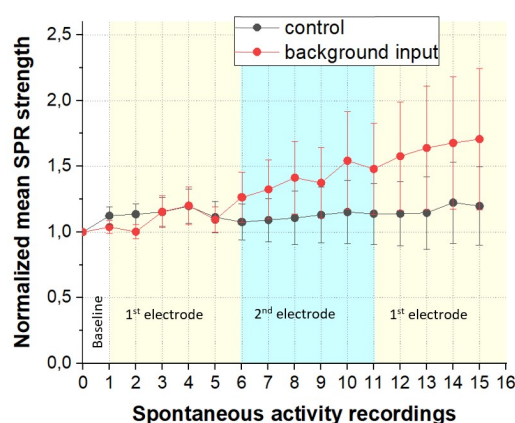


Figure 3.6 - Normalized mean SPR strengths throughout the duration of control and background input experiments. Control experiments (black line) showed no considerable differences from baseline values. Background input experiments exhibited also no significant differences. Comparison between the two sets of experiments displayed no significant differences between them.

Discussion

Developing cortical cultures have been used as a slow-wave-sleep (SWS) model due to their naturally occurring network bursts (Zhang et al., 2020). Over the past years, optogenetics had a vast contribution in unraveling the role of sleep in memory consolidation (Frazer et al., 2021). In this study we evaluated the effect of random background input through optogenetic stimulation on virally transduced network's expressing ChR2. We aimed to examine network activity, excitability along with the assessment of memory trace formation. For this cause we performed three sets of experiments; 1) optogenetic stimulation experiments in which the response in different stimulation frequencies (0.1-5 Hz) was tested; 2) control memory experiments where we evaluated if virally transduced cultures expressing ChR2 are capable of forming memory traces and consolidate them in response to electrical stimuli; 3) background input memory experiments in which we assessed the effect of random, background optogenetic input on memory formation and consolidation of electrical cues.

From these experiments the main findings were: 1) Amongst different stimulation frequencies (0.1-5 Hz), stimulation at 5 Hz did not significantly affect activity but reduced network excitability during stimulation periods. 2) Activity patterns did not alter in response to 5 Hz background optogenetic stimulation. 3) Network excitability during spontaneous activity recordings remain unchanged in response to background optogenetic input 4) In control and background input cultures, repeated electrical stimulation from both stimulation electrodes could not elicit significant connectivity changes, that would lead in memory trace formation.

4.1 Effect of different light stimulation frequencies on activity & excitability

It is critical to evaluate neuronal culture's response to different stimulation frequencies in order to understand how stimulation frequency affects activity patterns and network excitability. From these results we designed the optogenetic stimulation protocol for

background input memory experiments.

At low frequencies, MFR computed during light stimulation exhibited a marginally increasing trend but it was not significant compared to baseline values. The same behavior but with obvious changes is observed at BF values. While photoactivated with frequencies between 0.2 and 1 Hz cultures showed a significant enhancement in bursting rate (4-fold). These results were expected as wide-field stimulation provides concurrent activation of all ChR2-positive excitatory neurons and results in the synchronous induction of additional spikes (Zhang et al., 2020). This observation is in agreement with an in-vitro study on rat cortical neurons, that showed that bursting activity at 4 Hz is stimulus locked and the network can keep up and respond to each stimulus. However, at higher stimulation frequencies (16 and 46 Hz) a decrease in the number of spikes was detected probably due to neurotransmitter depletion at the synaptic level (Takahashi et al., 2012).

In addition, there are several studies which used tetanic electrical or optogenetic stimulation and were able to suppress synchronized network bursts (Dranijs et al., 2015; Mendez et al., 2018; Norimoto et al., 2018; Wagenaar et al., 2005b; Zhang et al., 2020). Interestingly, neither MFR nor BF were significantly higher than baseline when stimulated at 5 Hz. We suggest that this “peak” at 1 Hz in BF might indicate the limit where higher stimulation frequencies lead to depression of BF. This evidence could be more concrete if we could stimulate at higher rates and monitor if depression would further persist. In our study, a clear stimulus response was evident when stimulating with at least 100ms-long pulses which set the minimum of the inter-stimulus intervals (ISIs) distribution to 100 ms. Furthermore, ISIs were randomly chosen so the distribution needed to be sufficiently large. Thus, we were restrained to use 5 Hz as the maximal stimulation frequency.

It is still debatable whether optogenetic stimulation can induce changes in network activity that persist post-stimulation. El Hady et al. followed a very similar stimulation protocol with ours and showed that low-frequency light pulses (1 Hz) administered to hippocampal cultures induced enhanced post – stimulation firing rate and occurrence of network bursts (El Hady et al., 2013). These results could not be confirmed in cortical cultures as changes in MFR and BF also during spontaneous activity recordings right after stimulation period, were not significant for both parameters. Apparently, even the maximum frequency utilized (5Hz) was not sufficient to induce detectable after-effects in cortical cultures, possibly due to differences in cellular or synaptic properties of hippocampal and cortical neurons.

In general, network excitability can be defined as the ease of inducing a network response when a stimulus is applied (Le Feber et al., 2014). Thus, we examined the mean network response to stimulation for each stimulation frequency (Fig 2A). The efficacy of optogenetic stimulation considerably dropped with increasing stimulation frequency. We observed a reduction of 60% at maximum frequency which is indicative of

reduced network excitability. This is consistent with two studies that used tetanic light stimulation in neuronal cultures to show that the number of spikes detected dropped markedly as stimulation frequency increased, resulting in a 80% and 60% decline at maximum frequency of 100 and 10 Hz, respectively (Lignani et al., 2013; Wong Fong Sang et al., 2021). Decreased efficacy of stimulation may be caused by short-term depression mechanisms due to depletion of the ready-pool neurotransmitter vesicles at synapses, as suggested by Takahashi et al. (Takahashi et al., 2012). Possible after effects on network excitability were assessed during spontaneous activity recordings through SPR strengths. Excitability in these periods tended to decrease after periods with higher stimulation frequency, but differences were not significant. In contrast, a recent in-vivo study in rats hippocampus revealed that light stimulation with 10 Hz reduced evidently synaptic excitability 24 hour post-stimulation (Mendez et al., 2018). A possible explanation to this difference might lie in the small sample size (n=4) for stimulation at 5 Hz, which may have failed to reveal significant differences. Another reason might be that the range of stimulation frequencies is short and higher stimulation frequencies may be able to unveil such a phenomenon.

In a number of in-vitro and in-vivo studies high-frequency light stimulation was applied in order to assess synaptic plasticity alterations (Lignani et al., 2013; Moulin et al., 2019), learning (Zhang et al., 2020) and memory (Mendez et al., 2018; Norimoto et al., 2018; Takahashi et al., 2012) in neuronal networks. Indeed, tetanic optogenetic stimulation seems to depress excitability (Mendez et al., 2018; Moulin et al., 2019), and reduce network bursts (Dranijs et al., 2015; Norimoto et al., 2018; Zhang et al., 2020). Although network excitability during spontaneous activity recordings seemed to be unaffected, during stimulation periods excitability depressed with increasing frequency. Thus, we concluded that 5 Hz optogenetic stimulation had the most robust effect on network excitability during stimulation periods. Hence, we applied stimulation pulses at 5 Hz mean frequency for the *background input memory experiments*.

4.2 Background optogenetic input at 5 Hz did not alter activity patterns

Activity levels in control and background input cultures showed no noticeable changes neither during spontaneous activity recordings nor stimulation periods. Activity of the network was monitored by calculating the mean firing rate (MFR) and bursting frequency (BF) of the cultures.

During periods of electrical stimulation control cultures displayed elevated values of MFR and BF but not significantly different from baseline values. Interestingly, simultaneous electrical and optogenetic stimulation (background input) exhibited similar values of MFR and BF compared to control suggesting that 5 Hz light pulses did not

contribute considerably in modifying activity patterns. This is in line with *optogenetic stimulation experiments* in which stimulation with 5 Hz pulses alone did not induce changes in MFR (Fig 3.1A) and BF (Fig 3.1B) compared to baseline. A study in which optical and electrical stimulation were coupled and applied in auditory neurons, revealed a 3-fold increase in MFR which comes in contrast to our findings (Hart et al., 2020). However, in our experiments optical stimulation served more as a background activation rather than time-locked stimuli to electrical pulses which might explain such differences.

In spontaneous activity periods, we observed no significant after-effects in MFR and BF for both control and background input cultures. A study done by Vajda et al. (Vajda et al., 2008) contradicts our results as they managed to induce stereotypical transition in activity of cortical networks with low-frequency (0.2 Hz) electrical pulses. They interpret the observed activity changes as a result of transitions between attractor states caused by slow electrical stimuli. A reason that such a phenomenon is not evident in our experiments might be the viral transduction which possibly lowered network excitability and electrical stimuli could not drive the network to a different activity state (Suriano et al., 2021). In background input cultures in which light pulses were also introduced we observed similar values as in control cultures. This is in accordance with *optogenetic stimulation experiments* in which, illumination with 5 Hz pulses demonstrated no significant after-effects in MFR and BF during spontaneous activity recordings.

4.3 Network excitability during spontaneous activity recordings remain unchanged in response to background input

Administration of 5 Hz background optogenetic input did not alter network excitability as measured by mean single pulse response (SPR) strengths during spontaneous activity recordings. These findings were somewhat expected as in *optogenetic stimulation experiments* activation with 5 Hz light pulses alone did not reveal any effect on network excitability. However, we observed a slight increase of SPR strengths in background input cultures after stimulation with the 2nd electrode (6-15 hours) but the change was not significant. Similarly, control cultures exhibited mean SPR strength values around the baseline with no significant changes throughout the duration of the experiment. In a recent in-vitro study on hippocampal neurons it was shown that 10 Hz optogenetic stimulation decreased excitatory and increased inhibitory synaptic currents, suggesting a reduction in neuronal excitability (Mendez et al., 2018). This was

not evident in our experiments as we were restrained to a maximal frequency of 5 Hz.

4.4 Repeated electrical stimulation could not elicit memory trace formation in virally transfected cultures expressing ChR2.

Low frequency electrical stimulation was not able to induce significant connectivity changes as calculated from Euclidean distances in cultures expressing ChR2 through viral transduction. It is suggested that cultured networks in the absence of external input can maintain an activity-connectivity balance (Le Feber et al., 2014). In the presence of a sufficiently strong external stimuli this balance can be disrupted and drive the network to a new activity-connectivity equilibrium. Thus, an observable change in connectivity may reflect such a transition to a new balance and the adapted activity patterns can indicate the formation of a memory trace in response to the external stimuli (le Feber et al., 2015). Previous studies have demonstrated that electrical stimulation of cortical networks can lead to memory trace formation (Dias et al., 2021; le Feber et al., 2015). In our experiments, although we applied the same stimulation protocol, control cultures did not exhibit any significant connectivity changes in response to electrical cues from both stimulation electrodes. A possible explanation could be due to the fact that our control cultures were transduced with an AAV vector to achieve ChR2 expression. A recent study showed that AAV-mediated gene delivery strikingly disrupted synaptic transmission and reduced dendritic complexity in the adult rodent cortex (Suriano et al., 2021). This suggests that AAV transduction of cortical networks potentially lowered network excitability so that electrical stimulation could not elicit significant connectivity changes. There is a growing body of evidence that reduced network excitability is associated with poor consolidation of memories and memory performance (Dias et al., 2021; Frazer et al., 2021; Yiu et al., 2014). A study done by Dias et al. (Dias et al., 2021) showed that repeated electrical stimulation could not induce memory trace formation in response to high cholinergic input probably due to decreased network excitability. Another study demonstrated that memory allocation is a 'competition' between neurons in which higher excitable neurons are involved in memory formation (Yiu et al., 2014). Thus, we suggest that AAV-mediated gene delivery reduced network excitability and hampered memory trace formation. Although connectivity changes were not significantly different, patterns of ED were quite similar with the study done by (Dias et al., 2021). Particularly, ED_0 followed the same trend (Fig 3.5) the first stimulation period elicited a larger connectivity change compared to subsequent stimulation periods on that electrode.

For cultures in which 5 Hz background optogenetic stimulation was administered we

observed the same pattern. Repeated electrical stimulation from both electrodes could not elicit any significant connectivity changes that could lead in memory trace formation. Again, this may be attributed to AAV transduction which might have lowered the excitability of the network. Indeed, as illustrated in Figure 3.5, in cultures where background input was administered no significant effect on network excitability was evident. Therefore, we assume that network excitability is still on a low level due to viral transduction and electrical stimulation could not induce significant changes in connectivity even when background input was administered. Additionally, error bars in *background input memory* were remarkably larger than *control memory experiments* impeding even more the detection of a significant connectivity change. Nevertheless, we cannot be certain about the causal factors of this phenomenon once network excitability as calculated by SPR analysis did not differ significantly from control cultures although the same increase in error bars is evident.

4.5 Efficacy of electrical stimulation

Efficacy of electrical stimulation was quantified through the area under the curve (AUC) of the mean post-stimulus time histogram (PSTH). In both control and background input cultures, the calculated AUC was quite balanced suggesting that all cultures were responsive to electrical stimulation for the entire experiment. This excludes the possibility that the insignificant connectivity changes observed were due to ineffective electrical stimulation. Moreover, the similarity between AUCs of PSTH curves of control and background input memory experiments indicates that optogenetic background input did not hamper or enhance substantially effectiveness of electrical stimulation . Unfortunately, we could not construct a corresponding metric to quantify effectiveness of optogenetic stimulation once the period of analysis was overlapping with subsequent light pulses.

Conclusions

Overall, we studied the effect of random, background optogenetic stimulation on memory formation and consolidation in rat cortical cultures. By testing different light stimulation frequencies we found that light stimulation at 5 Hz had the most prominent effect on network excitability during direct photoactivation although activity patterns did not change. Thus, we decided to use this value as stimulation frequency for *background input memory experiments*.

In control cultures memory trace formation was not possible. We hypothesize that due to reduced network excitability inferred by viral transduction, repeated electrical stimulation could not induce significant connectivity changes that could lead in memory trace formation. These findings support that memory consolidation possibly requires higher states of network excitability. During background light pulses at 5 Hz memory trace formation was also not possible but network excitability during spontaneous activity recordings remained unchanged compared to control. This comes in contrast with our initial hypothesis (stated in section 1.6) in which background input would hamper memory trace formation due to reduced network excitability. Nevertheless, we cannot be certain about the effects of background input once memory trace formation was not possible also in control cultures.

Study limitations and future perspectives

In our study we were limited to use 5 Hz as the maximal frequency for optogenetic random, background stimulation. At first, we would like to have a large enough distribution from where inter-stimulus intervals (ISIs) were chosen in order not to lose 'randomness'. Secondly, in the majority of the cultures we observed a clear stimulus response during probing at 100 ms pulse width which restricted the minimum of the ISIs distribution to be at 5 Hz.

In memory experiments we used in total 27 cultures (18 control, 9 background input) from which 11 of them were excluded post-analysis once they did not respond to electrical stimulation throughout the entire duration of the experiment. Thus, we based our study on 16 cultures only (8 control, 8 background input) which is quite a small number considering the initial sample size. However, higher sample sizes were not possible due to time restrictions.

Additionally, in *background input memory experiments* we were restrained to use a commercialized culture medium compared to a custom-made from our lab which was used in all other experiments. The two mediums contained the same substances however, we cannot be sure that concentrations in our custom-made culture medium were the same once concentrations of the commercialized are not publicly available. As stated in section 1.3 pH or medium composition can affect the amplitude of photocurrents. Although we did not observe significant differences in the network properties of the cultures that contained different mediums, considerably less cultures were excluded in *background input memory experiments*. This may be attributed to the difference of the two culture media.

Interestingly, in our study we could not reveal the effect of background input optogenetic stimulation since we were unable to induce memory trace formation in control cultures. A possible explanation is that viral transduction probably reduced network excitability. This is a hypothesis based on a study where AAV-mediated gene delivery disrupted synaptic transmission and reduced dendritic complexity ([Suriano et al.](#),

2021). However, this study did not examine specifically what happens in network excitability. In the future, we could design a study to evaluate more thoroughly the effect of AAV transduction on network properties. According to these findings we could adapt the stimulation protocols for both electrical and light stimulation. A possibility would be to stimulate electrically with pulse trains and test higher stimulation frequencies for light stimulation. With these studies, we could unveil any correlation between excitability state of the network and memory trace formation.

Bibliography

URL https://commons.wikimedia.org/wiki/File:Action_potential.svg.

Nikolai Axmacher, Florian Mormann, Guillen Fernández, Christian E Elger, and Juer-gen Fell. Memory formation by neuronal synchronization. *Brain research reviews*, 52(1):170–182, 2006.

Thomas Baltz and Thomas Voigt. Interaction of electrically evoked activity with intrinsic dynamics of cultured cortical networks with and without functional fast gabaergic synaptic transmission. *Frontiers in cellular neuroscience*, 9:272, 2015.

Mireille Bélanger and Pierre J Magistretti. The role of astroglia in neuroprotection. *Dialogues in clinical neuroscience*, 2022.

Christopher Bertucci, Ryan Koppes, Courtney Dumont, and Abigail Koppes. Neural responses to electrical stimulation in 2d and 3d in vitro environments. *Brain Research Bulletin*, 152:265–284, 2019.

J Gordon Betts, Kelly A Young, James A Wise, Eddie Johnson, Brandon Poe, Dean H Kruse, Oksana Korol, Jody E Johnson, Mark Womble, and Peter DeSaix. *Anatomy and physiology*. 2013.

Guo-qiang Bi and Mu-ming Poo. Synaptic modifications in cultured hippocampal neurons: dependence on spike timing, synaptic strength, and postsynaptic cell type. *Journal of neuroscience*, 18(24):10464–10472, 1998.

Mohammad Zaki Bin Ibrahim, Amrita Benoy, and Sreedharan Sajikumar. Long-term plasticity in the hippocampus: maintaining within and ‘tagging’between synapses. *The FEBS Journal*, 289(8):2176–2201, 2022.

B Blausen. Neuron - wikipedia, 2022. URL <https://en.wikipedia.org/wiki/Neuron>.

Tim VP Bliss and Terje Lømo. Long-lasting potentiation of synaptic transmission in the dentate area of the anaesthetized rabbit following stimulation of the perforant path. *The Journal of physiology*, 232(2):331–356, 1973.

- Luca Leonardo Bologna, Valentina Pasquale, Matteo Garofalo, Mauro Gandolfo, Pieter Laurens Baljon, Alessandro Maccione, Sergio Martinoia, and Michela Chiappalone. Investigating neuronal activity by spycode multi-channel data analyzer. *Neural Networks*, 23(6):685–697, 2010.
- Edward S Boyden, Feng Zhang, Ernst Bamberg, Georg Nagel, and Karl Deisseroth. Millisecond-timescale, genetically targeted optical control of neural activity. *Nature neuroscience*, 8(9):1263–1268, 2005.
- David Cabrera-Garcia, Davide Warm, Pablo de la Fuente, M Teresa Fernández-Sánchez, Antonello Novelli, and Joaquín M Villanueva-Balsera. Early prediction of developing spontaneous activity in cultured neuronal networks. *Scientific reports*, 11(1):1–13, 2021.
- Ami Citri and Robert C Malenka. Synaptic plasticity: multiple forms, functions, and mechanisms. *Neuropsychopharmacology*, 33(1):18–41, 2008.
- Michael A Corner, Jaap van Pelt, PS Wolters, RE Baker, and RH Nuytinck. Physiological effects of sustained blockade of excitatory synaptic transmission on spontaneously active developing neuronal networks—an inquiry into the reciprocal linkage between intrinsic biorhythms and neuroplasticity in early ontogeny. *Neuroscience & Biobehavioral Reviews*, 26(2):127–185, 2002.
- Inês Dias, Marloes R Levers, Martina Lamberti, Gerco C Hassink, Richard Van Wezel, and Joost Le Feber. Consolidation of memory traces in cultured cortical networks requires low cholinergic tone, synchronized activity and high network excitability. *Journal of neural engineering*, 18(4):046051, 2021.
- Lynn E Dobrunz and Charles F Stevens. Heterogeneity of release probability, facilitation, and depletion at central synapses. *Neuron*, 18(6):995–1008, 1997.
- Mark R Dranias, M Brandon Westover, Sidney Cash, and Antonius MJ VanDongen. Stimulus information stored in lasting active and hidden network states is destroyed by network bursts. *Frontiers in Integrative Neuroscience*, 9:14, 2015.
- Mattia D’Andola, Massimiliano Giullioni, Vittorio Dante, Paolo Del Giudice, and Maria V Sanchez-Vives. Control of cortical oscillatory frequency by a closed-loop system. *Journal of NeuroEngineering and Rehabilitation*, 16(1):1–14, 2019.
- Ahmed El Hady, Ghazaleh Afshar, Kai Bröking, Oliver M Schlüter, Theo Geisel, Walter Stühmer, and Fred Wolf. Optogenetic stimulation effectively enhances intrinsically generated network synchrony. *Frontiers in neural circuits*, 7:167, 2013.

- Michelle A Frazer, Yesenia Cabrera, Rockelle S Guthrie, and Gina R Poe. Shining a light on the mechanisms of sleep for memory consolidation. *Current Sleep Medicine Reports*, pages 1–11, 2021.
- F Fröhlich. Chapter 11—optical measurements and perturbations. *Network Neuroscience*, pages 145–159, 2016a.
- F Fröhlich. Synaptic plasticity. *Network Neuroscience*, pages 47–58, 2016b.
- S Gais, B Scharf, U Wagner, and J Born. Low acetylcholine during slow-wave sleep is critical for memory consolidation. In *JOURNAL OF PSYCHOPHYSIOLOGY*, volume 17, pages 148–148. HOGREFE & HUBER PUBLISHERS ROHNSWEG 25, D-37085 GOTTINGEN, GERMANY, 2003.
- Asaf Gal, Danny Eytan, Avner Wallach, Maya Sandler, Jackie Schiller, and Shimon Marom. Dynamics of excitability over extended timescales in cultured cortical neurons. *Journal of Neuroscience*, 30(48):16332–16342, 2010.
- William L Hart, Rachael T Richardson, Tatiana Kameneva, Alex C Thompson, Andrew K Wise, James B Fallon, Paul R Stoddart, and Karina Needham. Combined optogenetic and electrical stimulation of auditory neurons increases effective stimulation frequency—an in vitro study. *Journal of Neural Engineering*, 17(1):016069, 2020.
- B Katz. Miledi r. *The role of calcium in neuromuscular facilitation*. *J Physiol*, 195: 481–492, 1968.
- Antranik Kizirian. Synaptic transmission by somatic motoneurons, 2022. URL <https://antranik.org/synaptic-transmission-by-somatic-motoneurons/>.
- Sophie Kussauer, Robert David, and Heiko Lemcke. ipscs derived cardiac cells for drug and toxicity screening and disease modeling: what micro-electrode-array analyses can tell us. *Cells*, 8(11):1331, 2019.
- Martina Lamberti, Michael Hess, Inês Dias, Michel van Putten, Joost le Feber, and Sarah Marzen. Maximum entropy models provide functional connectivity estimates in neural networks. *Scientific Reports*, 12(1):1–10, 2022.
- Jakob le Feber, WLC Rutten, J Stegenga, PS Wolters, GJA Ramakers, and J Van Pelt. Conditional firing probabilities in cultured neuronal networks: a stable underlying structure in widely varying spontaneous activity patterns. *Journal of neural engineering*, 4(2):54, 2007.
- Joost Le Feber, Jan Stegenga, and Wim LC Rutten. The effect of slow electrical stimuli to achieve learning in cultured networks of rat cortical neurons. *PloS one*, 5(1):e8871, 2010.

- Joost Le Feber, Irina I Stoyanova, and Michela Chiappalone. Connectivity, excitability and activity patterns in neuronal networks. *Physical biology*, 11(3):036005, 2014.
- Joost le Feber, Tim Witteveen, Tamar M van Veenendaal, and Jelle Dijkstra. Repeated stimulation of cultured networks of rat cortical neurons induces parallel memory traces. *Learning & memory*, 22(12):594–603, 2015.
- Joost le Feber, Stelina Tzafi Pavlidou, Niels Erkamp, Michel JAM van Putten, and Jeannette Hofmeijer. Progression of neuronal damage in an in vitro model of the ischemic penumbra. *PLoS One*, 11(2):e0147231, 2016.
- Joost Le Feber, Anneloes Dummer, Gerco C Hassink, Michel JAM Van Putten, and Jeannette Hofmeijer. Evolution of excitation–inhibition ratio in cortical cultures exposed to hypoxia. *Frontiers in cellular neuroscience*, 12:183, 2018.
- Gabriele Lignani, Enrico Ferrea, Francesco Difato, Jessica Amarù, Eleonora Ferroni, Eleonora Lugarà, Stefano Espinoza, Raul R Gainetdinov, Pietro Baldelli, and Fabio Benfenati. Long-term optical stimulation of channelrhodopsin-expressing neurons to study network plasticity. *Frontiers in molecular neuroscience*, 6:22, 2013.
- Gabriele Lignani, Pietro Baldelli, and Vincenzo Marra. Homeostatic plasticity in epilepsy. *Frontiers in Cellular Neuroscience*, page 197, 2020.
- Pedro Mateos-Aparicio and Antonio Rodríguez-Moreno. The impact of studying brain plasticity. *Frontiers in cellular neuroscience*, 13:66, 2019.
- Pablo Mendez, Thomas Stefanelli, Carmen E Flores, Dominique Muller, and Christian Lüscher. Homeostatic plasticity in the hippocampus facilitates memory extinction. *Cell reports*, 22(6):1451–1461, 2018.
- Thiago C Moulin, Lyvia L Petiz, Danielle Rayêe, Jessica Winne, Roberto G Maia, Rafael V Lima da Cruz, Olavo B Amaral, and Richardson N Leão. Chronic in vivo optogenetic stimulation modulates neuronal excitability, spine morphology, and hebbian plasticity in the mouse hippocampus. *Hippocampus*, 29(8):755–761, 2019.
- Lynn Nadel, A Hupbach, R Gomez, and K Newman-Smith. Memory formation, consolidation and transformation. *Neuroscience & Biobehavioral Reviews*, 36(7):1640–1645, 2012.
- Georg Nagel, Martin Brauner, Jana F Liewald, Nona Adeishvili, Ernst Bamberg, and Alexander Gottschalk. Light activation of channelrhodopsin-2 in excitable cells of *Caenorhabditis elegans* triggers rapid behavioral responses. *Current Biology*, 15(24):2279–2284, 2005.

- Hiroaki Norimoto, Kenichi Makino, Mengxuan Gao, Yu Shikano, Kazuki Okamoto, Tomoe Ishikawa, Takuya Sasaki, Hiroyuki Hioki, Shigeyoshi Fujisawa, and Yuji Ikegaya. Hippocampal ripples down-regulate synapses. *Science*, 359(6383):1524–1527, 2018.
- Thoralf Opitz, Ana D De Lima, and Thomas Voigt. Spontaneous development of synchronous oscillatory activity during maturation of cortical networks in vitro. *Journal of neurophysiology*, 88(5):2196–2206, 2002.
- Clara Ortega-de San Luis and Tomás J Ryan. Understanding the physical basis of memory: Molecular mechanisms of the engram. *Journal of Biological Chemistry*, 298(5), 2022.
- Valentina Pasquale, Sergio Martinoia, and Michela Chiappalone. Stimulation triggers endogenous activity patterns in cultured cortical networks. *Scientific reports*, 7(1): 1–16, 2017.
- Anssi Pelkonen, Cristiana Pistono, Pamela Klecki, Mireia Gómez-Budia, Antonios Dougalis, Henna Konttinen, Iveta Stanová, Ilkka Fagerlund, Ville Leinonen, Paula Korhonen, et al. Functional characterization of human pluripotent stem cell-derived models of the brain with microelectrode arrays. *Cells*, 11(1):106, 2021.
- Gertrudis Perea, Marta Navarrete, and Alfonso Araque. Tripartite synapses: astrocytes process and control synaptic information. *Trends in neurosciences*, 32(8):421–431, 2009.
- Dale Purves and S. Mark Williams. *Neuroscience*. Sinauer Associates, 2001.
- JoM Ritchie and RB Rogart. Density of sodium channels in mammalian myelinated nerve fibers and nature of the axonal membrane under the myelin sheath. *Proceedings of the National Academy of Sciences*, 74(1):211–215, 1977.
- HJ Romijn, F Van Huizen, and PS Wolters. Towards an improved serum-free, chemically defined medium for long-term culturing of cerebral cortex tissue. *Neuroscience & Biobehavioral Reviews*, 8(3):301–334, 1984.
- Sohrab Saberi-Moghadam, Alessandro Simi, Hesam Setareh, Cyril Mikhail, and Mehdi Tafti. In vitro cortical network firing is homeostatically regulated: a model for sleep regulation. *Scientific reports*, 8(1):1–14, 2018.
- Takuya Sasaki, Norio Matsuki, and Yuji Ikegaya. Action-potential modulation during axonal conduction. *Science*, 331(6017):599–601, 2011.
- Philipp Schoenenberger, Yan-Ping Zhang Schärer, and Thomas G Oertner. Channel-rhodopsin as a tool to investigate synaptic transmission and plasticity. *Experimental physiology*, 96(1):34–39, 2011.

- Chumin Sun, KC Lin, Yu-Ting Huang, Emily SC Ching, Pik-Yin Lai, and CK Chan. Directed effective connectivity and synaptic weights of in vitro neuronal cultures revealed from high-density multielectrode array recordings. *bioRxiv*, 2020.
- Christos M Suriano, Jessica L Verpeut, Neerav Kumar, Jie Ma, Caroline Jung, and Lisa M Boulanger. Adeno-associated virus (aav) reduces cortical dendritic complexity in a tlr9-dependent manner. *BioRxiv*, 2021.
- Hirokazu Takahashi, Takeshi Sakurai, Hideo Sakai, Douglas J Bakkum, Jun Suzurikawa, and Ryohei Kanzaki. Light-addressed single-neuron stimulation in dissociated neuronal cultures with sparse expression of chr2. *Biosystems*, 107(2): 106–112, 2012.
- Huihui Tian, Ke Xu, Liang Zou, and Ying Fang. Multimodal neural probes for combined optogenetics and electrophysiology. *Isience*, page 103612, 2021.
- Elisenda Tibau and Jordi Soriano. Analysis of spontaneous activity in neuronal cultures through recurrence plots: Impact of varying connectivity. *The European Physical Journal Special Topics*, 227(10):999–1014, 2018.
- Nai-Wen Tien and Daniel Kerschensteiner. Homeostatic plasticity in neural development. *Neural development*, 13(1):1–7, 2018.
- Ildikó Vajda, Jaap Van Pelt, Pieter Wolters, Michela Chiappalone, Sergio Martinoia, Eus Van Someren, and Arjen Van Ooyen. Low-frequency stimulation induces stable transitions in stereotypical activity in cortical networks. *Biophysical journal*, 94(12): 5028–5039, 2008.
- Inkeri A Välkki, Kerstin Lenk, Jarno E Mikkonen, Fikret E Kapucu, and Jari AK Hyttinen. Network-wide adaptive burst detection depicts neuronal activity with improved accuracy. *Frontiers in Computational Neuroscience*, 11:40, 2017.
- J Van Pelt, MA Corner, PS Wolters, WLC Rutten, and GJA Ramakers. Longterm stability and developmental changes in spontaneous network burst firing patterns in dissociated rat cerebral cortex cell cultures on multielectrode arrays. *Neuroscience letters*, 361(1-3):86–89, 2004.
- MJAM van Putten. *Dynamics of Neural Networks*. Springer, 2020.
- Daniel Wagenaar, Thomas B DeMarse, and Steve M Potter. Meabench: A toolset for multi-electrode data acquisition and on-line analysis. In *Conference Proceedings. 2nd International IEEE EMBS Conference on Neural Engineering, 2005.*, pages 518–521. IEEE, 2005a.

- Daniel A Wagenaar, Radhika Madhavan, Jerome Pine, and Steve M Potter. Controlling bursting in cortical cultures with closed-loop multi-electrode stimulation. *Journal of Neuroscience*, 25(3):680–688, 2005b.
- Jennifer Walinga and Charles Stangor. Introduction to psychology-1st canadian edition. 2014.
- Szu-Han Wang, Richard GM Morris, et al. Hippocampal-neocortical interactions in memory formation, consolidation, and reconsolidation. *Annual review of psychology*, 61(1):49–79, 2010.
- Oliver Weihberger, Samora Okujeni, Jarno E Mikkonen, and Ulrich Egert. Quantitative examination of stimulus-response relations in cortical networks in vitro. *Journal of neurophysiology*, 109(7):1764–1774, 2013.
- I Emeline Wong Fong Sang, Jonas Schroer, Lisa Halbhuber, Davide Warm, Jenq-Wei Yang, Heiko J Luhmann, Werner Kilb, and Anne Sinning. Optogenetically controlled activity pattern determines survival rate of developing neocortical neurons. *International Journal of Molecular Sciences*, 22(12):6575, 2021.
- Alan Woodruff. What is a neuron?, 2022. URL <https://qbi.uq.edu.au/brain/brain-anatomy/what-neuron>.
- Adelaide P Yiu, Valentina Mercaldo, Chen Yan, Blake Richards, Asim J Rashid, Hwa-Lin Liz Hsiang, Jessica Pressey, Vivek Mahadevan, Matthew M Tran, Steven A Kushner, et al. Neurons are recruited to a memory trace based on relative neuronal excitability immediately before training. *Neuron*, 83(3):722–735, 2014.
- Fleur Zeldenrust, Wytse J Wadman, and Bernhard Englitz. Neural coding with bursts—current state and future perspectives. *Frontiers in computational neuroscience*, 12:48, 2018.
- Xiaoyu Zhang, Fang-Chin Yeh, Han Ju, Yuheng Jiang, Gabriel Foo Wei Quan, and Antonius MJ VanDongen. Familiarity detection and memory consolidation in cortical assemblies. *Eneuro*, 7(3), 2020.
- Robert S Zucker, Wade G Regehr, et al. Short-term synaptic plasticity. *Annual review of physiology*, 64(1):355–405, 2002.

Appendix A

Overview of experiments

This section includes the main findings of each experiment conducted in *optogenetic stimulation experiments, control memory experiments and background input memory experiments*. In the beginning of each section there is a table which summarizes the properties of the culture (MEA number, days in-vitro (DIV)), the stimulation settings (light pulse width, % of maximal light intensity, electrical pulse amplitude) and if the culture met the exclusion criteria stated in section 2.3. If a culture met at least one exclusion then it was withdrawn from the analysis and the corresponding cell is coloured in red.

Next, detailed information for each individual experiment is given by graphical representation of the main readouts.

A.1 Optogenetic stimulation experiments

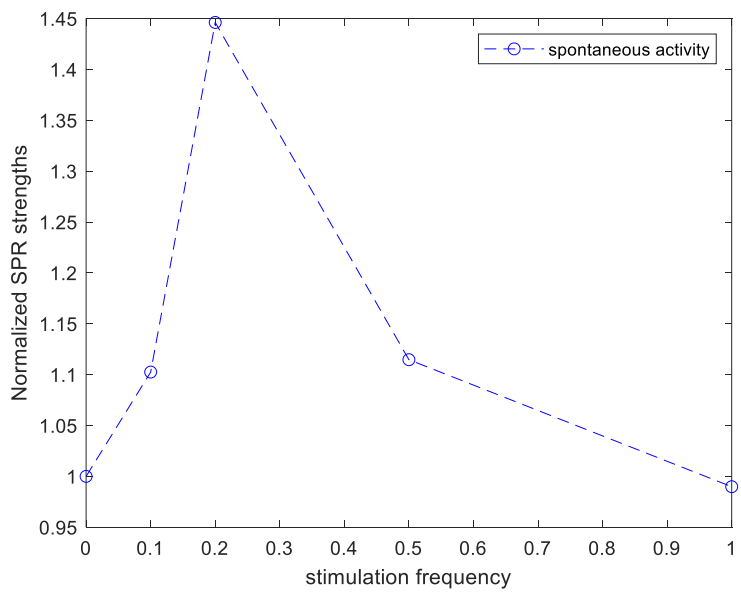
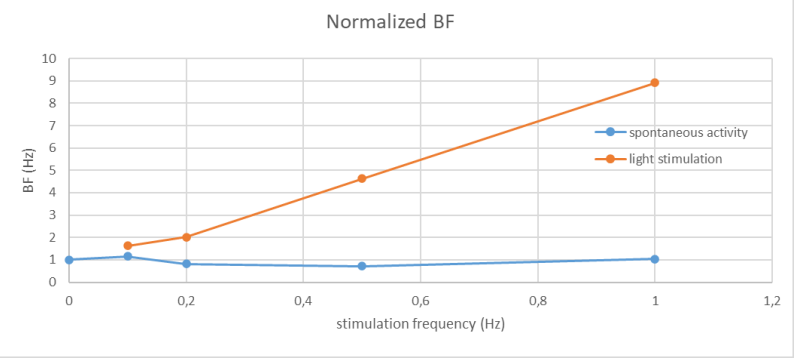
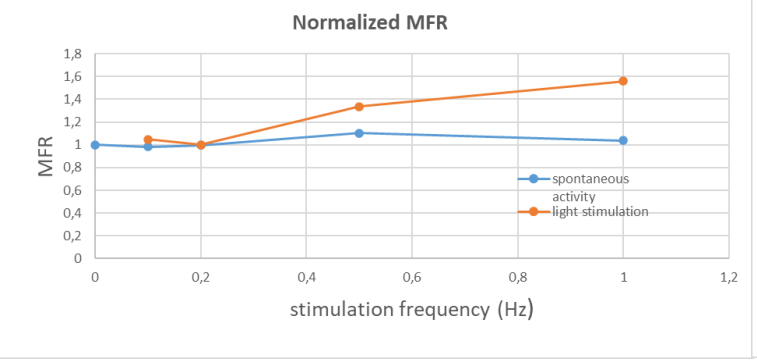
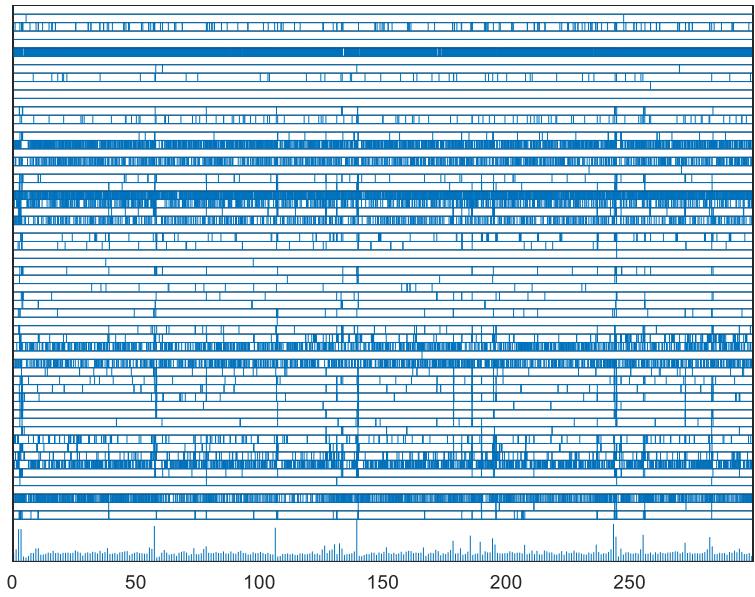
In each of these experiments we illustrate:

- A raster plot
- The normalized MFR and BF plotted during stimulation periods and during spontaneous activity recordings.
- A normalized graph of SPR strengths which serve as an estimate of network excitability during spontaneous activity recordings.
- Finally, whenever was possible an average network response graph which estimates network excitability during stimulation periods

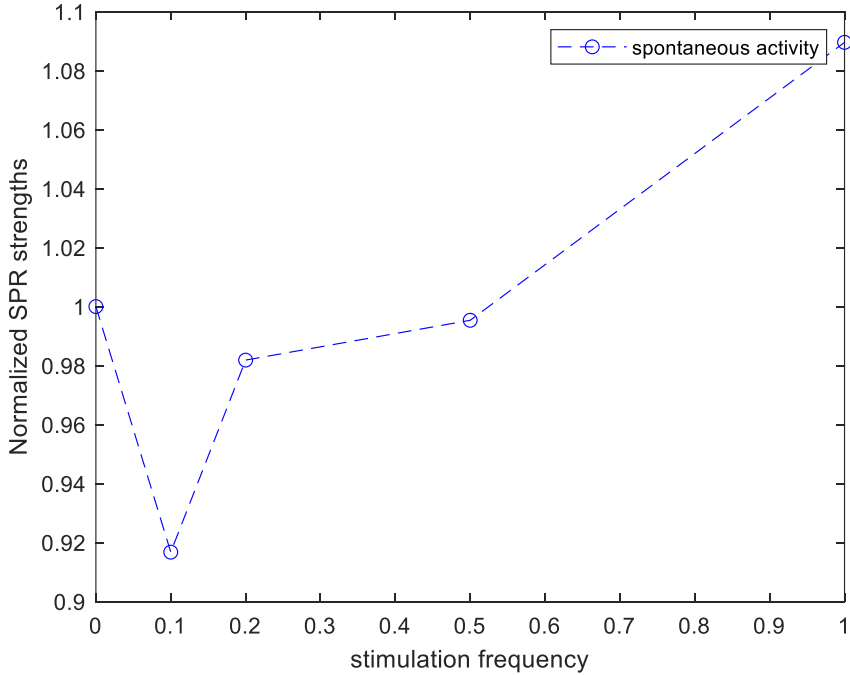
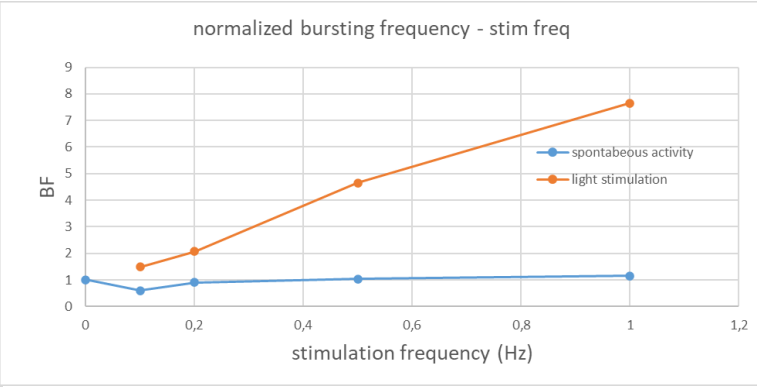
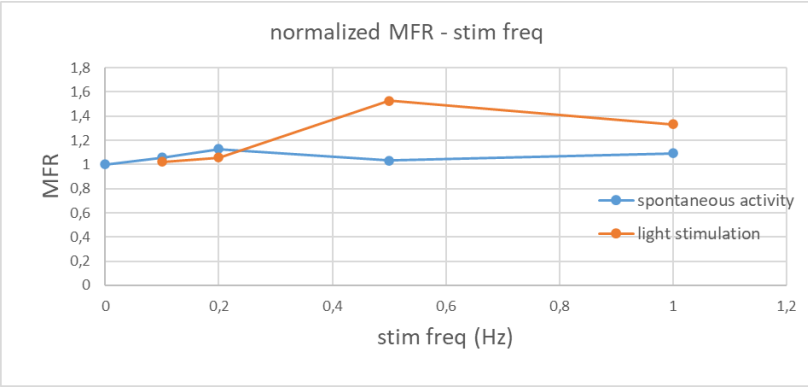
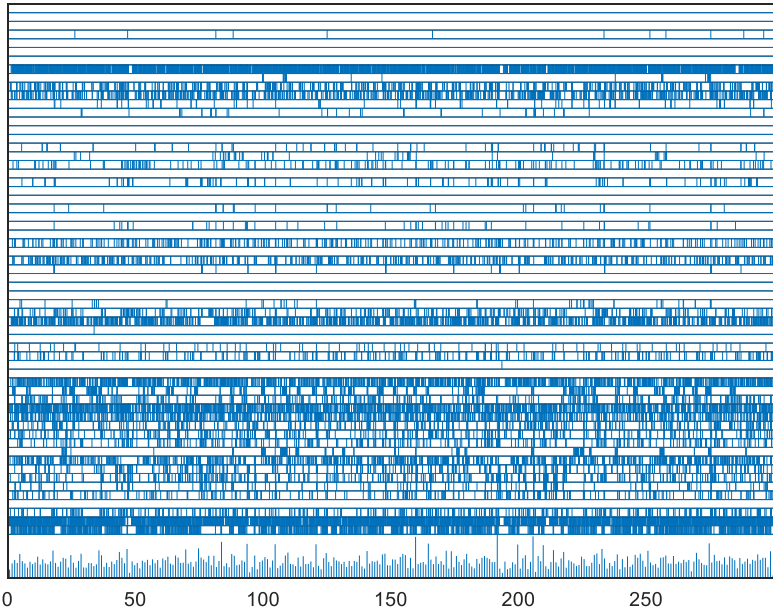
Table A.1 - Overview of optogenetic stimulation experiments

Experiment date	MEA nr.	DIV	Pulse width (ms)	Light intensity (%)	Active electrodes >15	Nr. of spikes > 2 ¹⁵
25/10/2021	38897	19	200	50	16	YES
28/10/2021	38856	22	200	50	26	YES
29/10/2021	38889	23	200	50	23	YES
24/11/2021	38857	20	5	40	34	YES
08/12/2021	38899	20	50	50	20	YES
16/12/2021	38860	24	5	50	13	NO
15/01/2022	38857	29	50	50	24	YES
16/01/2022	38897	30	100	50	14	YES
18/01/2022	38859	32	100	50	16	YES
01/02/2022	38900	18	100	50	16	YES
02/02/2022	24851	19	100	50	22	YES
15/02/2022	40319	19	100	50	32	NO
28/02/2022	38897	19	100	50	17	YES
01/03/2022	40459	22	100	50	30	YES
02/03/2022	38857	23	100	50	26	YES

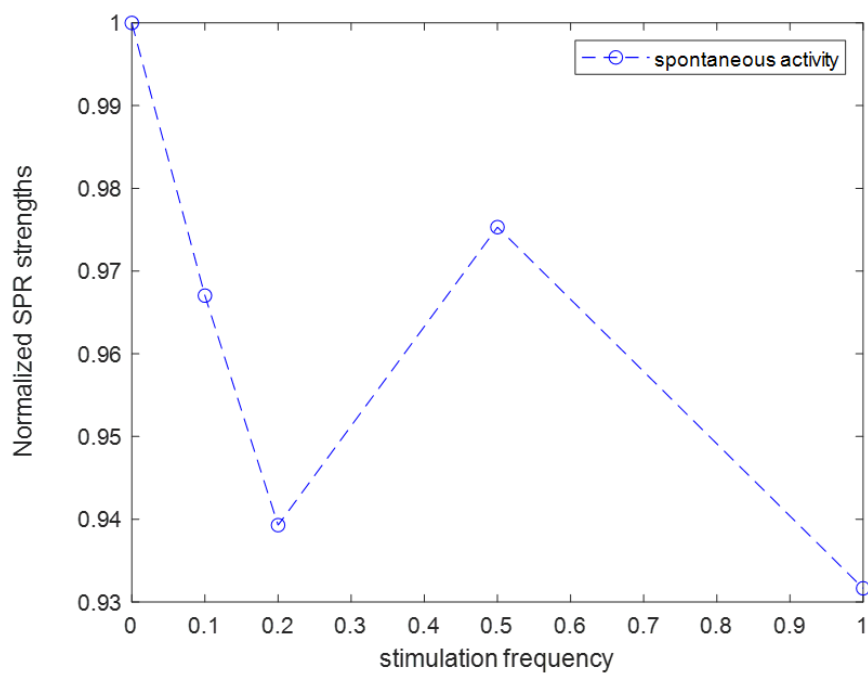
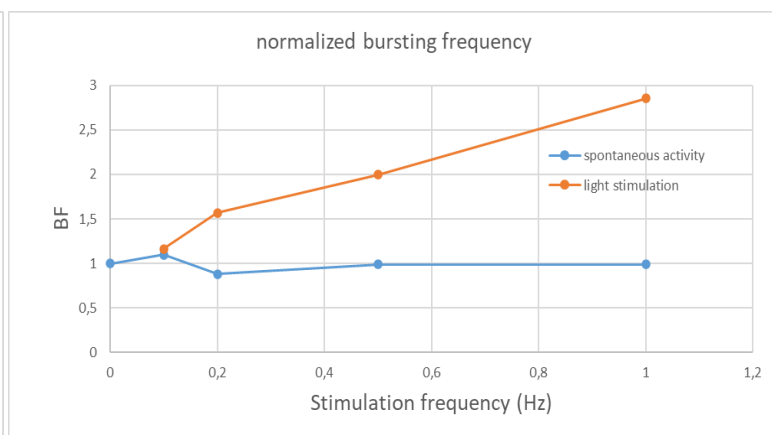
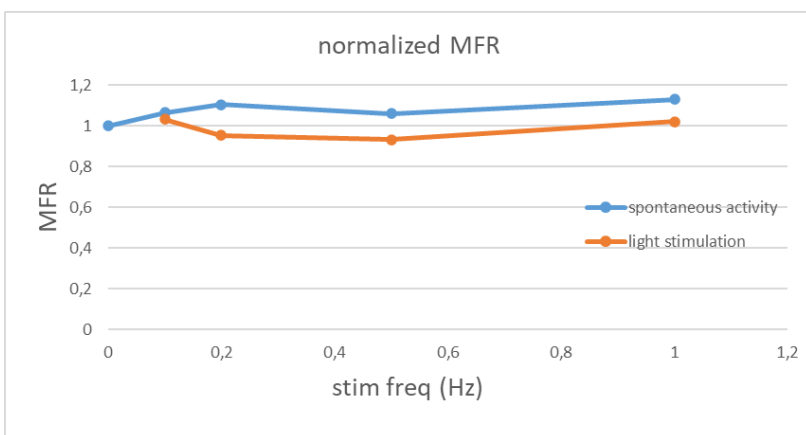
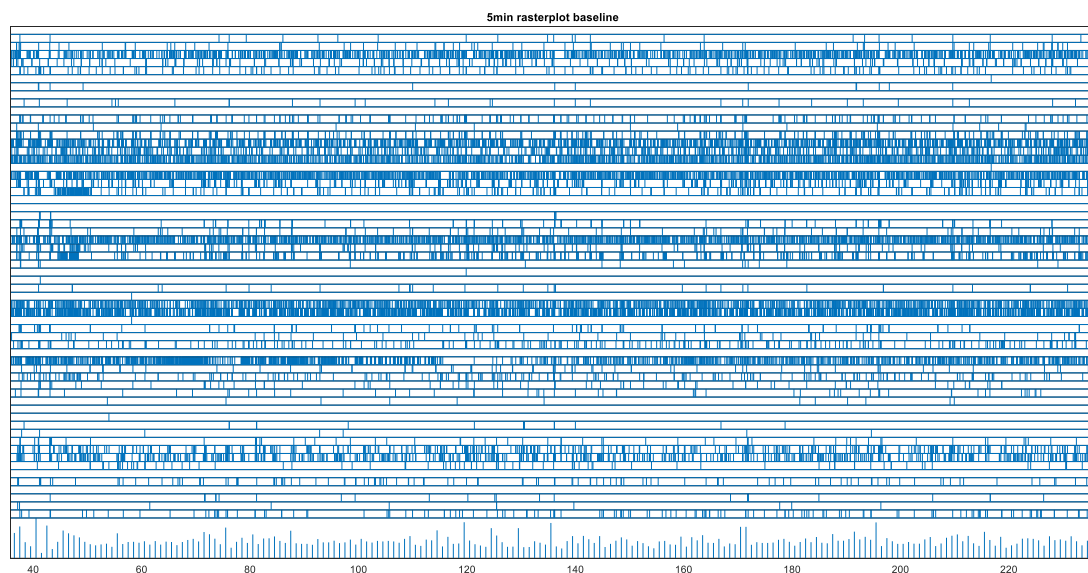
Experiment Date	25/10/2021
MEA	38897
Plating date	06/10/2021
Pulse width	200 ms
Light intensity	50%
artifacts removed from baseline	35,48%
active electrodes at baseline	16



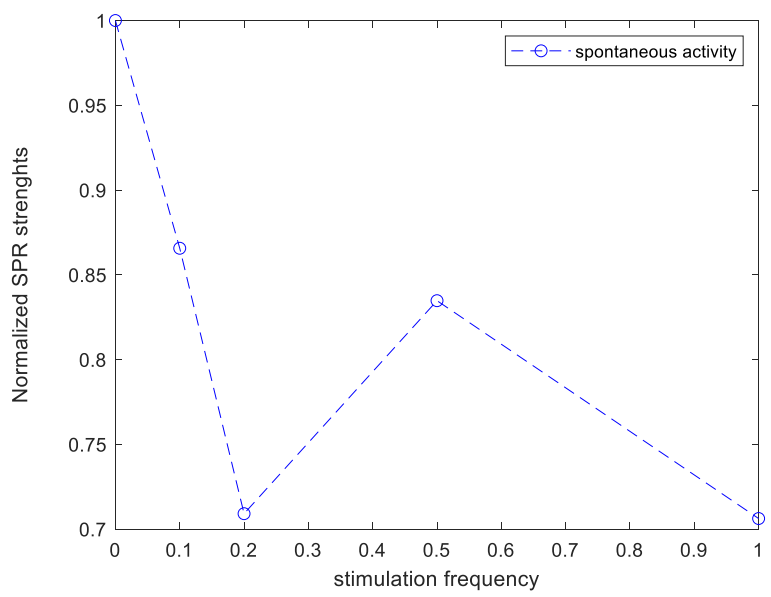
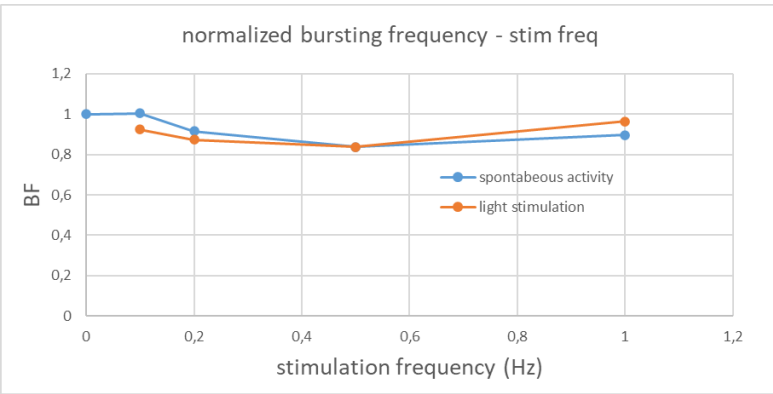
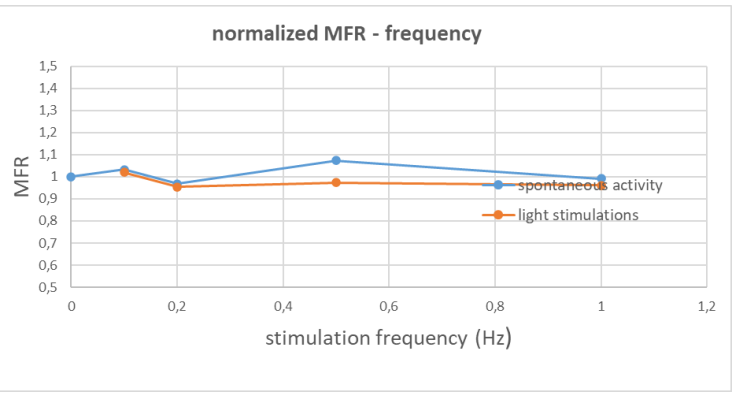
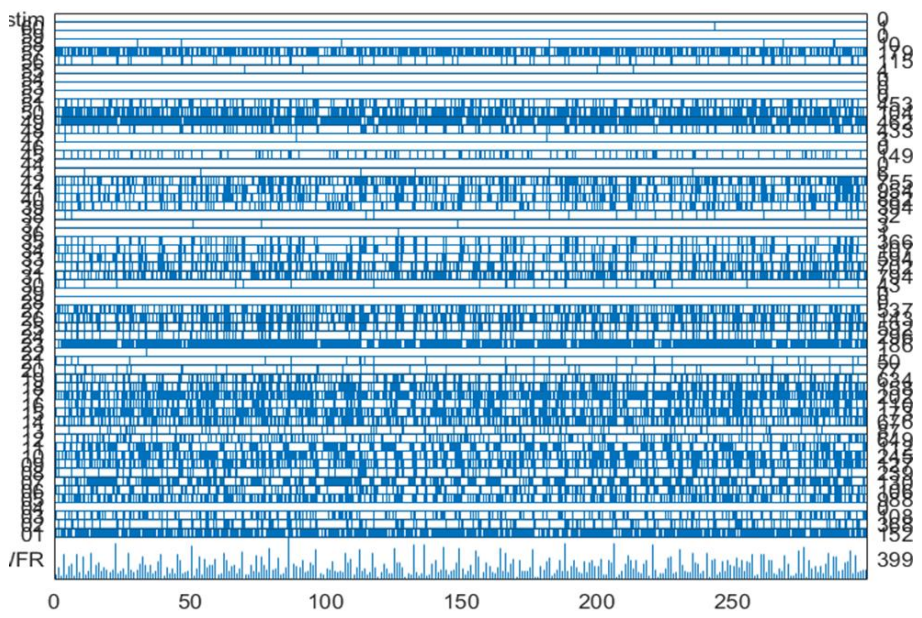
Experiment Date	28/10/2021
MEA	38856
Plating date	06/10/2021
Pulse width	200 ms
Light intensity	50%
artifacts removed from baseline	32,10%
active electrodes	26



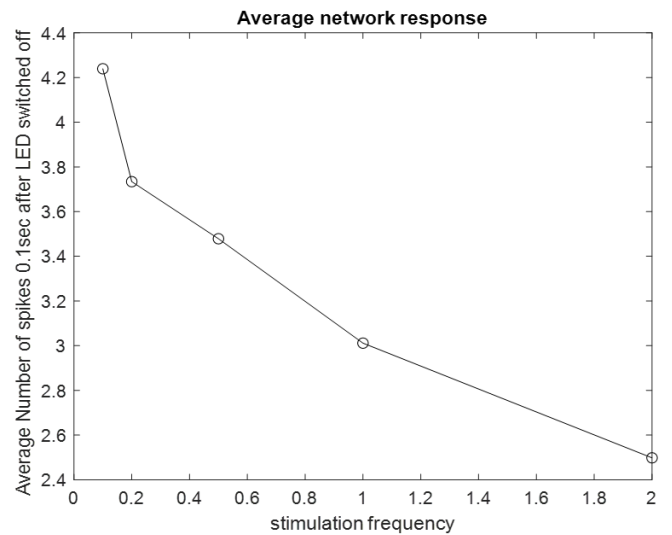
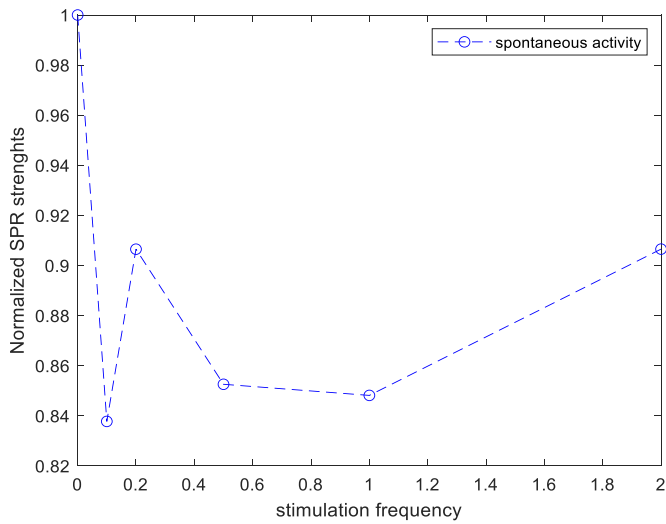
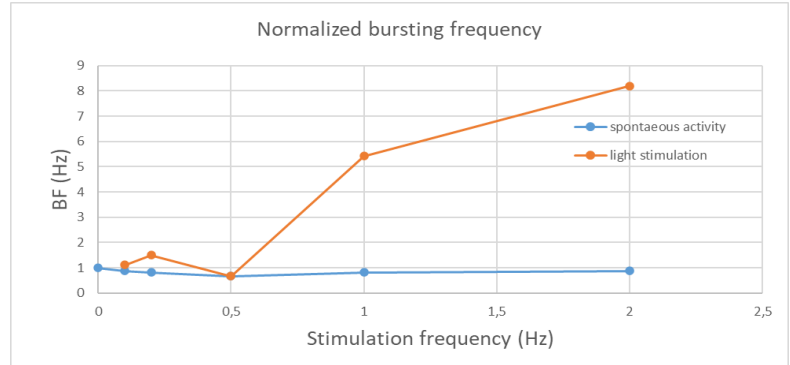
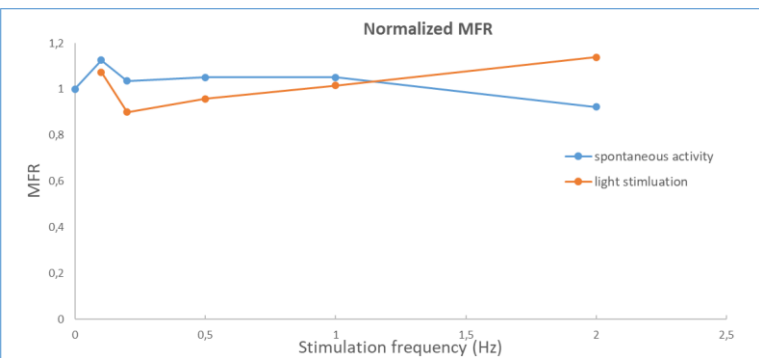
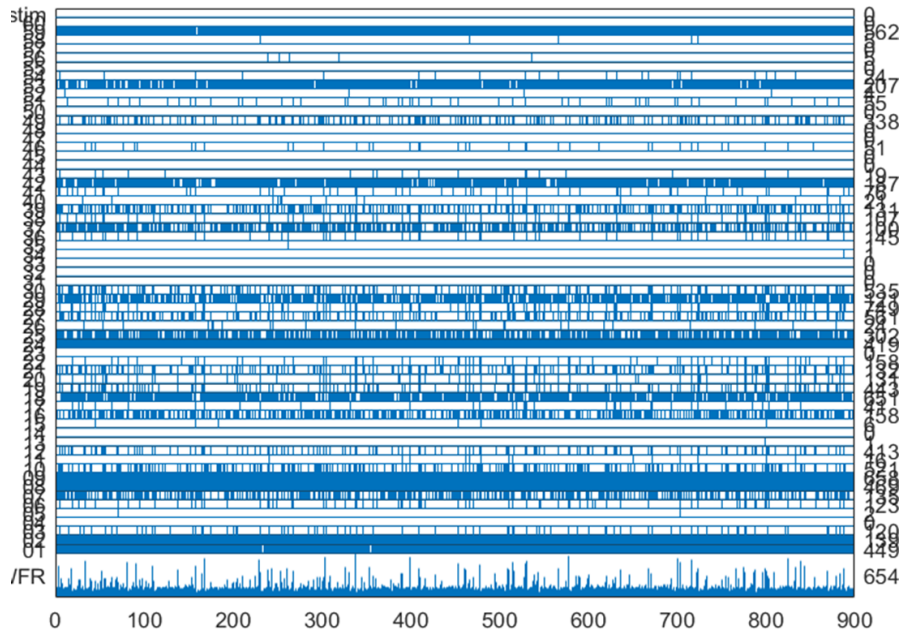
Experiment Date	29/10/2021
MEA	38889
Plating date	06/10/2021
Pulse width	200 ms
Light intensity	50%
artifacts removed from baseline	52,89%
active electrodes	23



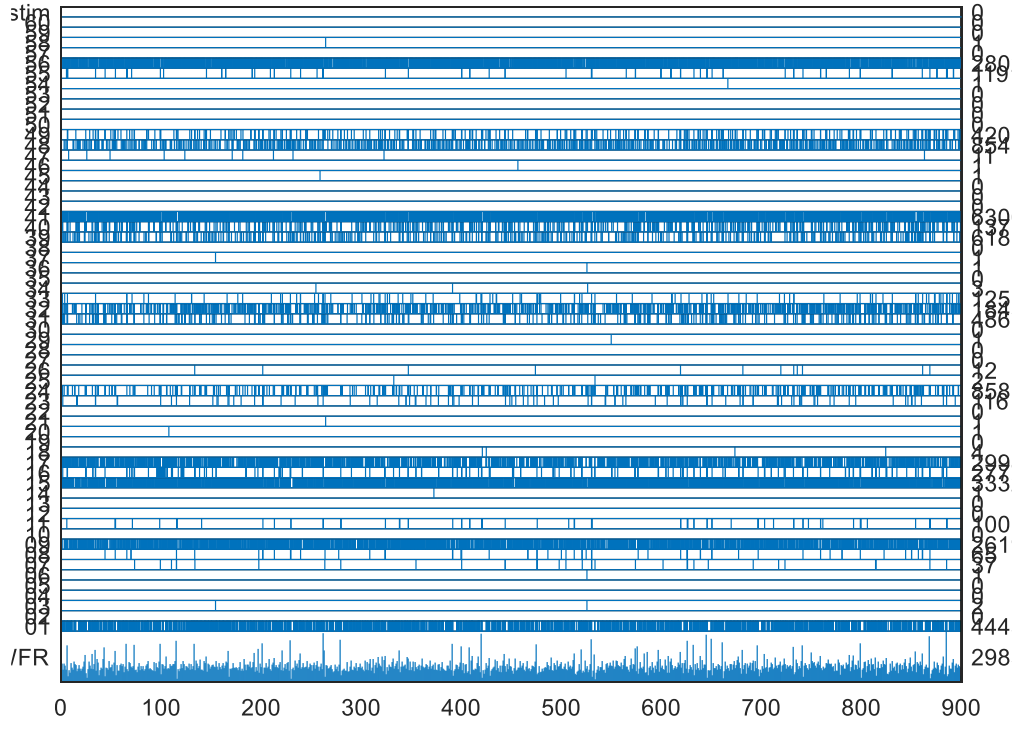
Experiment Date	24/11/2021
MEA	38857
Plating date	04/11/2021
Pulse width	5 ms
Light intensity	40%
artifacts removed from baseline	45,30%
active electrodes	34



Experiment Date	08.12.21
MEA	38899
Plating date	18/11/2021
Pulse width	50 ms
Light intensity	50%
artifacts removed from baseline	15,30%
active electrodes	20

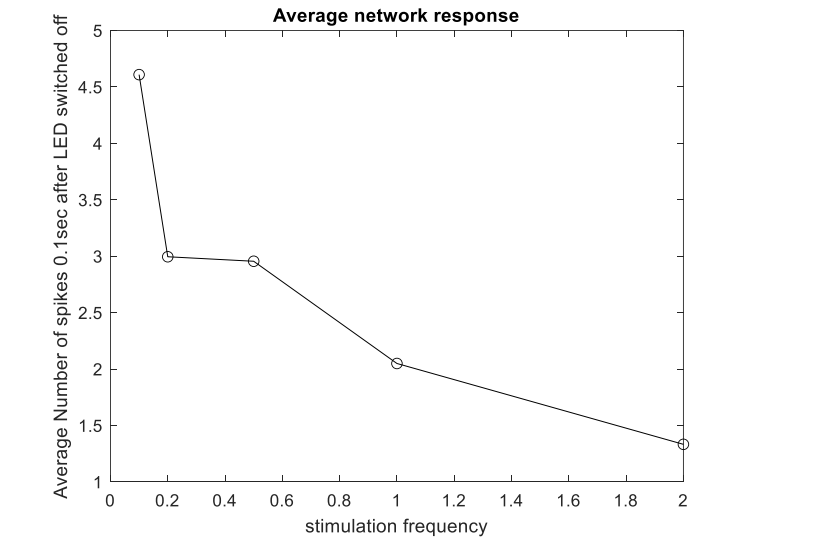
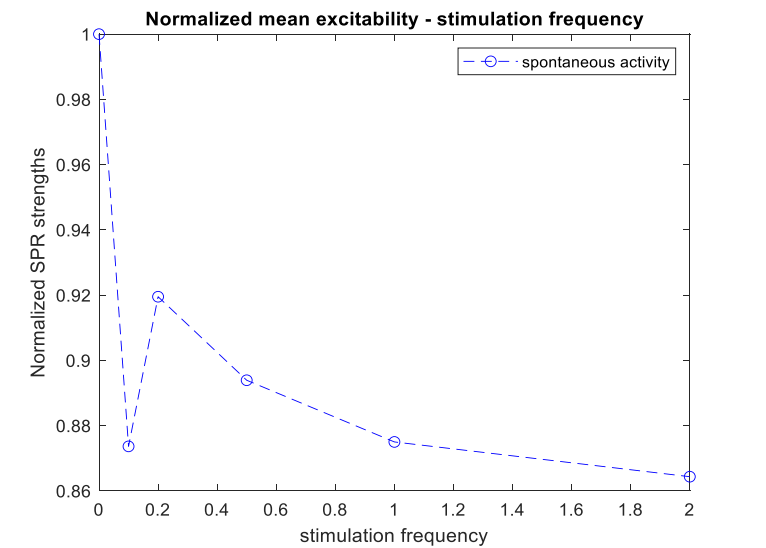
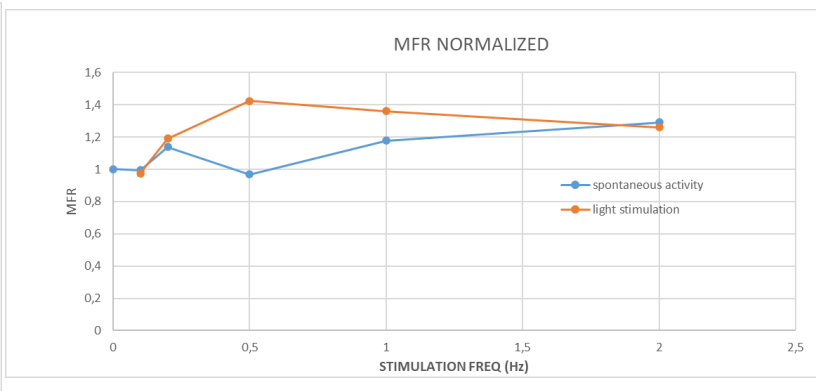
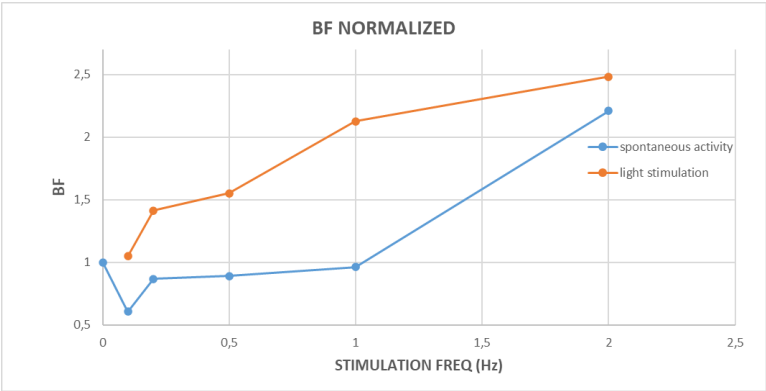
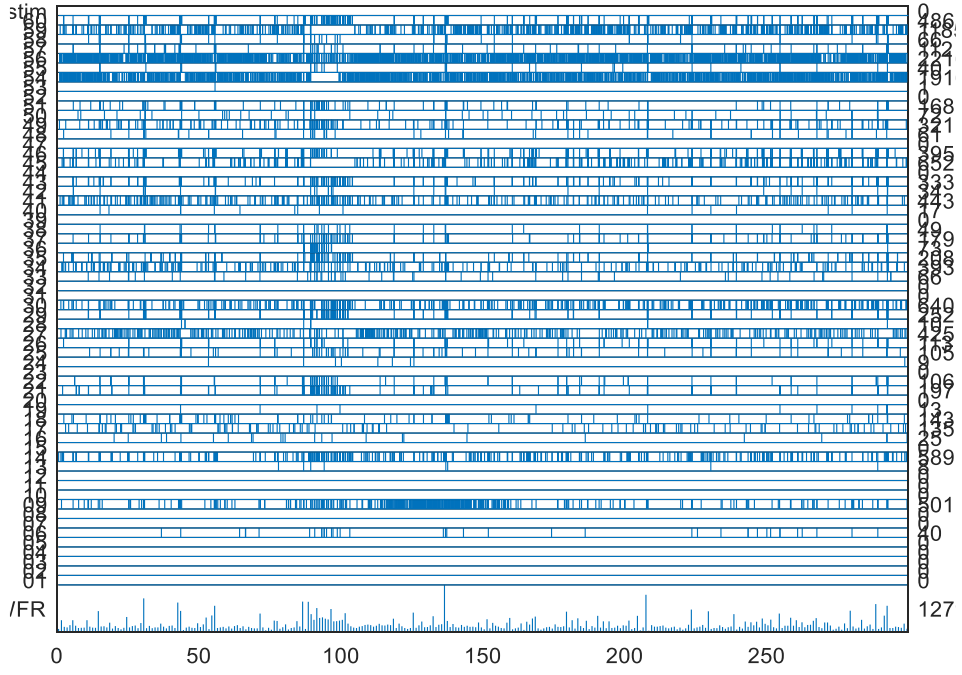


Experiment Date	16.12.21
MEA	38860
Plating date	18/11/2021
Pulse width	5 ms
Light intensity	50%
artifacts removed from baseline	46,16%
active electrodes baseline	13

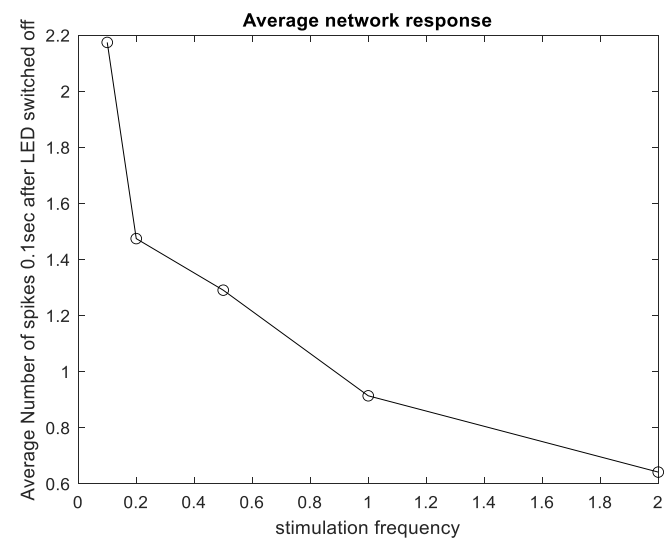
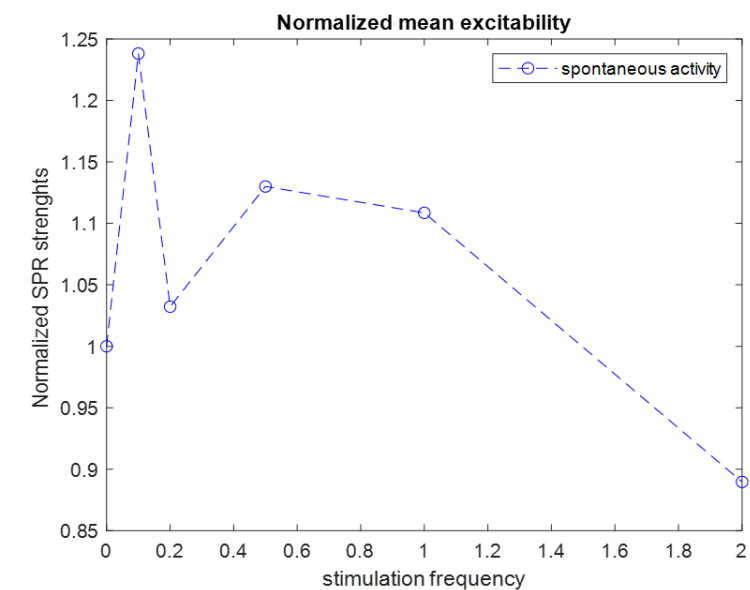
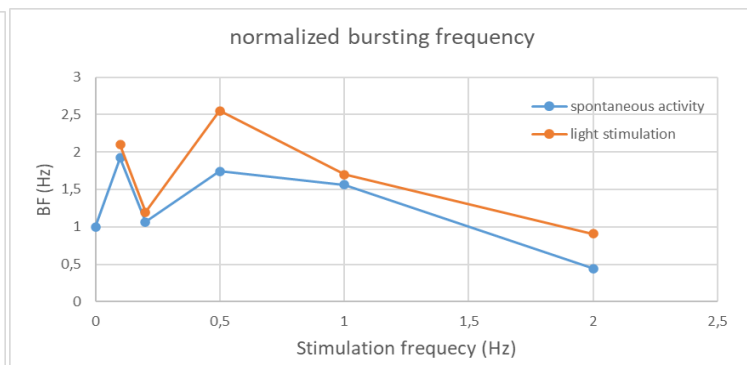
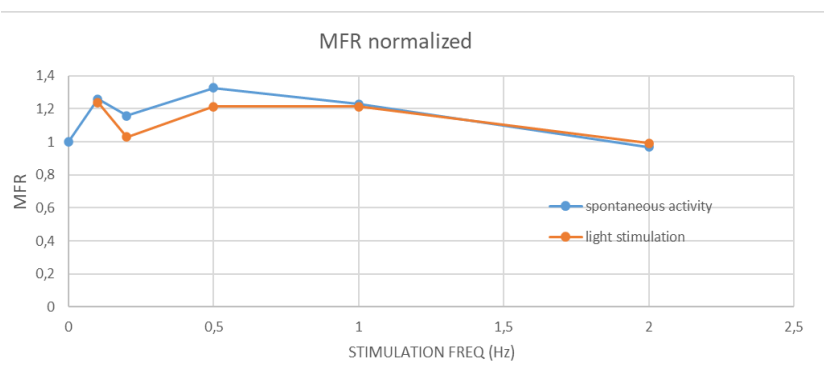
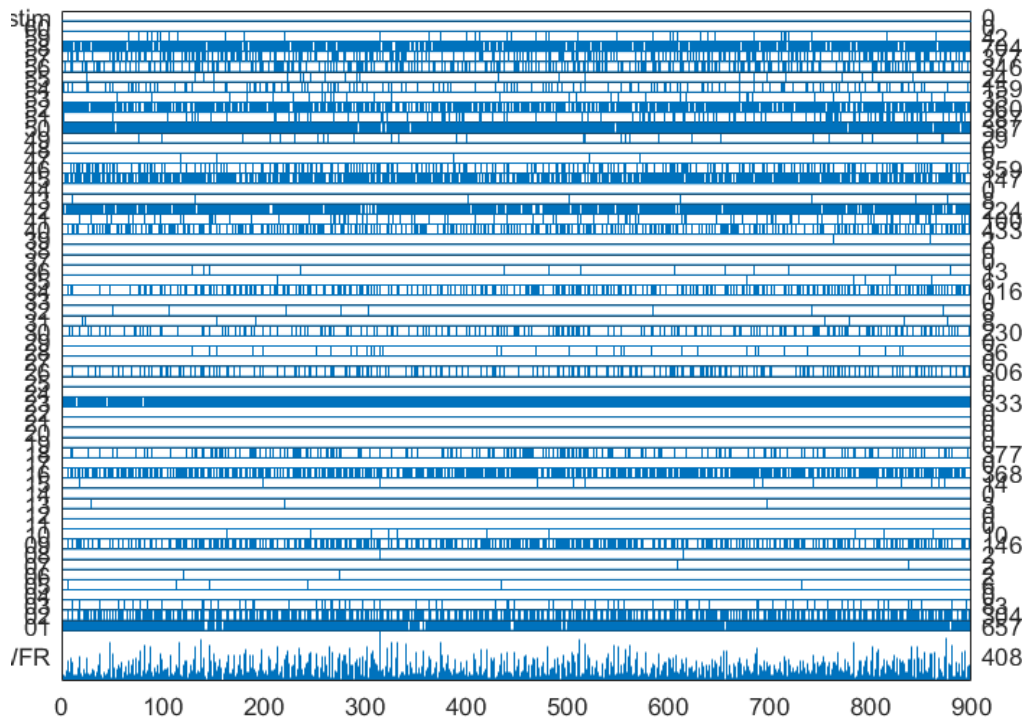


EXCLUDED BECAUSE ACTIVE ELECTRODES < 15

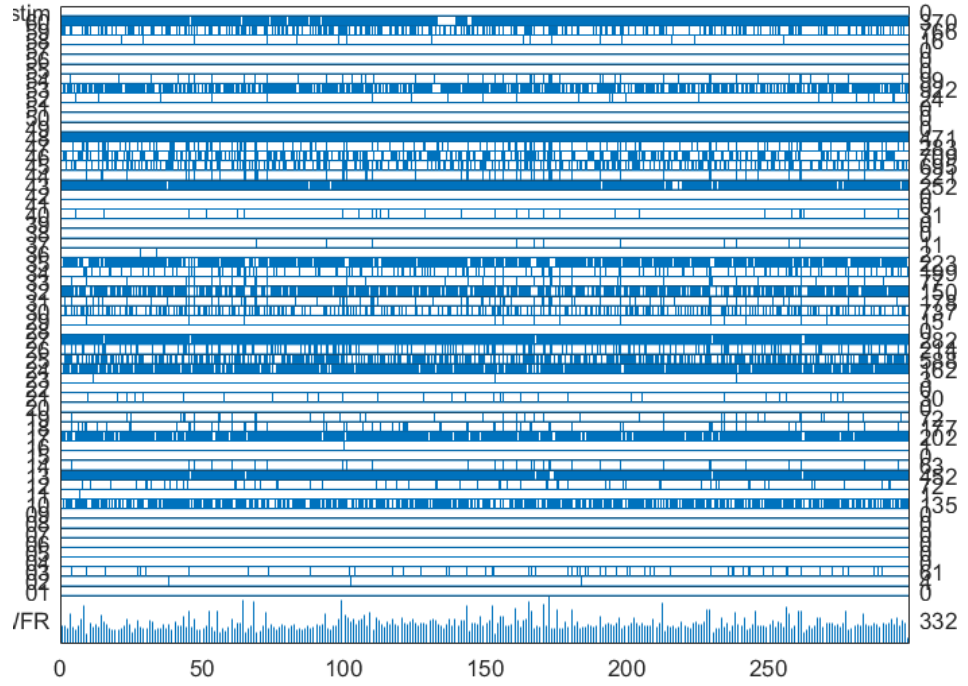
Experiment Date	15/01/2022
MEA	38857
Plating date	16/12/2021
Pulse width	50 ms
Light intensity	50%
artifacts removed from baseline	63,89%
active electrodes	24



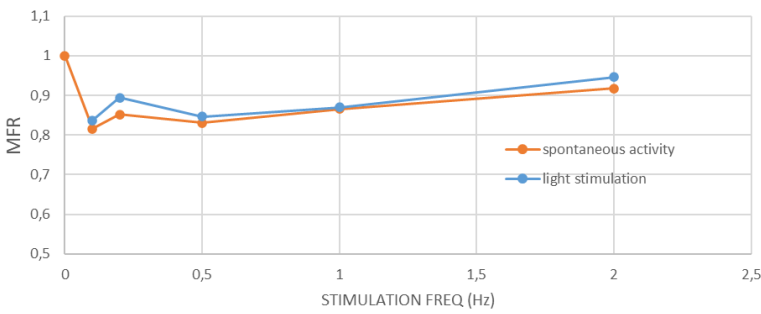
Experiment Date	18/01/2022
MEA	38859
Plating date	16/12/2021
Pulse width	100 ms
Light intensity	50%
artifacts removed from baseline	53,22%
active electrodes	16
non-zero connections (%)	56,888889



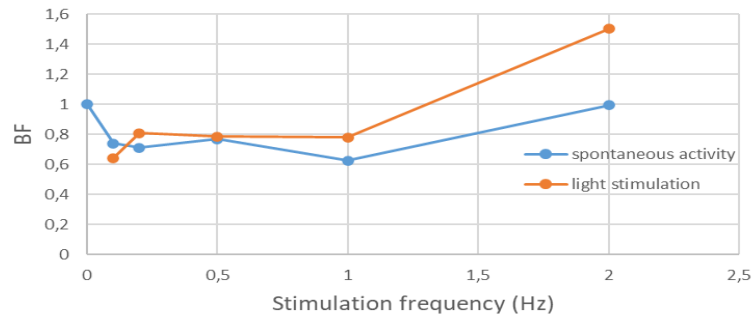
Experiment Date	01.02.22
MEA	38900
Plating date	13/01/2022
Pulse width	100 ms
Light intensity	50%
artifacts removed from baseline	33,17%
active electrodes	16



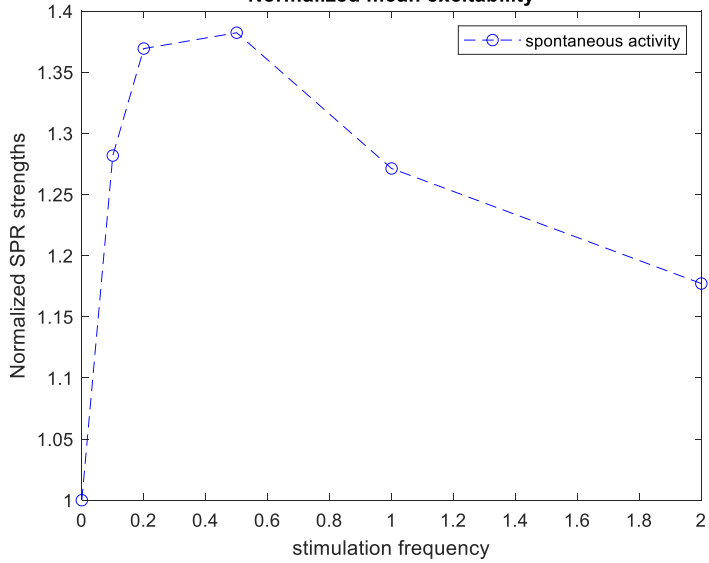
MFR normalized



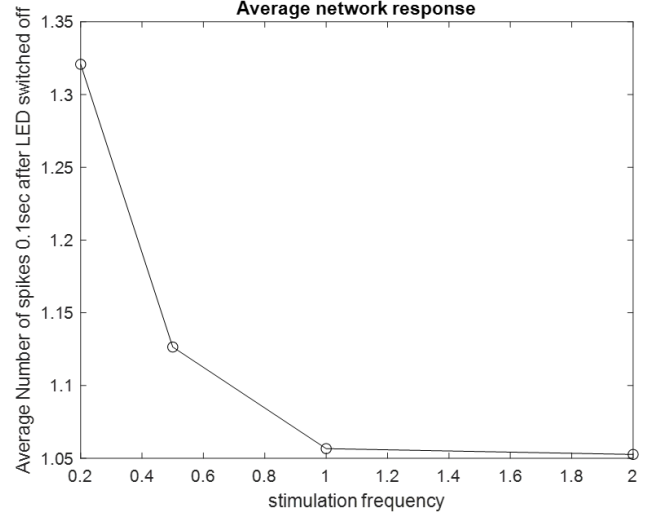
Normalized bursting frequency



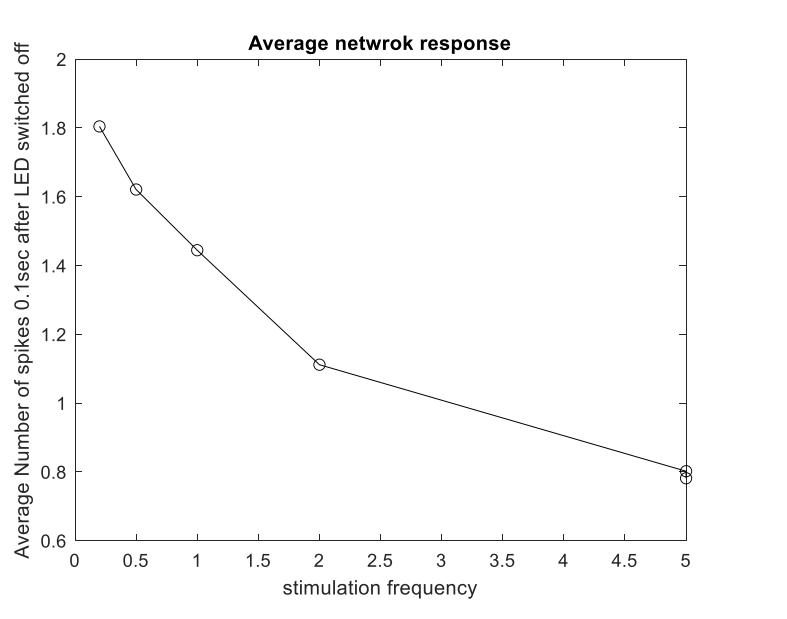
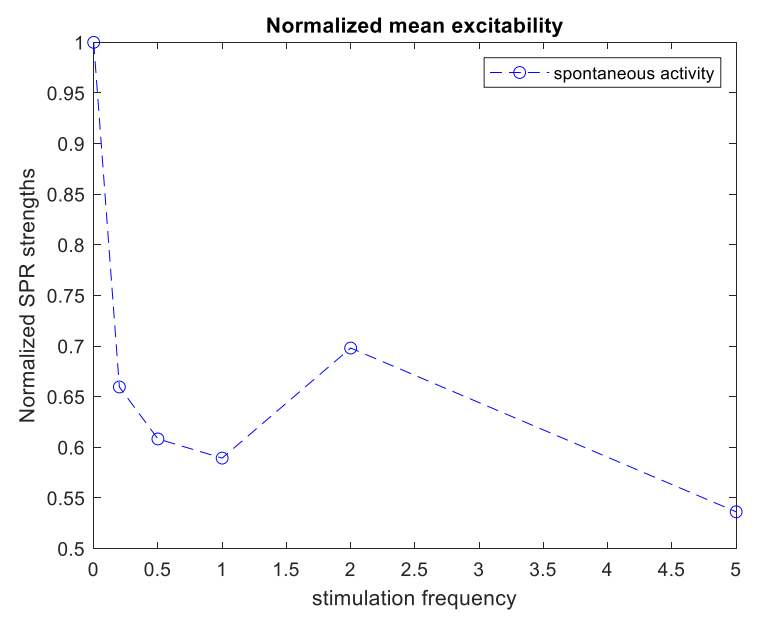
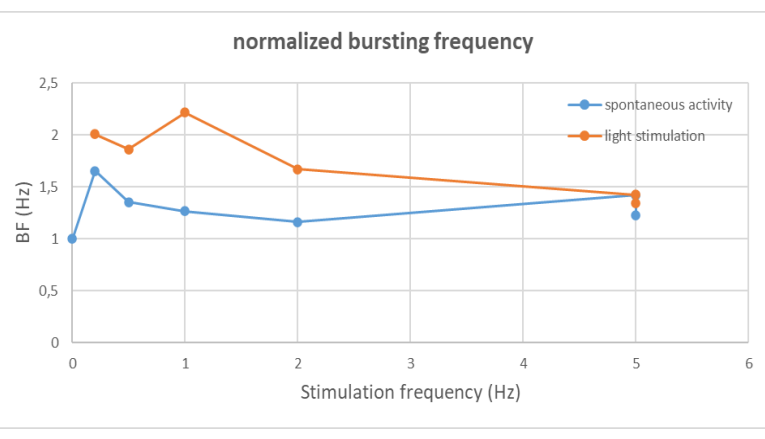
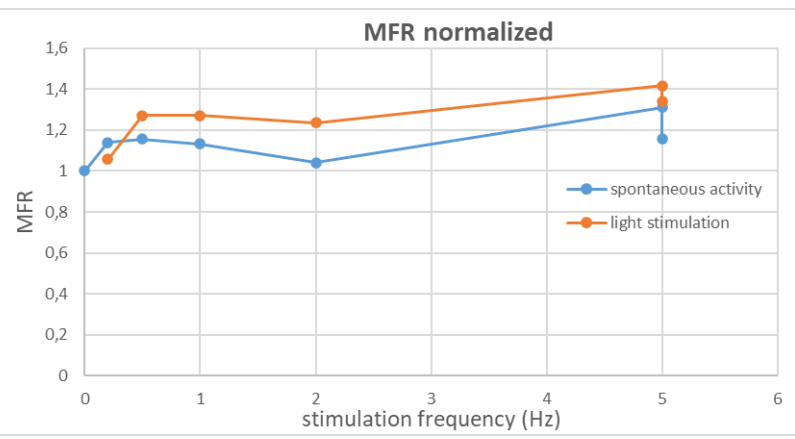
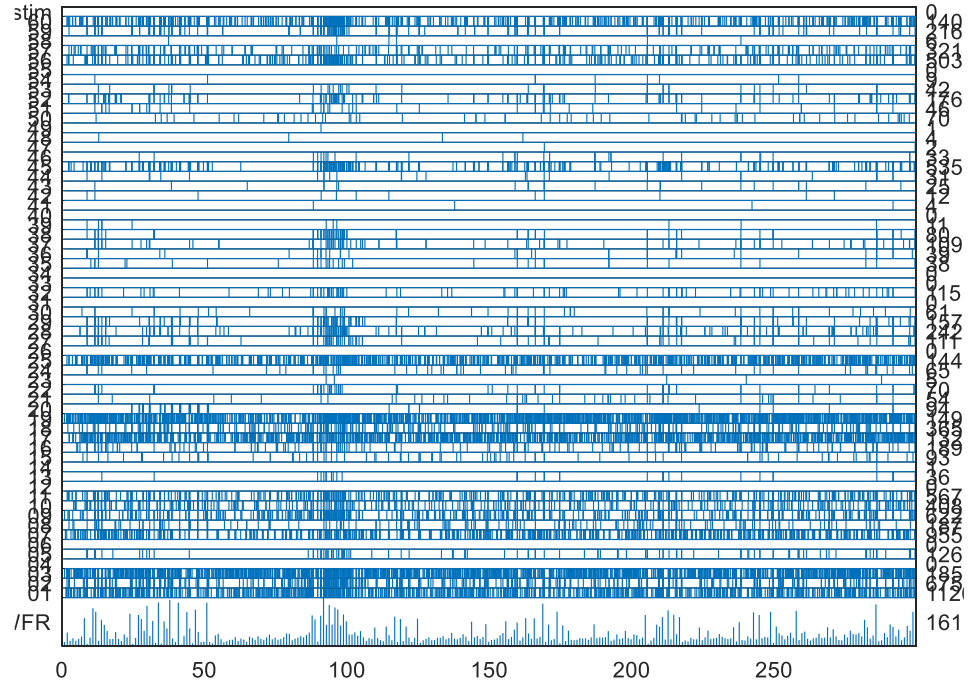
Normalized mean excitability



Average network response



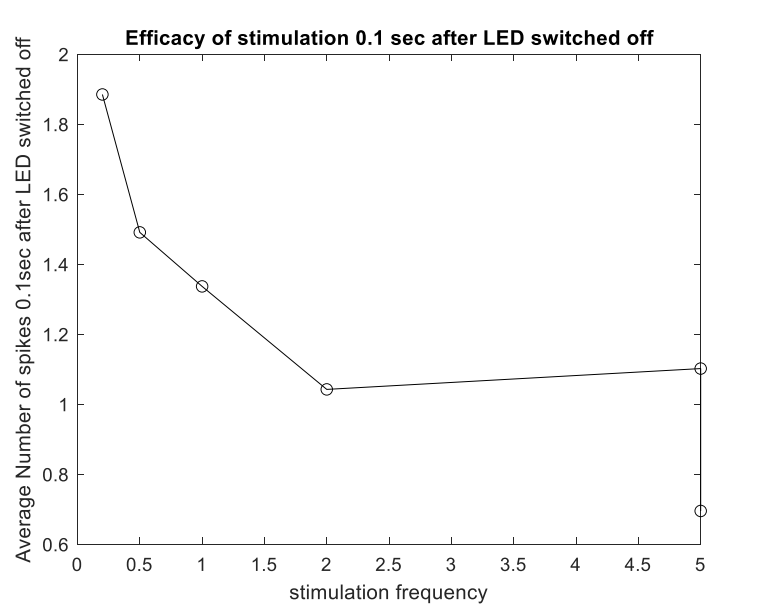
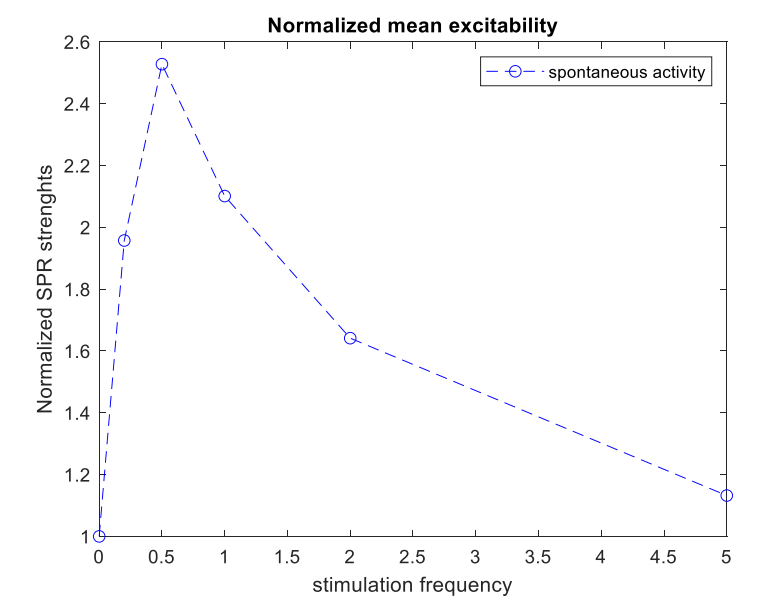
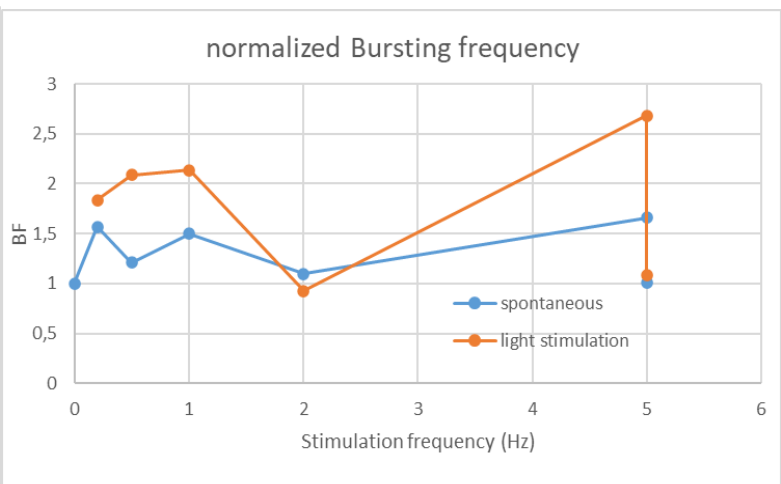
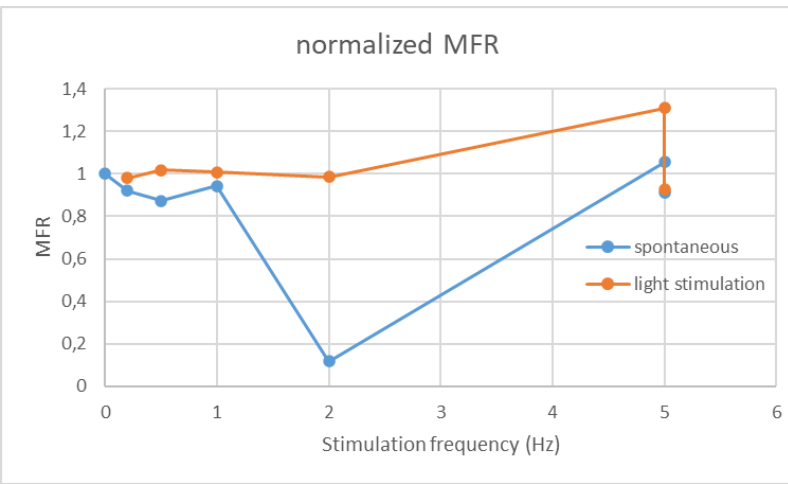
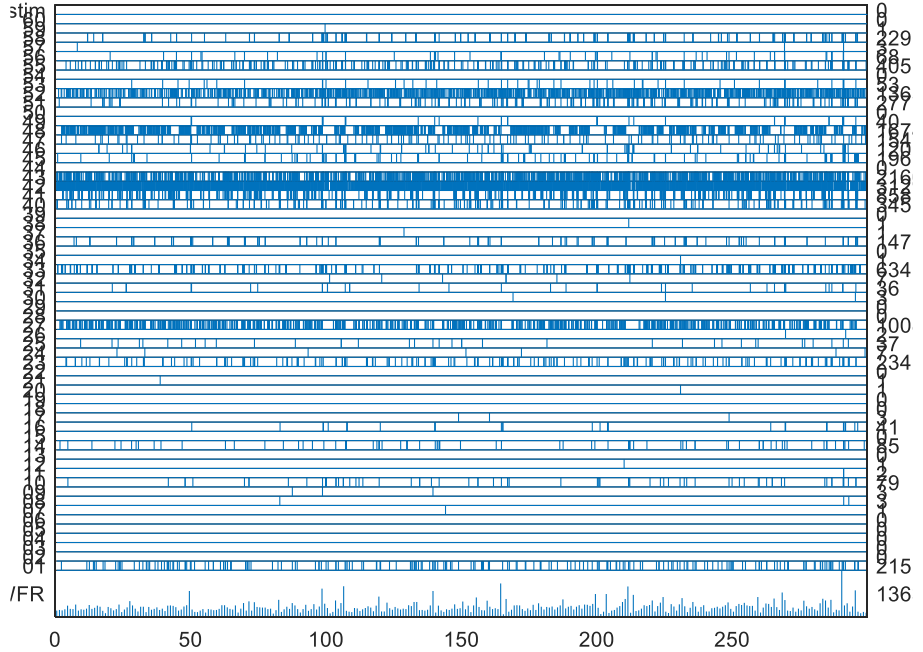
Experiment Date	02.02.22
MEA	24851
Plating date	13/01/2022
Pulse width	100 ms
Light intensity	50%
artifacts removed from baseline	31,52%
active electrodes	22



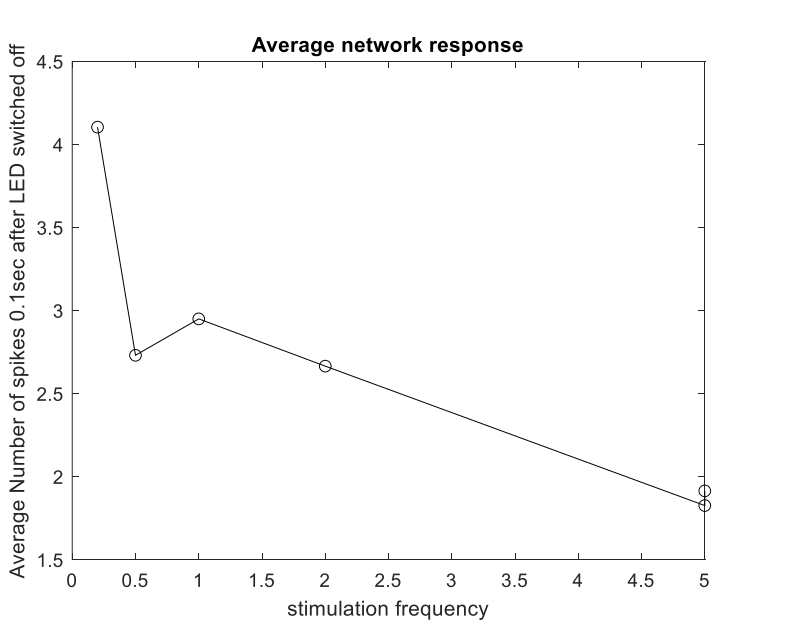
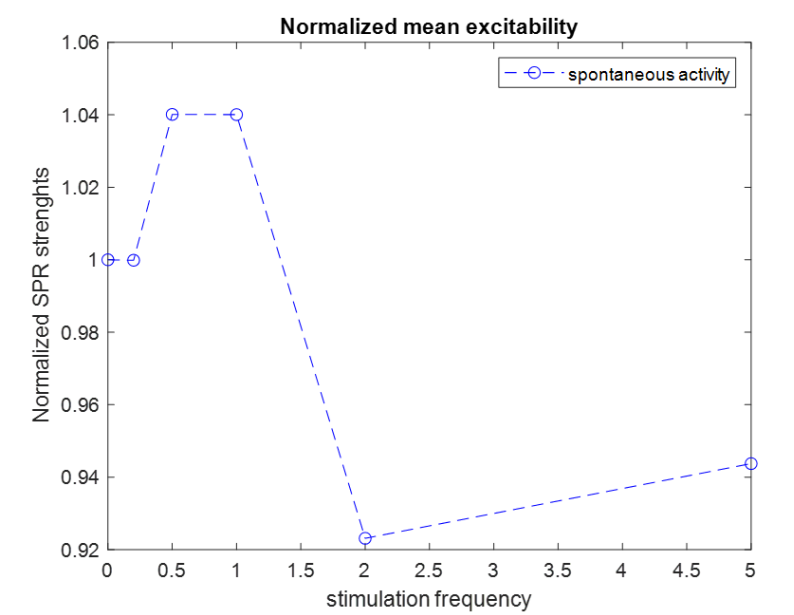
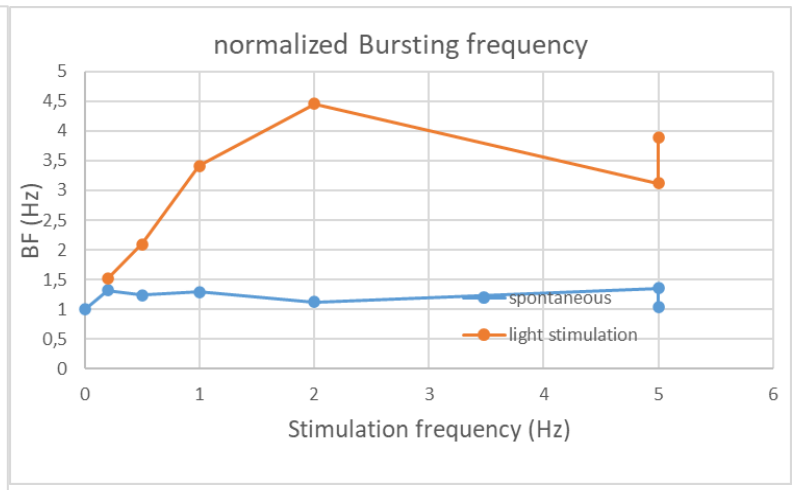
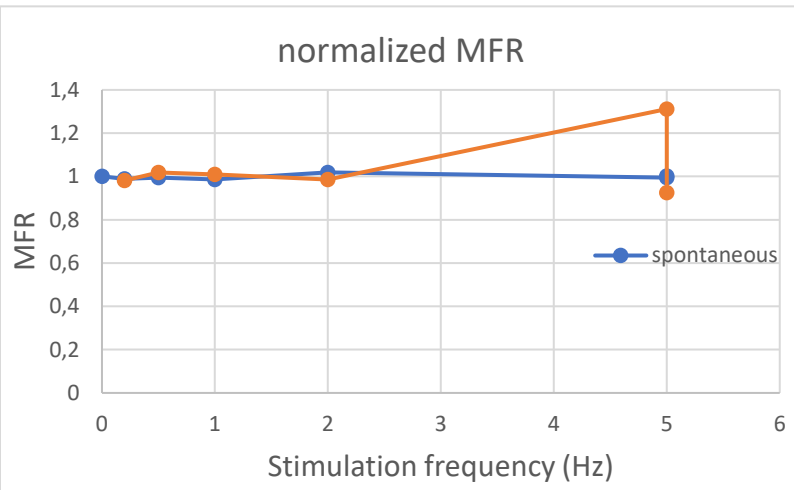
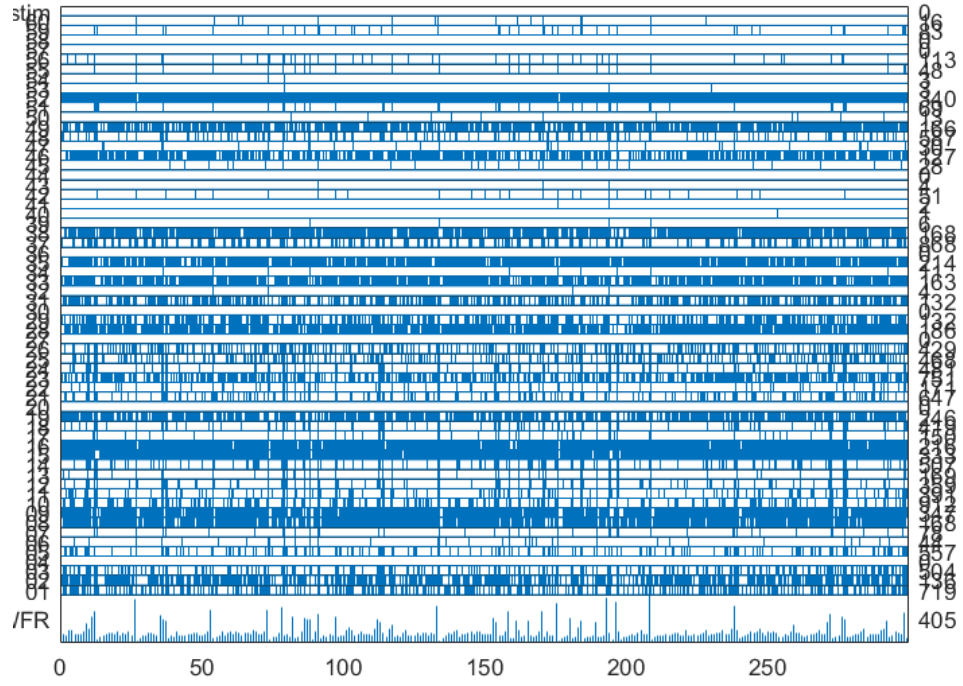
Experiment Date	15.02.22
MEA	40319
Plating date	27/01/2022
Pulse width	100 ms
Light intensity	50%
artifacts removed from baseline	43,50%
active electrodes	32

At 0.1 Hz stimulation frequency
the number of spikes $< 2^{15}$

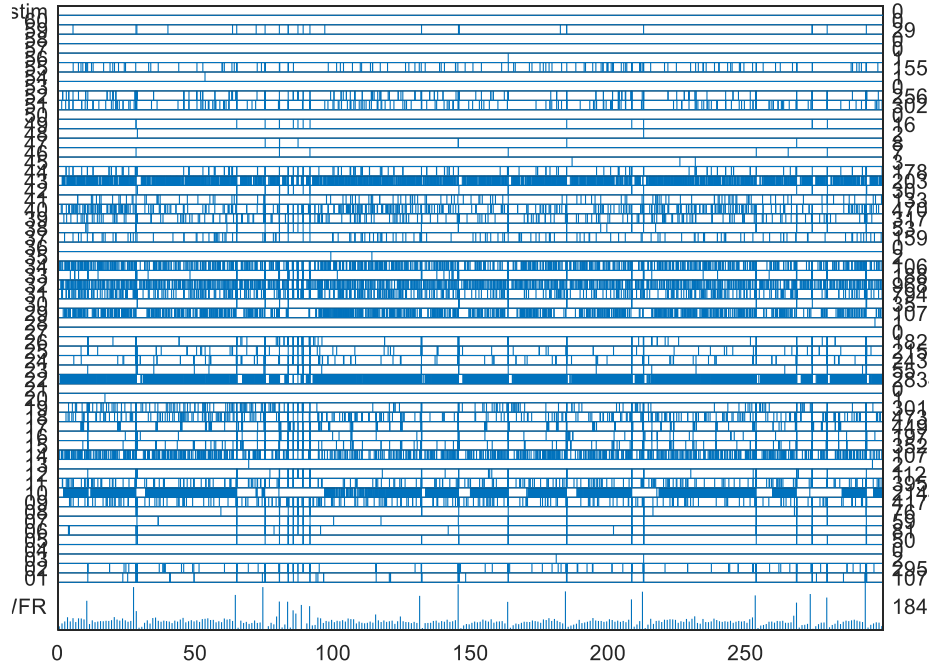
Experiment Date	28.02.22
MEA	38897
Plating date	09/02/2022
Pulse width	100 ms
Light intensity	50%
artifacts removed from baseline	
active electrodes	17



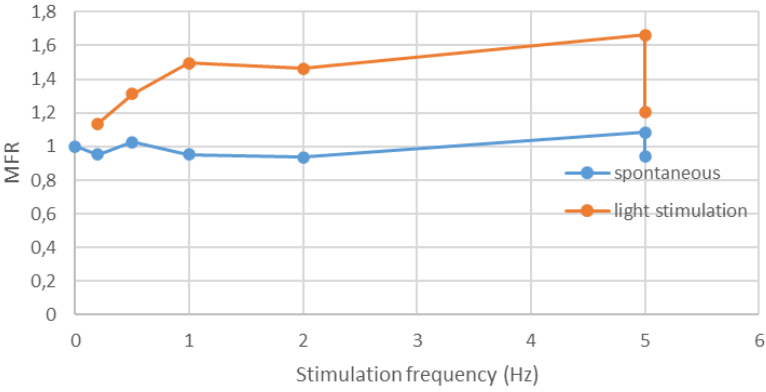
Experiment Date	01.03.22
MEA	40459
Plating date	09/02/2022
Pulse width	100 ms
Light intensity	50%
artifacts removed from baseline	
active electrodes	30



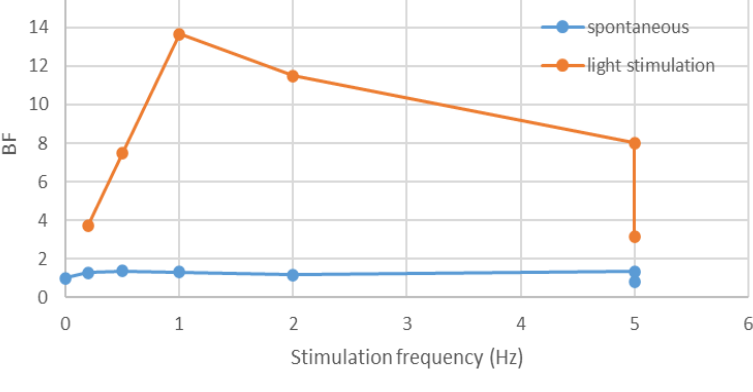
Experiment Date	02.03.22
MEA	38857
Plating date	09/02/2022
Pulse width	100 ms
Light intensity	50%
artifacts removed from baseline	
active electrodes	26



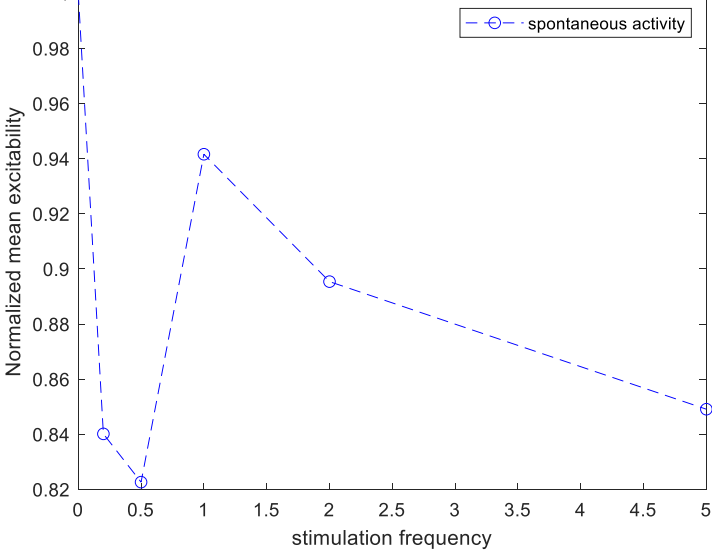
normalized MFR



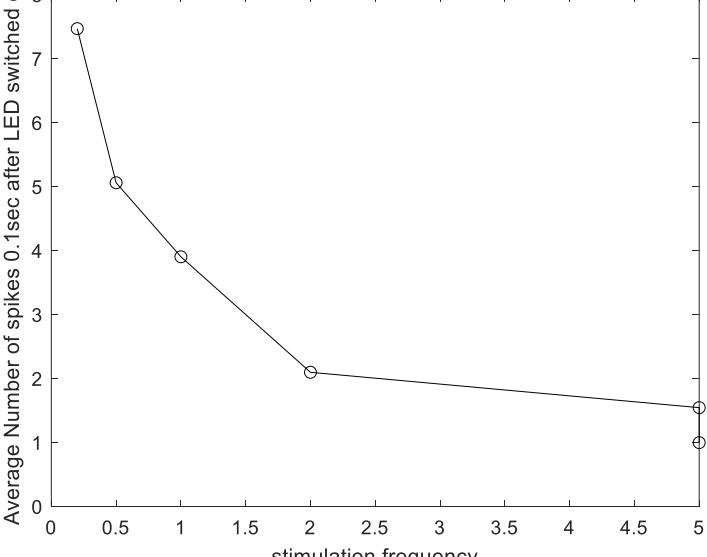
normalized Bursting frequency



Normalized mean excitability



Average network response



A.2 Control memory experiments

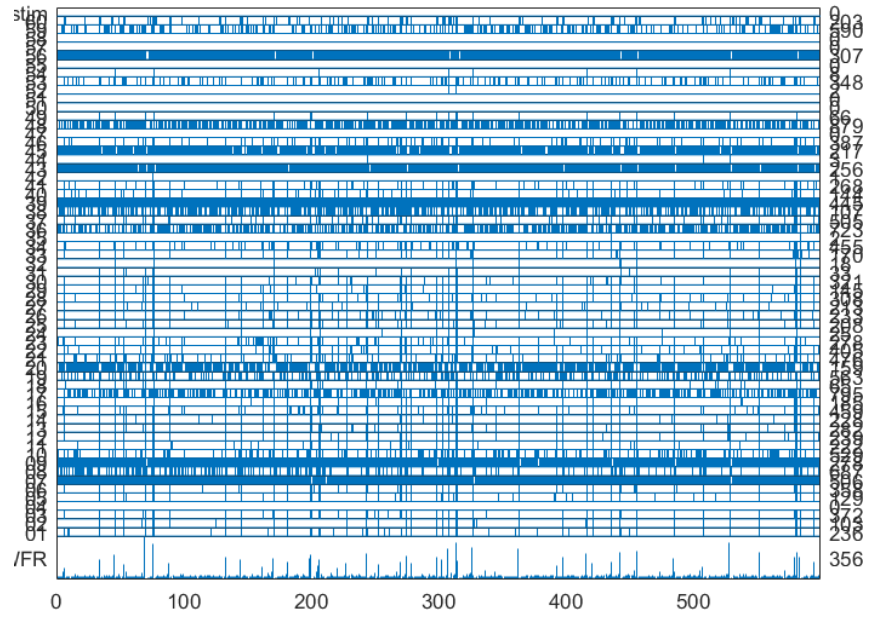
In each of these experiments we illustrate:

- A raster plot
- The area under the curve (AUC) of the mean post-stimulus time histogram (PSTH) which quantifies the effectiveness of electrical stimulation. If $AUC < 0$ the graph is depicted with a red border and this experiment is excluded.
- The Euclidean distance between baselines and spontaneous activity recordings (EDo) which quantifies connectivity changes in the network.
- The array-wide firing rate. This metric was not used in the main report illustrates the number of spikes detected from all the electrodes at any time of the experiment. If the detected spikes are $< 2^{15}$ then experiment is not included and the graph is illustrated with a red outline.
- Finally, we show a normalized graph of SPR strengths which serve as an estimate of network excitability during spontaneous activity recordings. This graph is only shown if the experiment was not meeting any of the exclusion criteria stated in section 2.3.

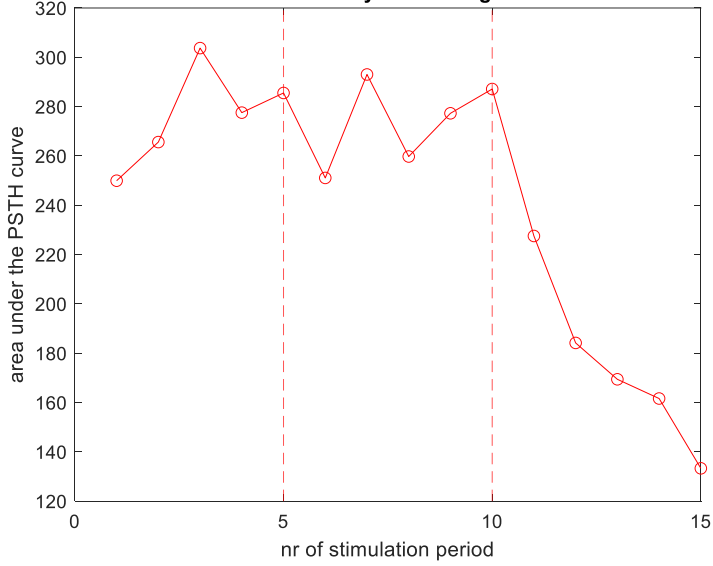
Table A.2 - Overview of control memory experiments

Experiment date	MEA nr.	DIV	Electrical pulse amplitude (μA)	Active electrodes >15	Nr. of spikes > 2^{15}	Response to electrical stim
27/10/2021	38897	21	24	30	YES	YES
28/10/2021	38856	22	24	27	YES	NO
03/11/2021	37619	28	24	25	YES	NO
26/11/2021	38857	22	24	27	YES	NO
08/12/2021	38899	20	24	21	YES	NO
16/12/2021	38860	28	36	16	YES	NO
14/01/2022	38897	29	12	30	YES	NO
15/01/2022	40314	30	24	35	YES	YES
16/01/2022	38857	31	24	22	YES	YES
18/01/2022	38859	33	24	19	YES	NO
02/02/2022	38900	20	12	18	YES	NO
07/02/2022	24851	25	36	18	YES	NO
22/02/2022	40319	26	24	20	YES	NO
01/03/2022	38897	21	24	20	YES	YES
02/03/2022	40459	22	24	27	YES	YES
04/03/2022	38857	25	24	23	YES	YES
21/06/2022	40314	19	24	24	YES	YES
23/06/2022	38898	21	32	18	YES	YES

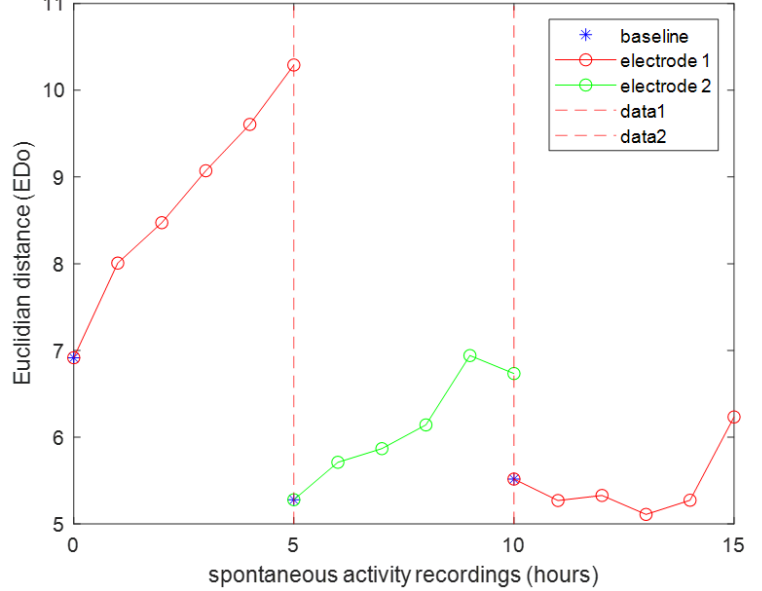
Experiment date	27/10/21
MEA nr	38897
Plating date	06/10/21
Amplitude (μA)	24
Grounded electrodes	0
Artifacts removed from baseline (%)	39,1 %
Active electrodes	30



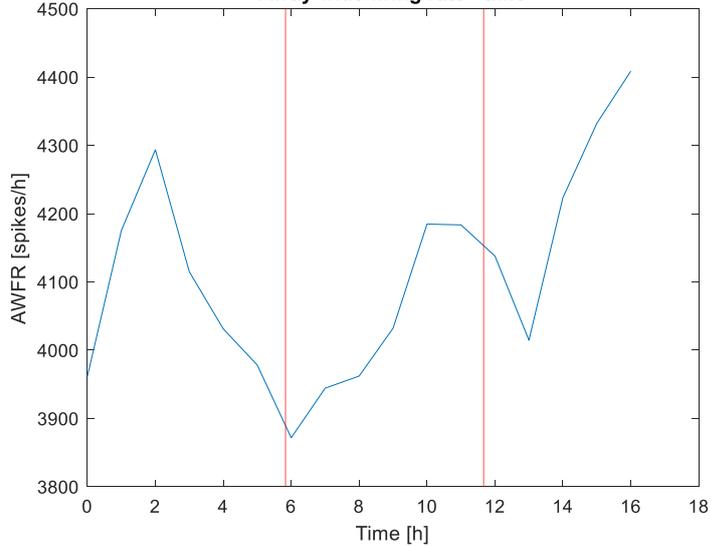
Validate effectiveness of stim by calculating area under PSTH curve



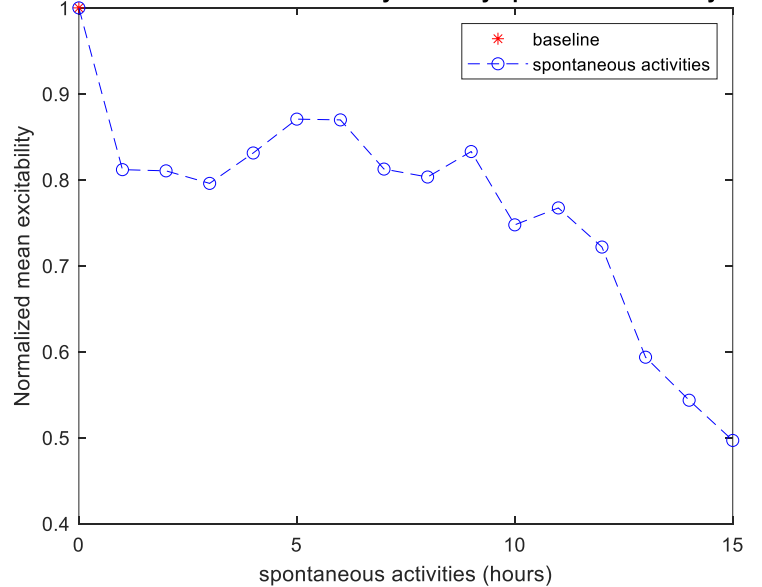
Euclidian distances with respect to a baseline recording (EDo)



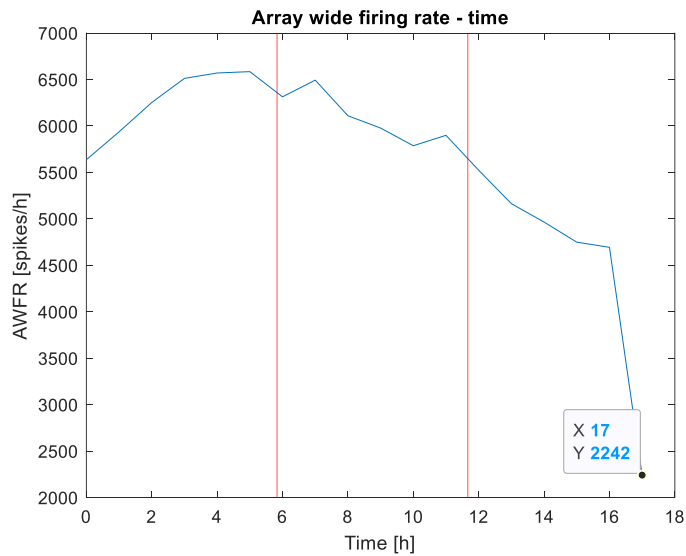
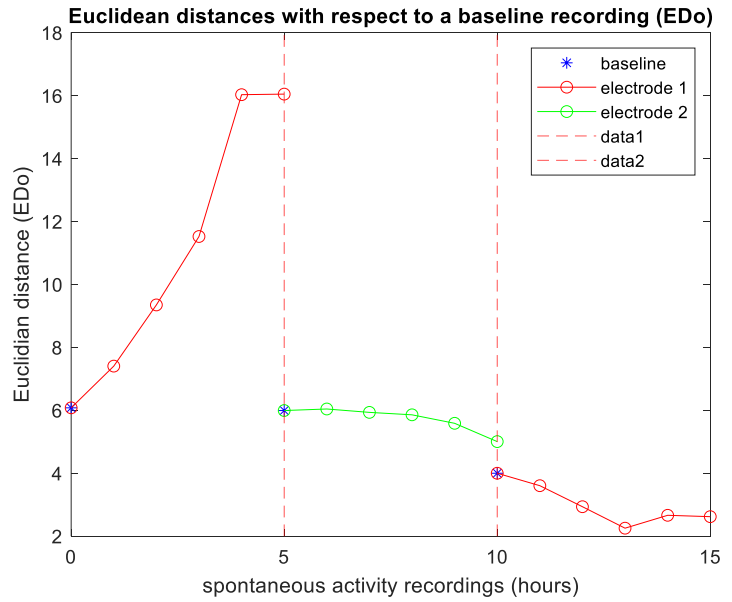
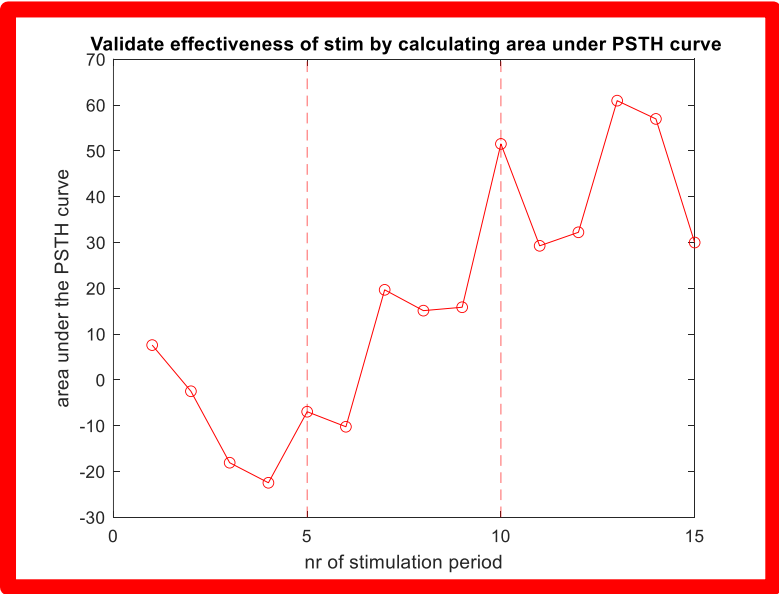
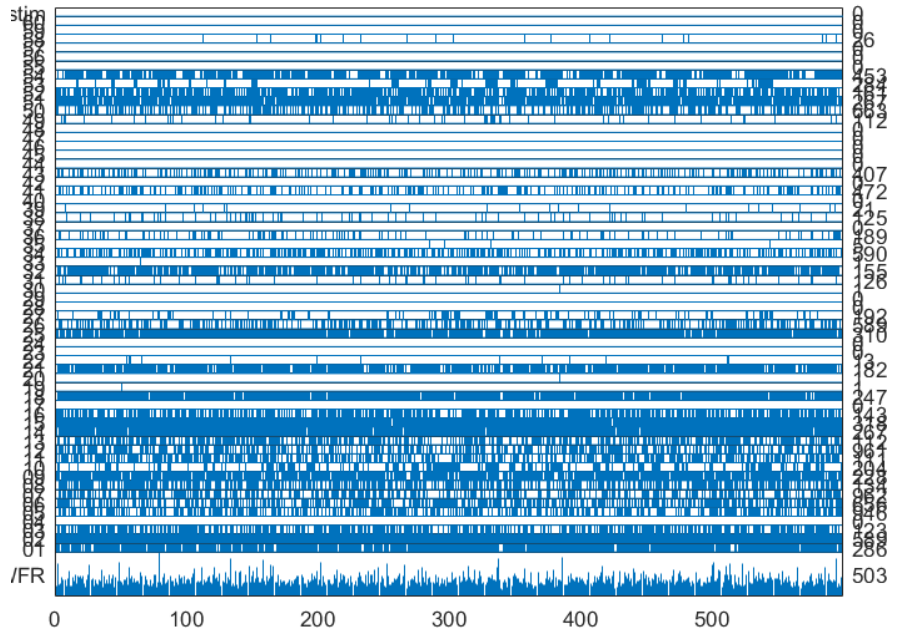
Array wide firing rate - time



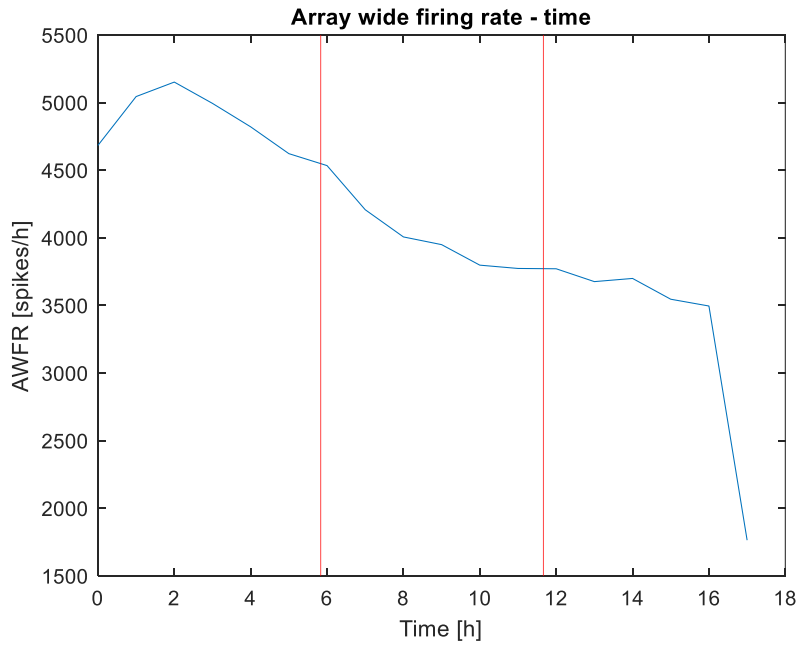
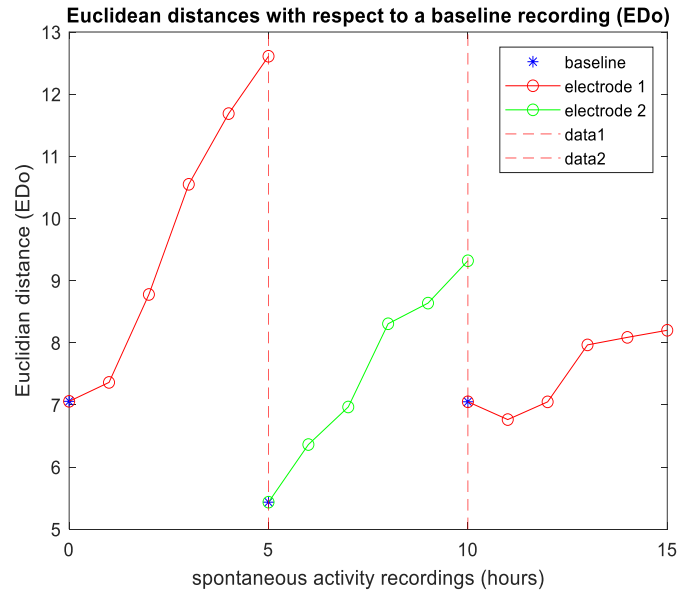
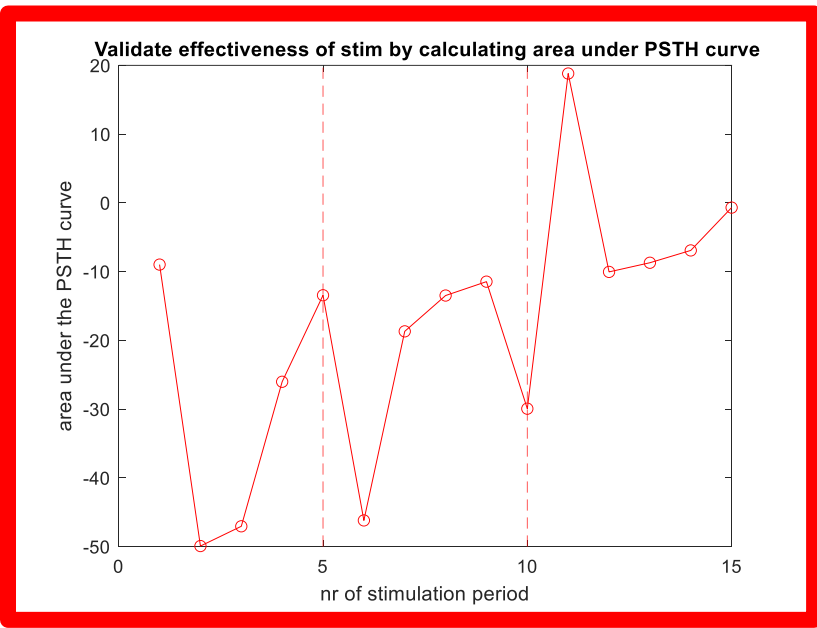
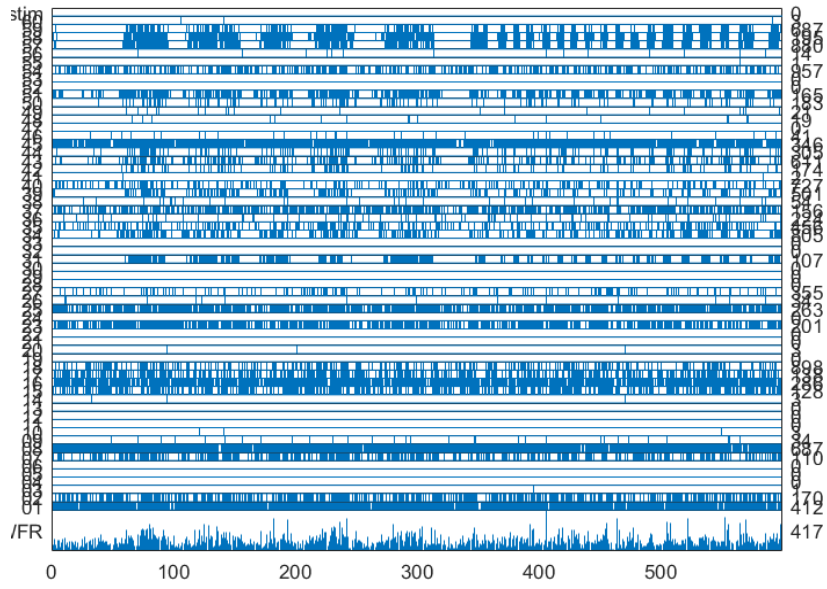
Normalized mean excitability for every spontaneous activity



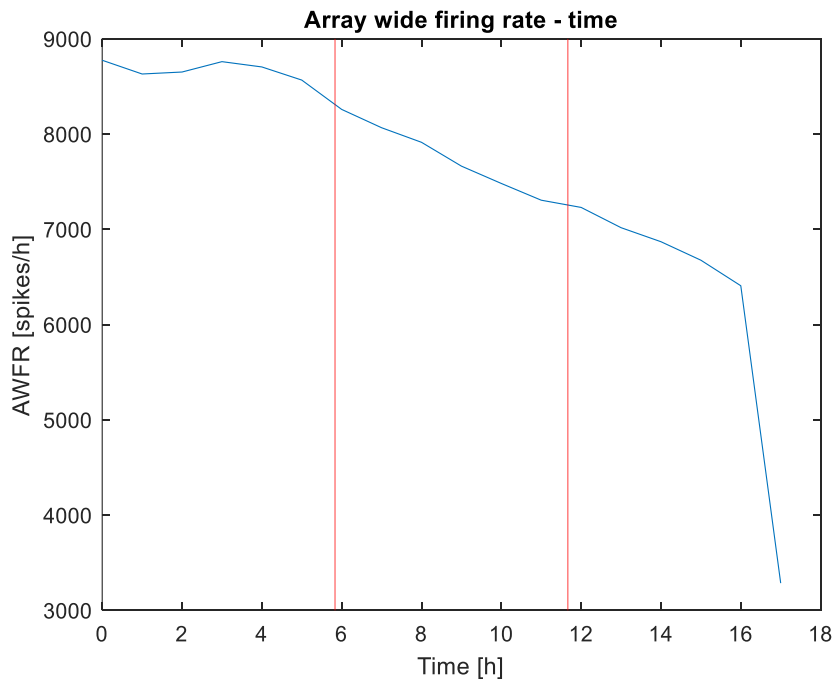
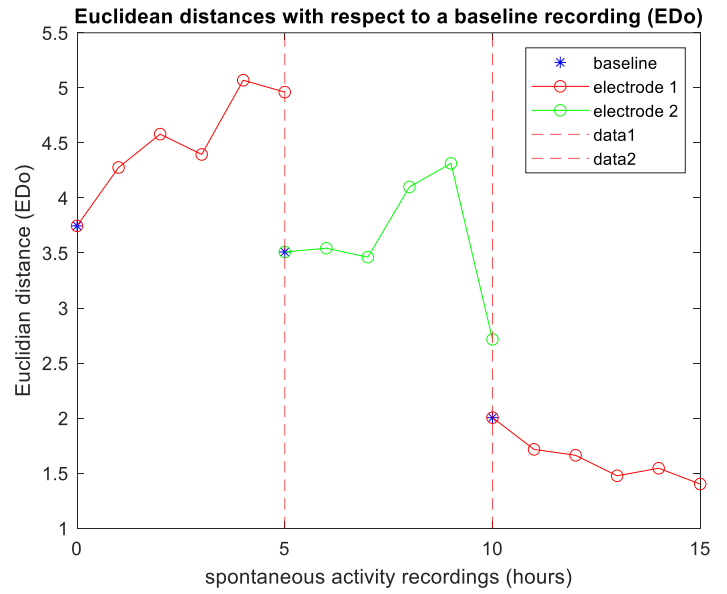
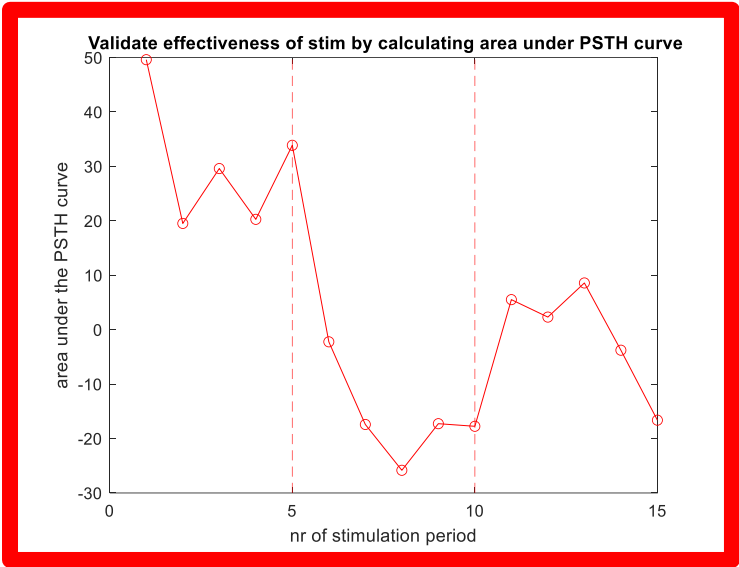
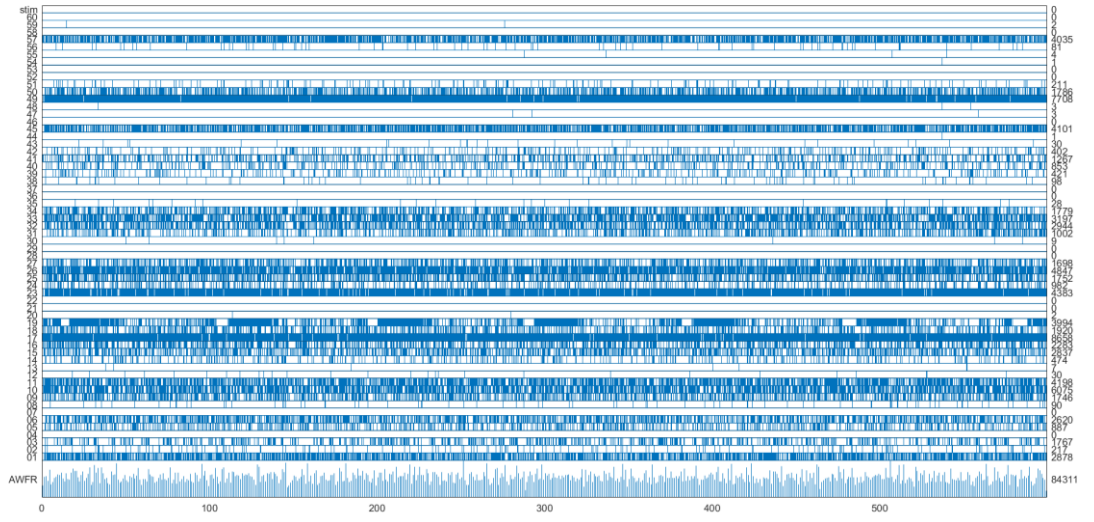
Experiment date	28/10/21
MEA nr	38856
Plating date	06/20/21
Amplitude (μ A)	24
Grounded electrodes	0
Artifacts removed from baseline (%)	30,17%
Active electrodes	27



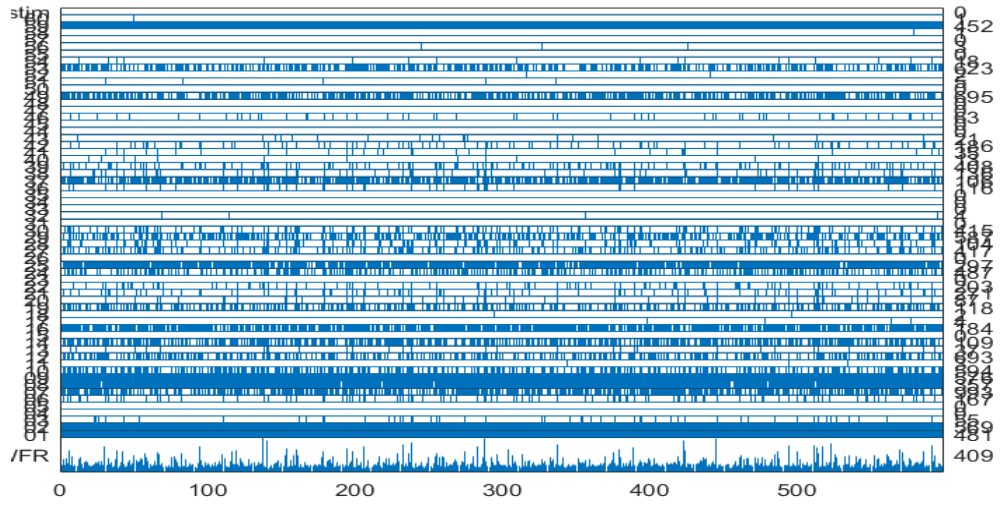
Experiment date	03/11/21
MEA nr	37619
Plating date	06/10/21
Amplitude (μA)	24
Grounded electrodes	10
Artifacts removed from baseline (%)	26,09 %
Active electrodes	25



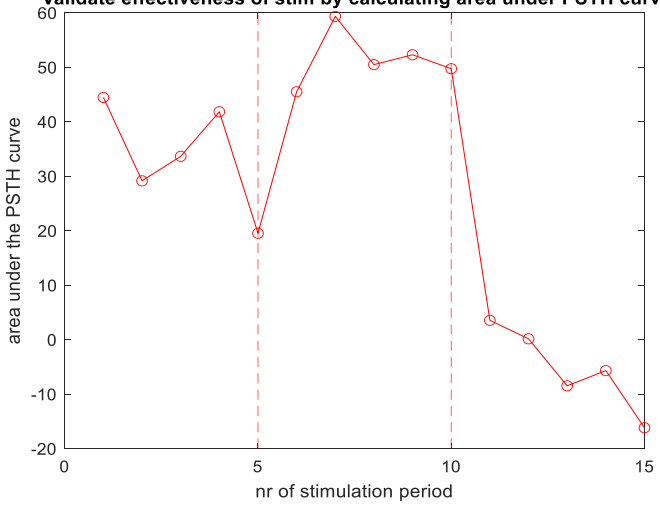
Experiment date	26/11/21
MEA nr	38857
Plating date	04/11/21
Amplitude (μA)	24
Grounded electrodes	7
Artifacts removed from baseline (%)	56,89%
Active electrodes	27



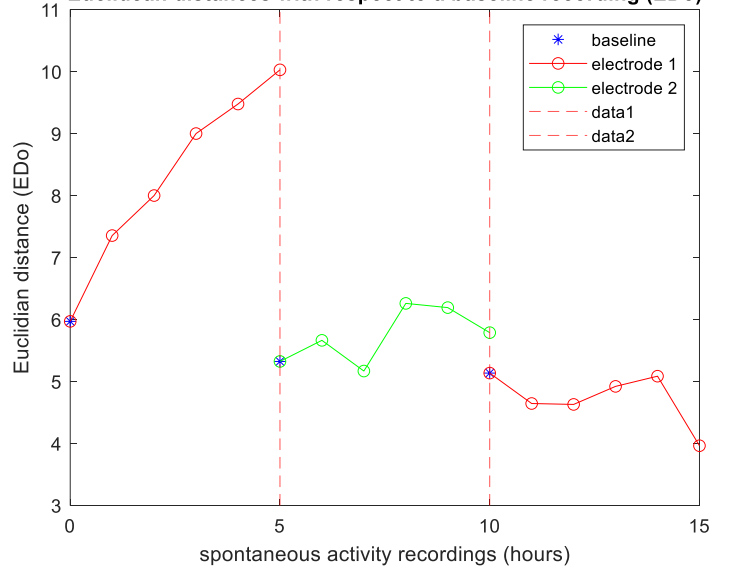
Experiment date	08/12/21
MEA nr	38857
Plating date	18/11/21
Amplitude (μ A)	24
Grounded electrodes	3
Artifacts removed from baseline (%)	18,95%
Active electrodes	21



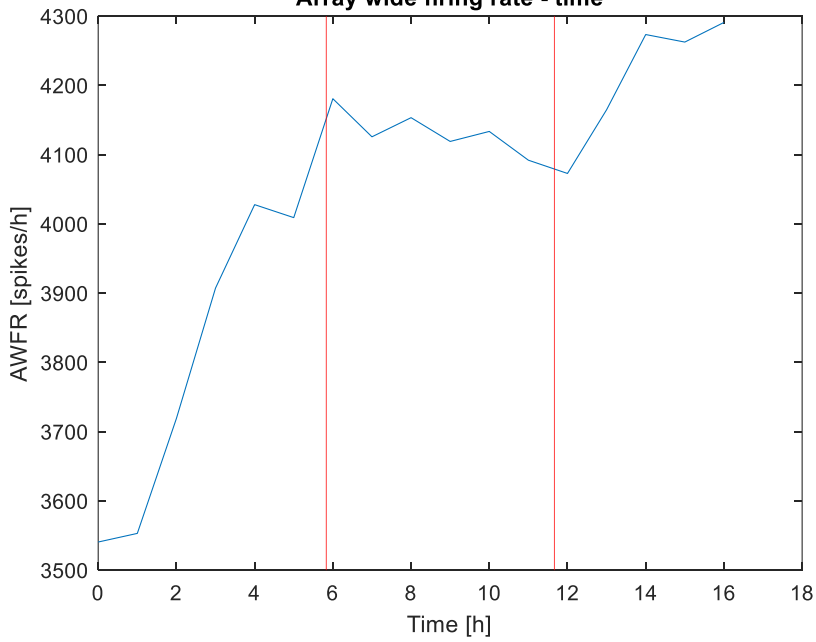
Validate effectiveness of stim by calculating area under PSTH curve



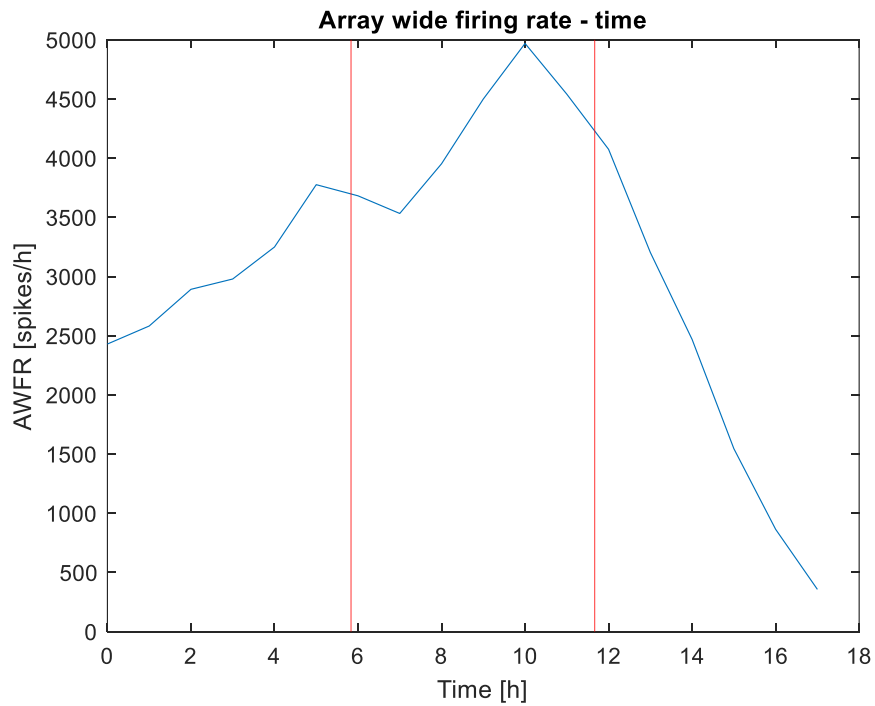
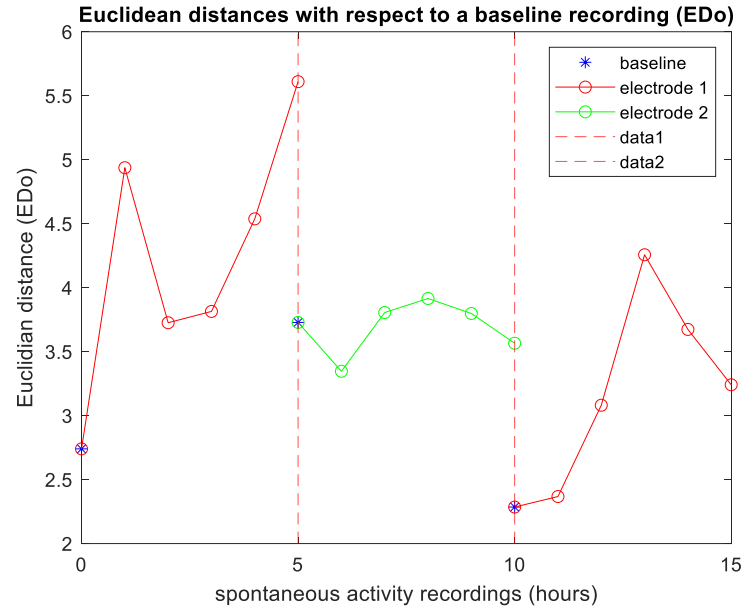
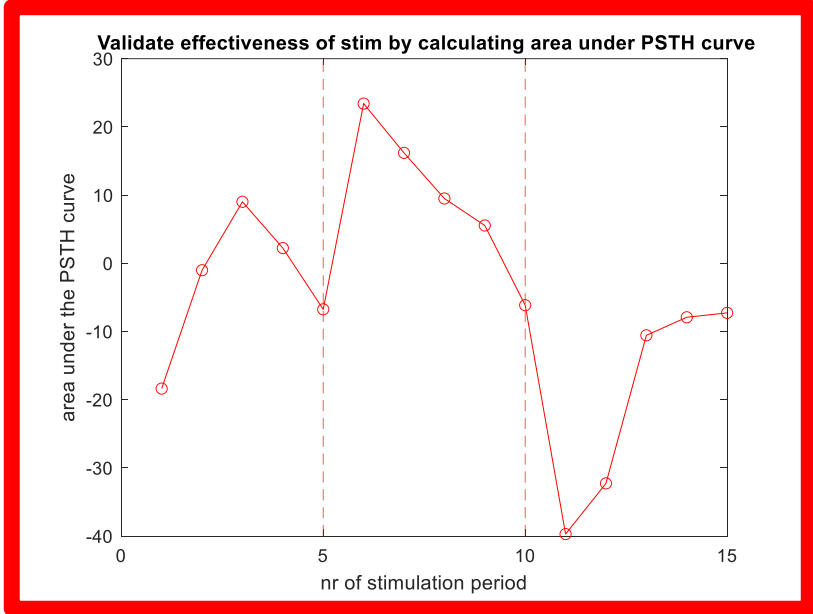
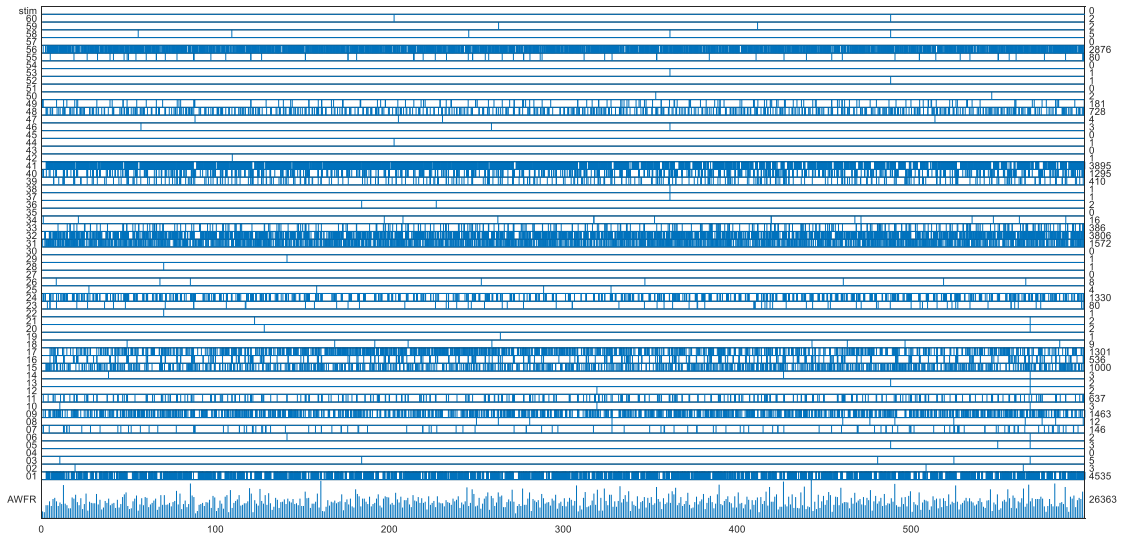
Euclidean distances with respect to a baseline recording (EDo)



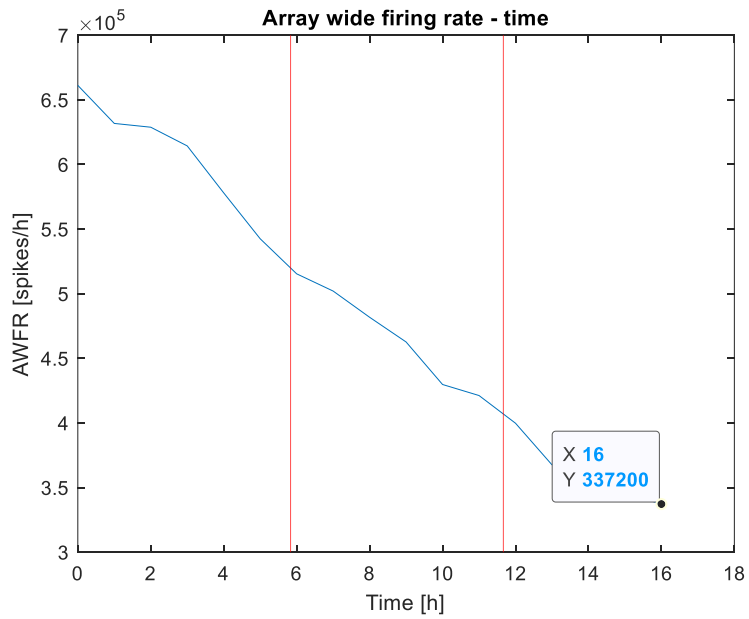
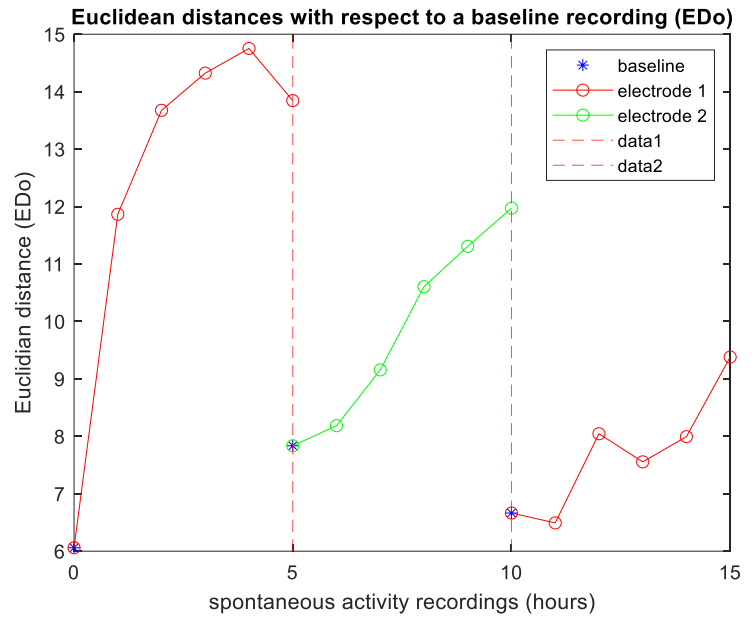
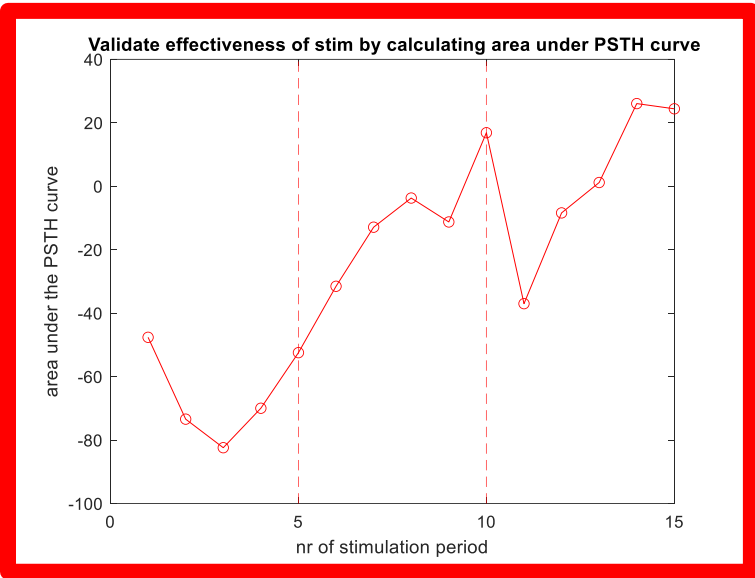
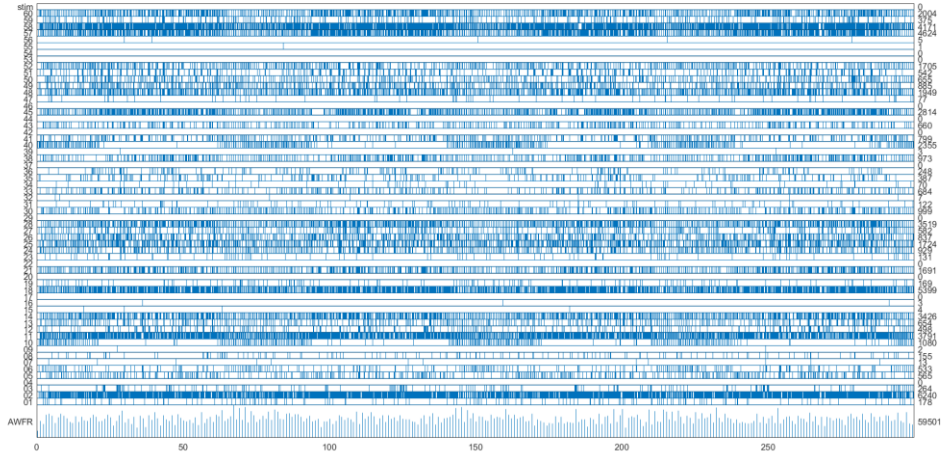
Array wide firing rate - time



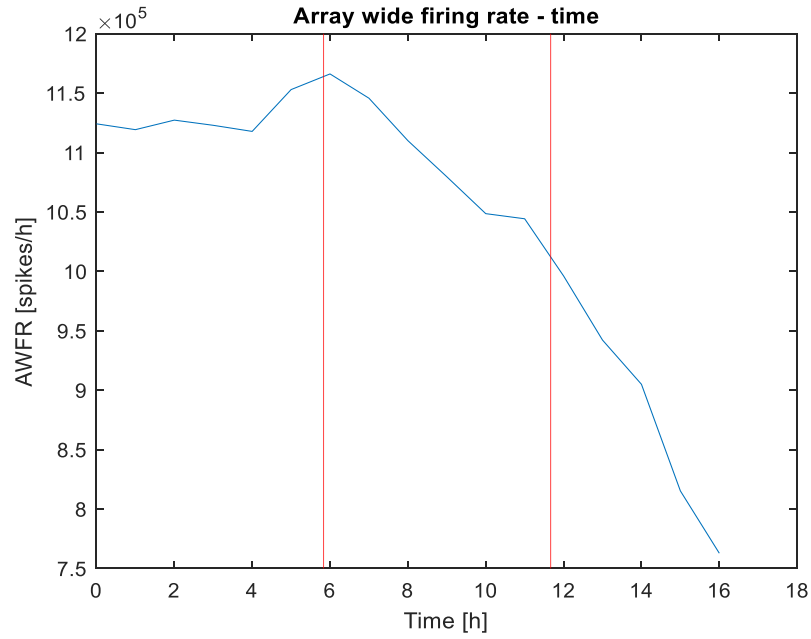
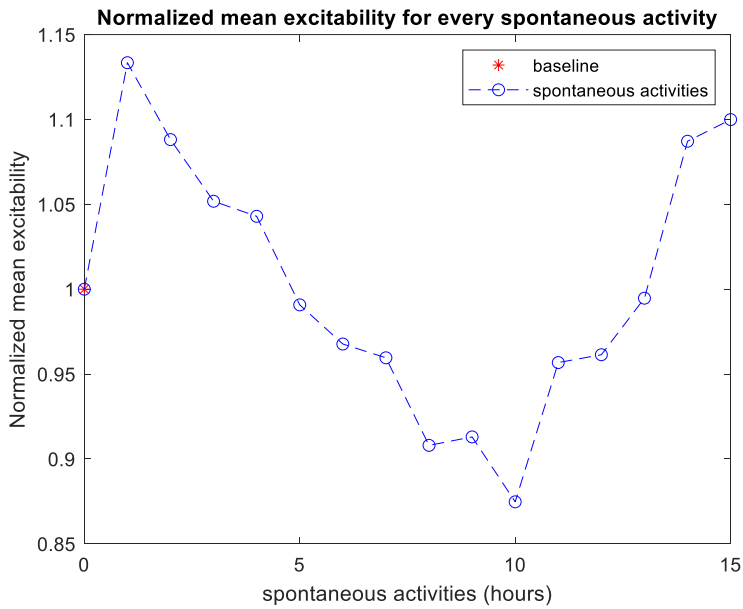
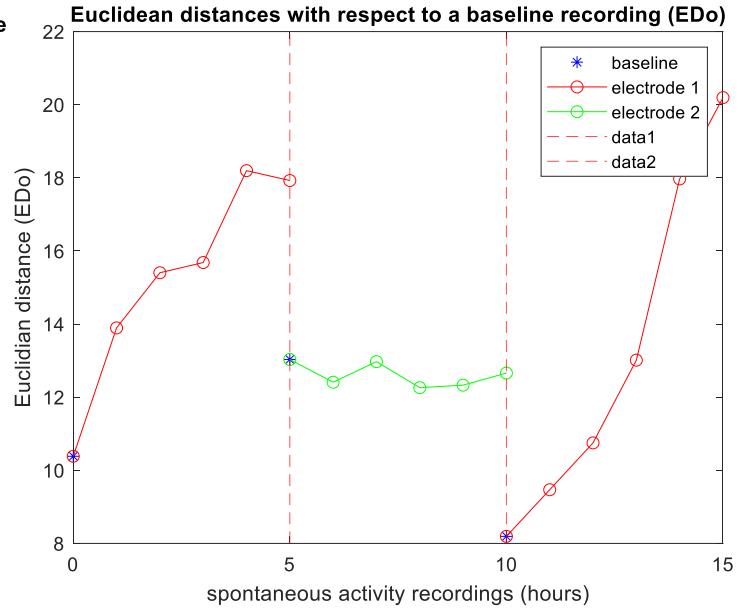
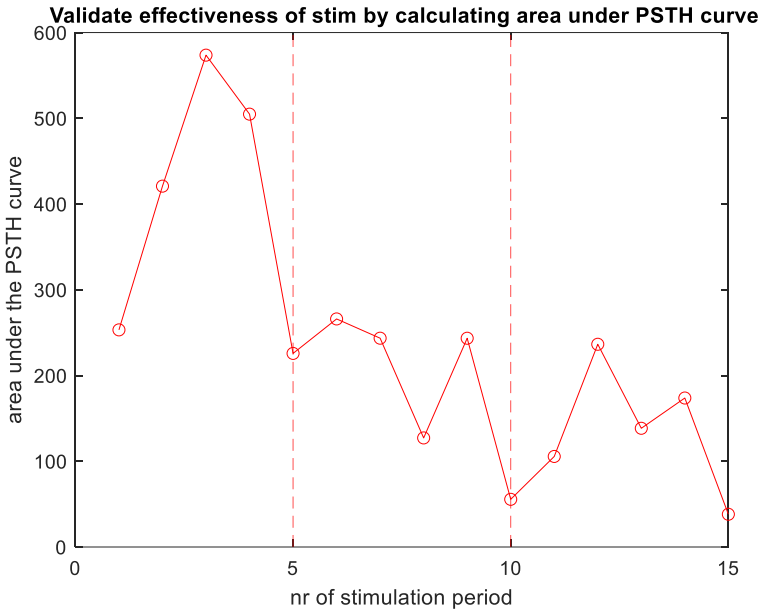
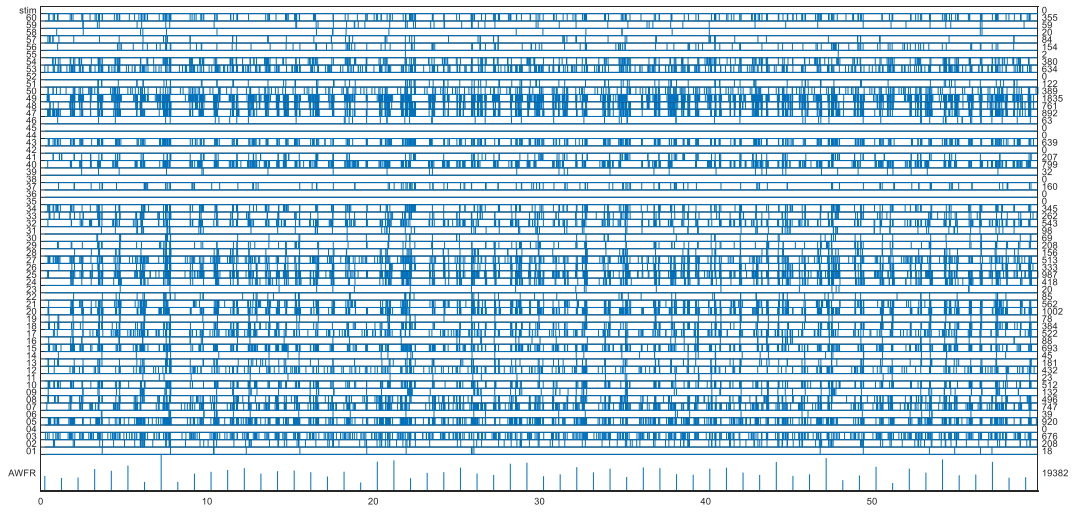
Experiment date	16/12/21
MEA nr	38860
Plating date	18/11/21
Amplitude (μA)	36
Grounded electrodes	27
Artifacts removed from baseline (%)	39,91
Active electrodes	16



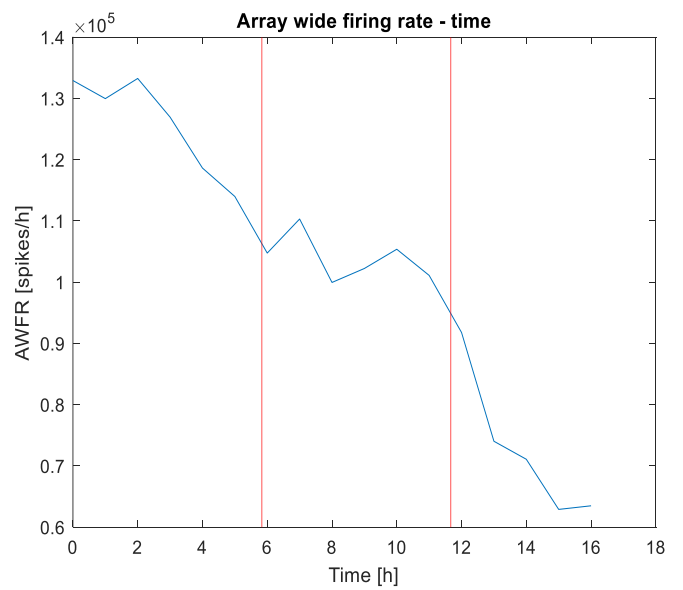
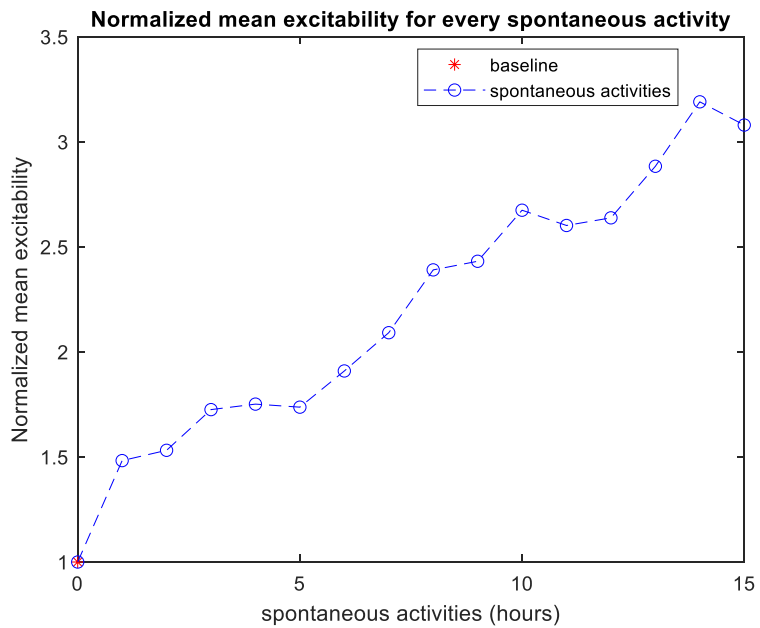
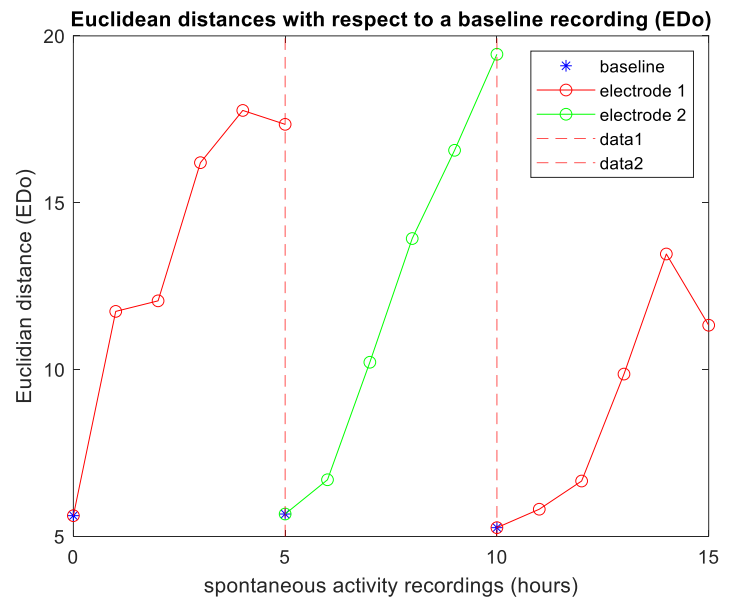
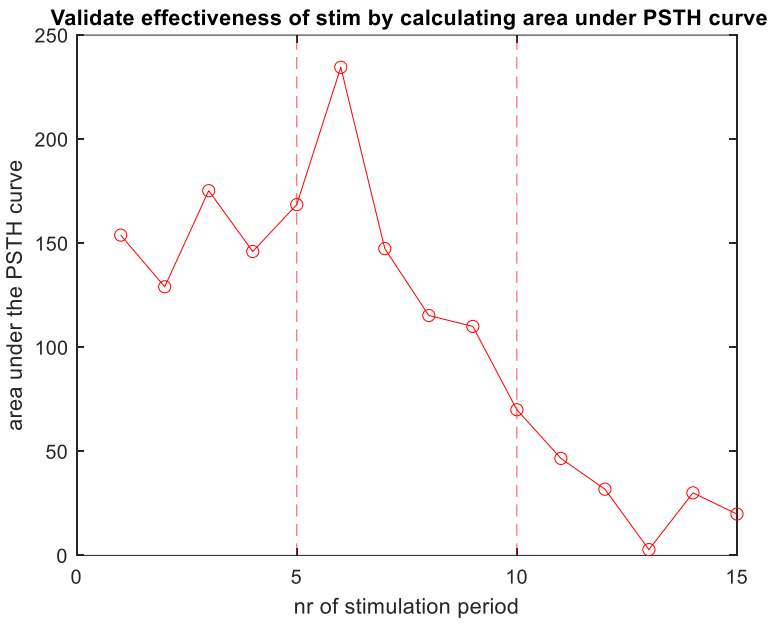
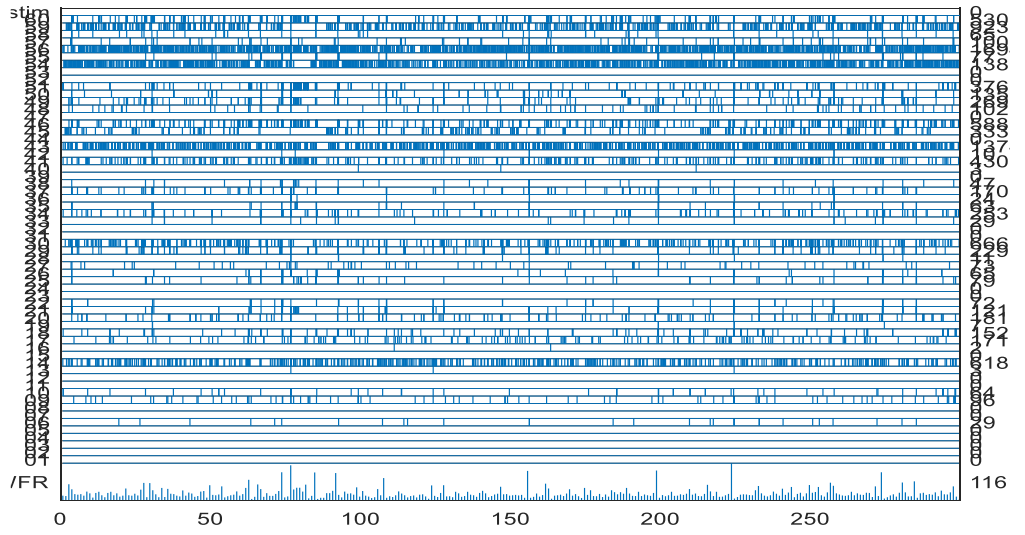
Experiment date	14/01/22
MEA nr	38897
Plating date	16/12/21
Amplitude (μA)	12
Grounded electrodes	8
Artifacts removed from baseline (%)	44,98%
Active electrodes	30



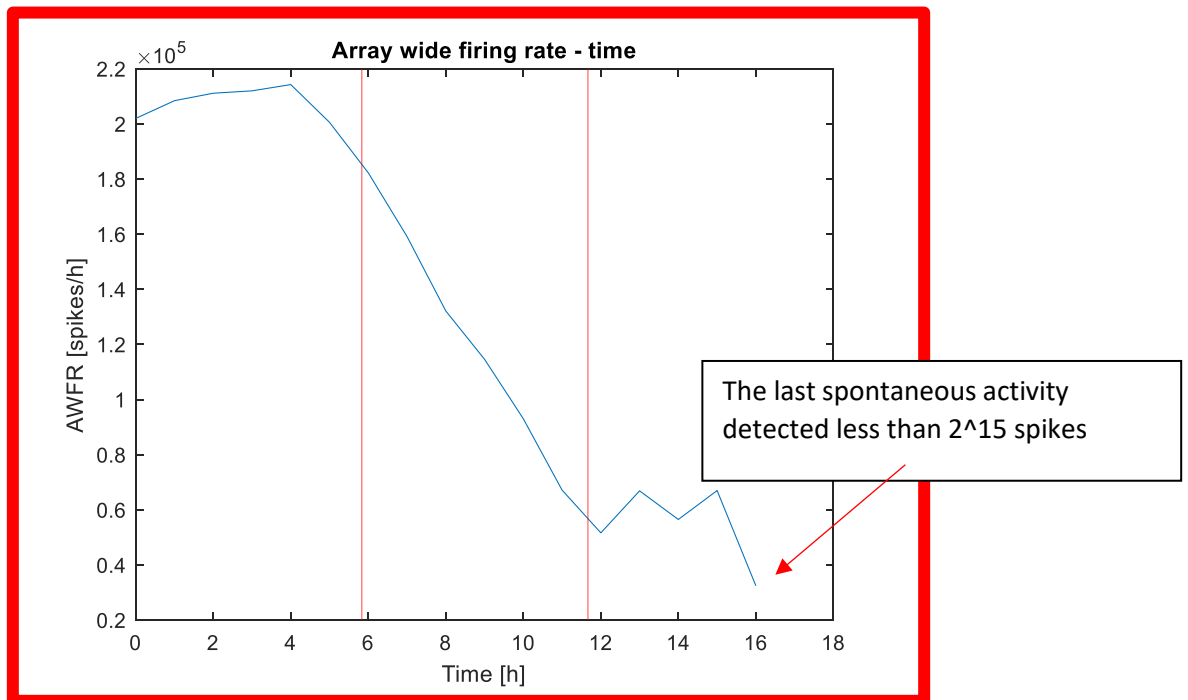
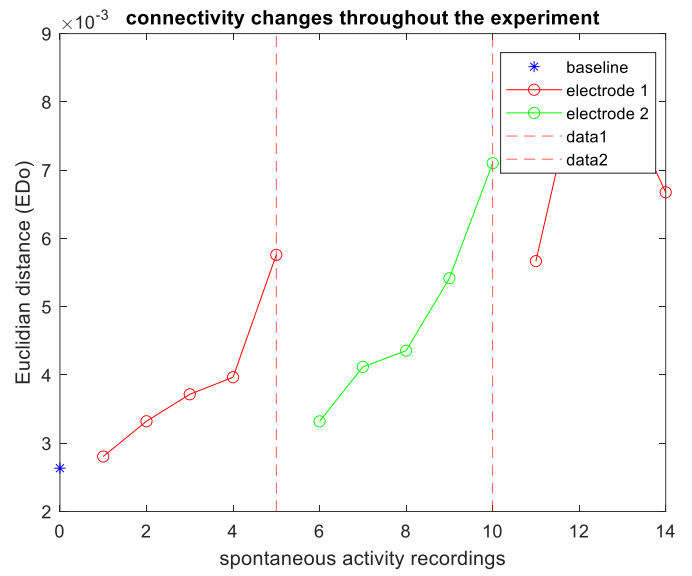
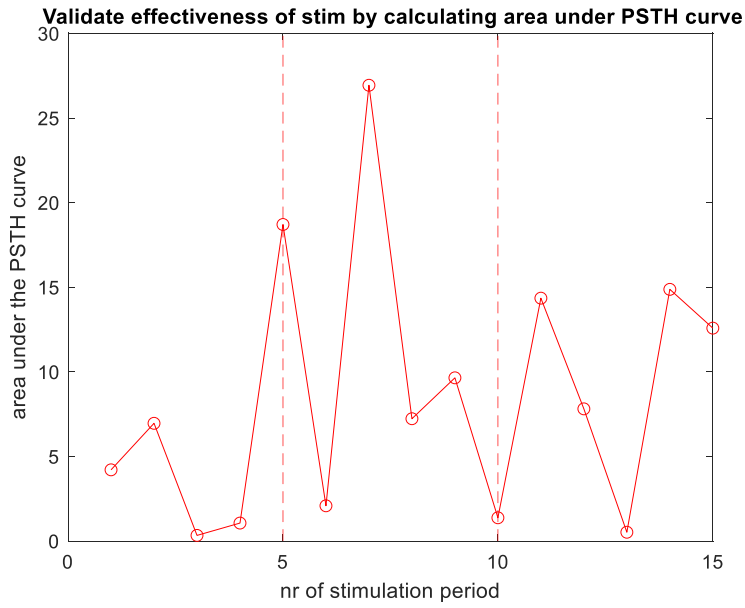
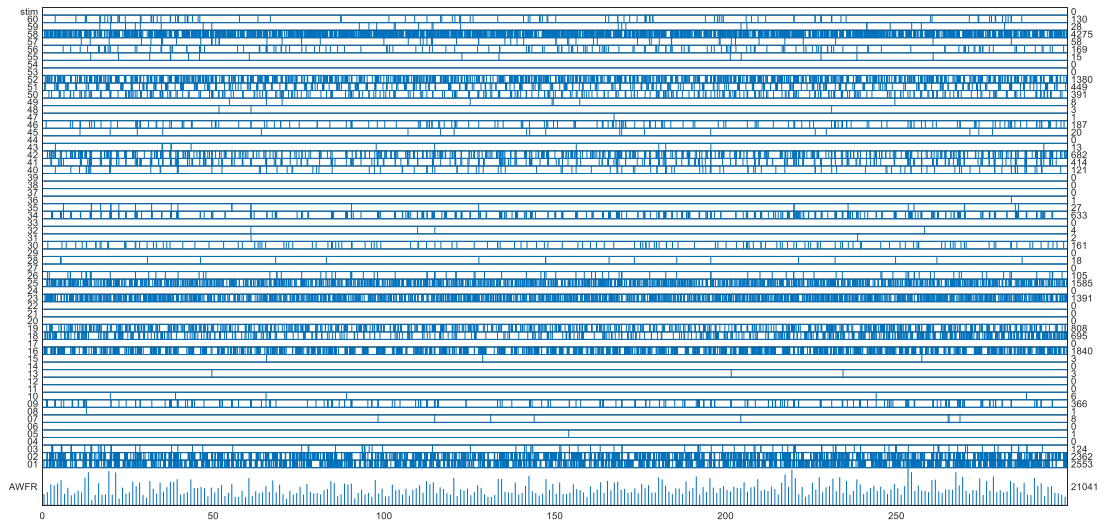
Experiment date	15/01/22
MEA nr	40314
Plating date	16/12/21
Amplitude (μA)	24
Grounded electrodes	7
Artifacts removed from baseline (%)	46,29%
Active electrodes	35



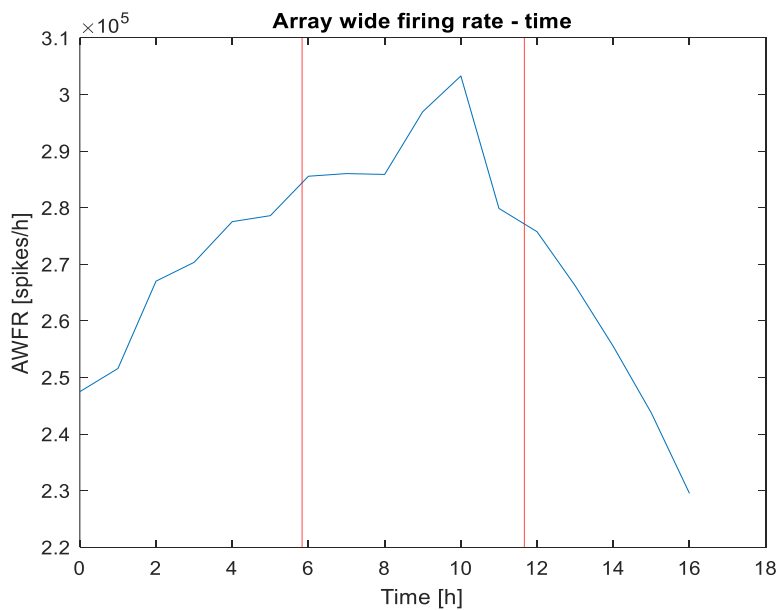
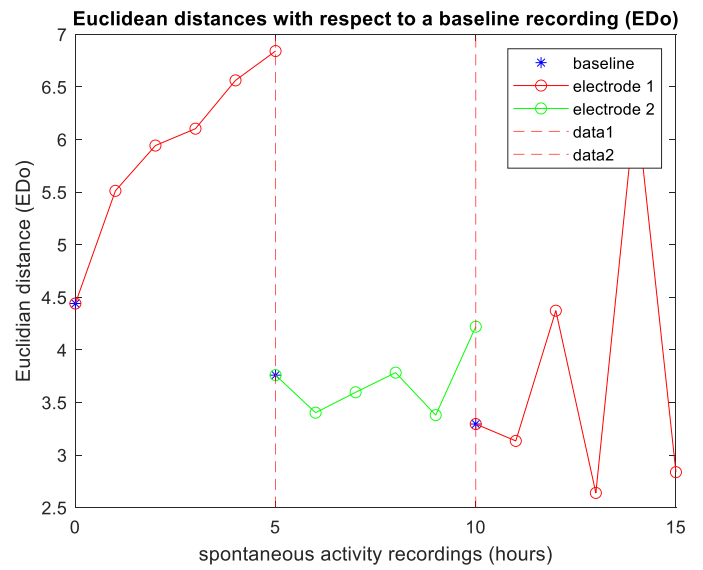
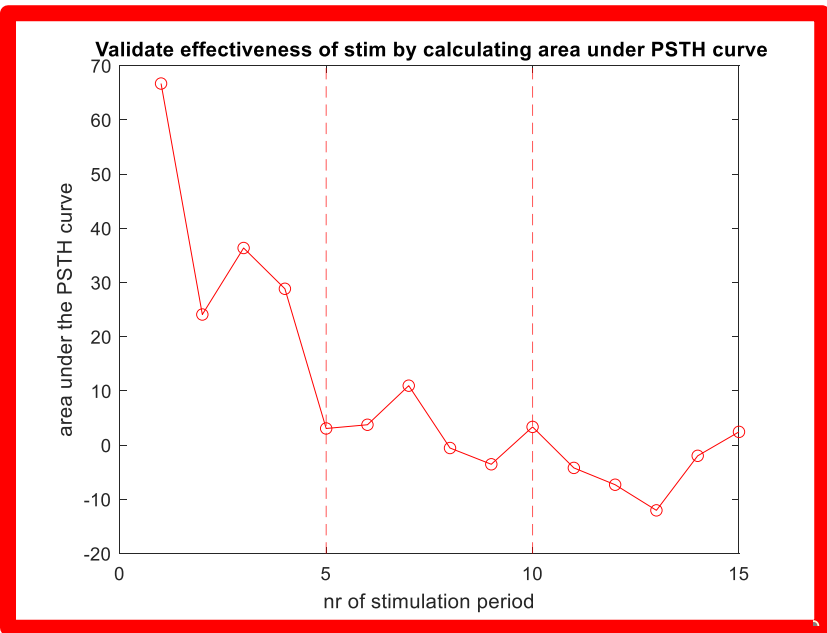
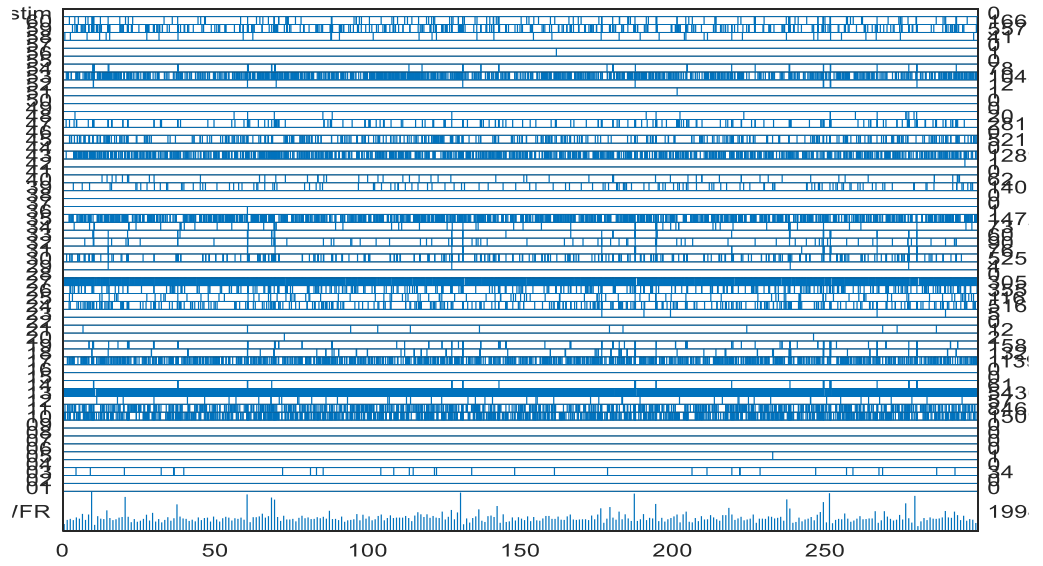
Experiment date	16/01/22
MEA nr	38857
Plating date	16/12/21
Amplitude (μA)	24
Grounded electrodes	2
Artifacts removed from baseline (%)	54,69%
Active electrodes	22



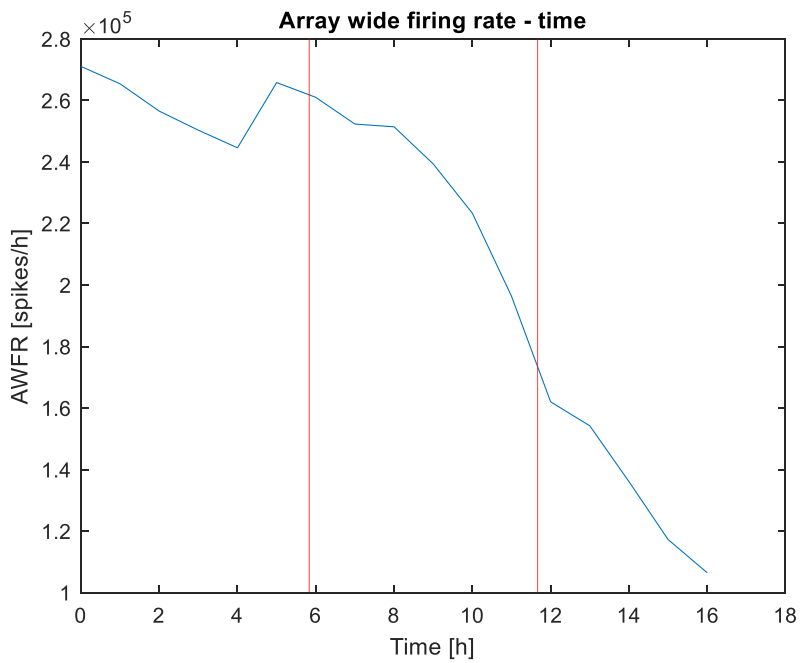
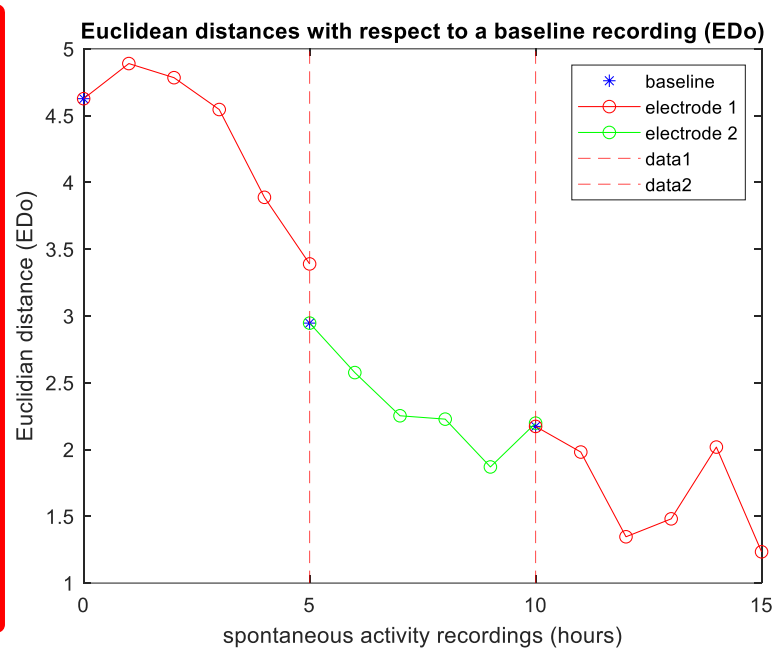
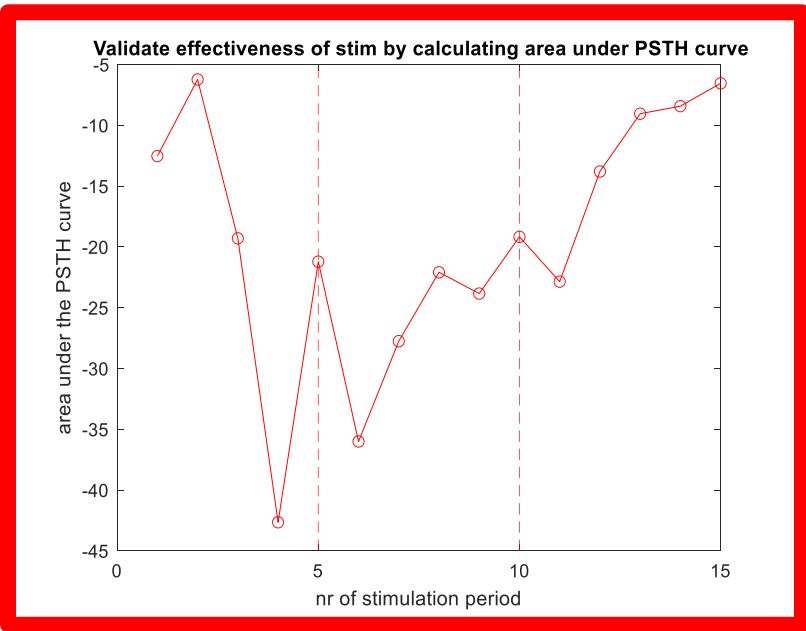
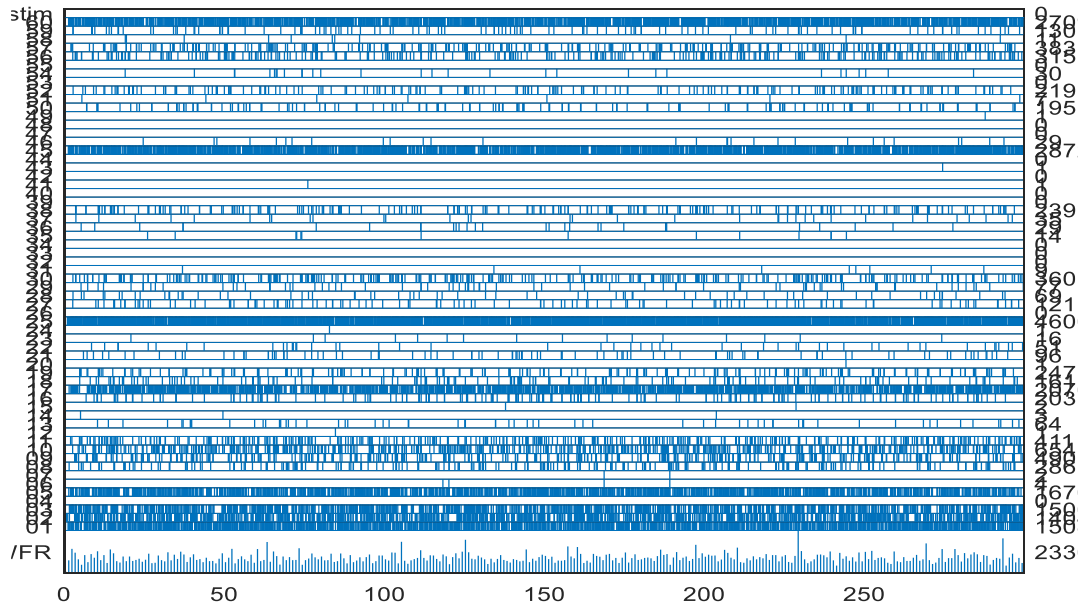
Experiment date	18/01/22
MEA nr	38859
Plating date	16/12/21
Amplitude (μA)	24
Grounded electrodes	10
Artifacts removed from baseline (%)	47,72%
Active electrodes	19



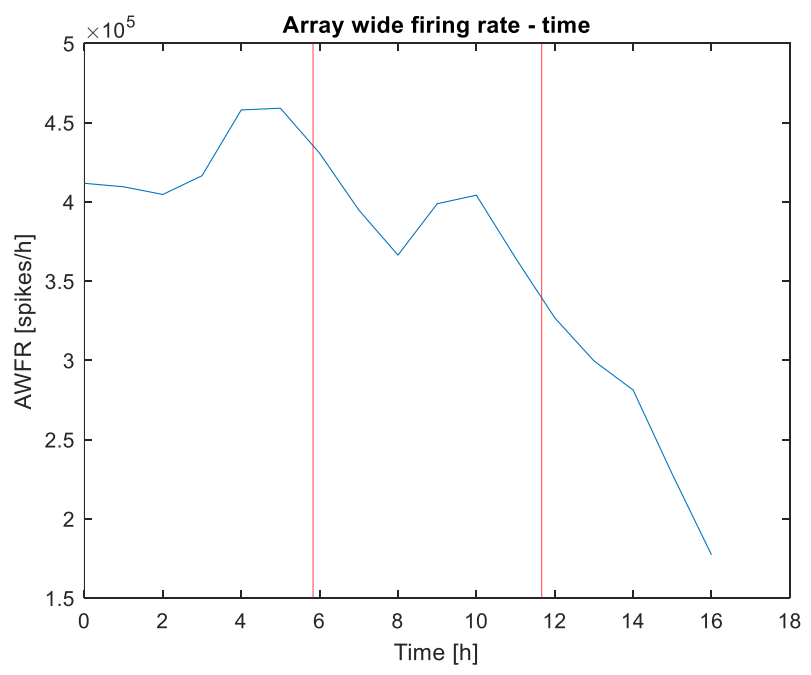
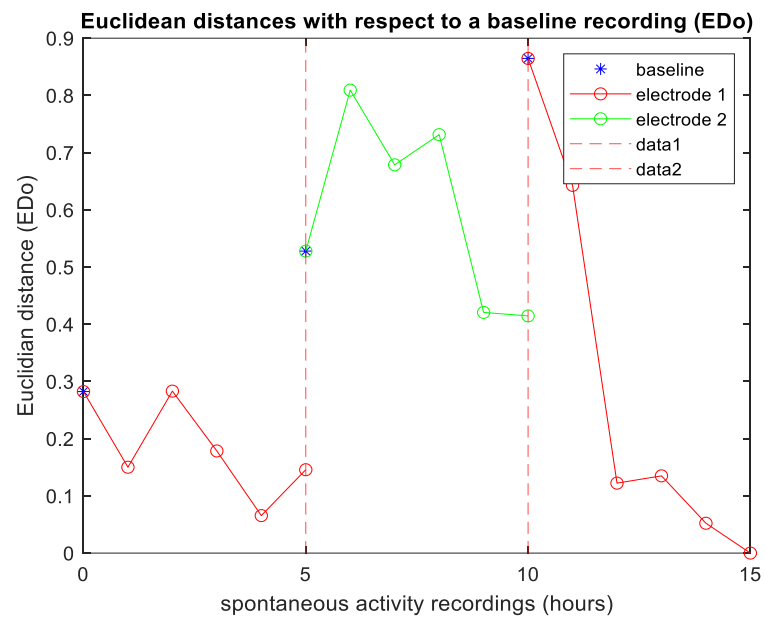
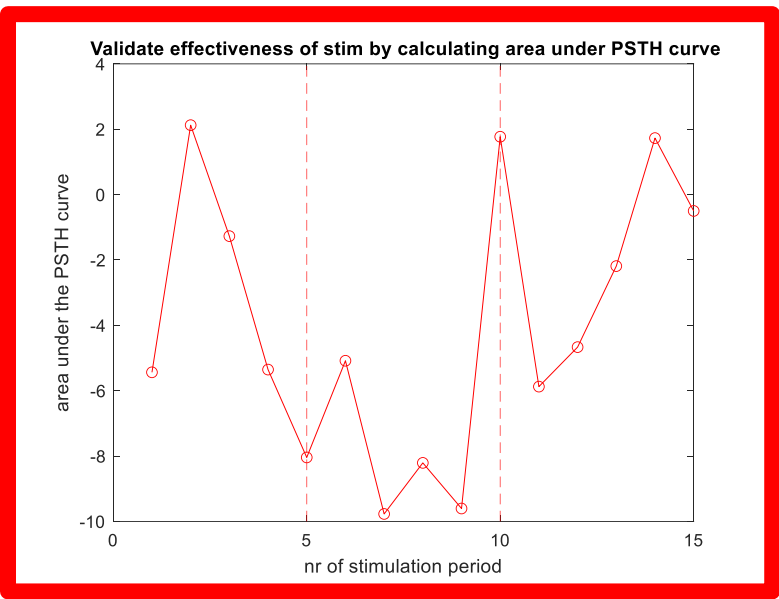
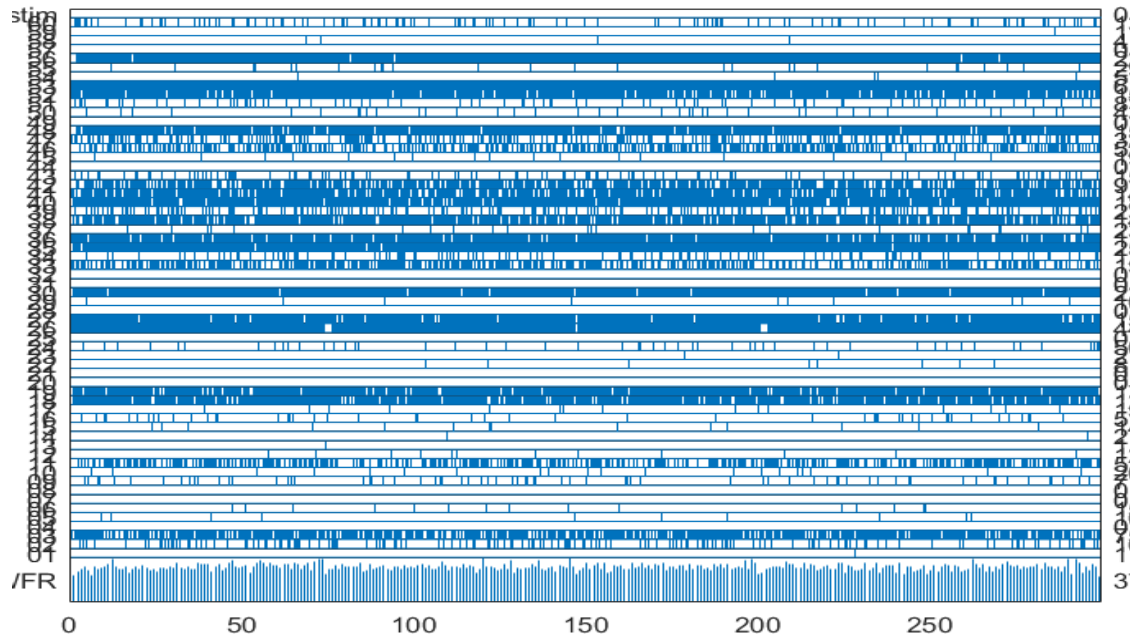
Experiment date	02/02/22
MEA nr	38900
Plating date	13/01/22
Amplitude (μA)	12
Grounded electrodes	3
Artifacts removed from baseline (%)	50,3 %
Active electrodes	18



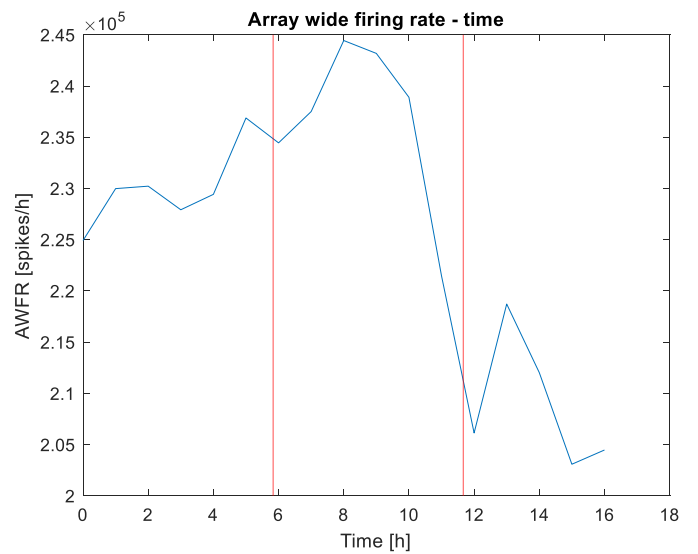
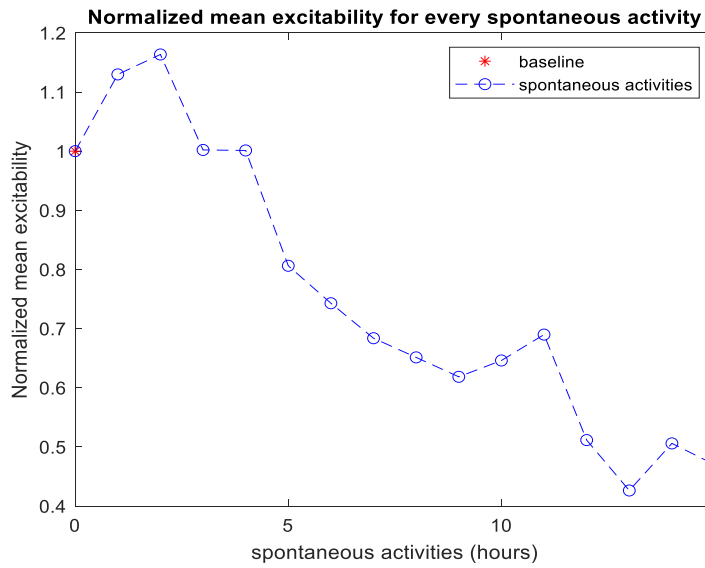
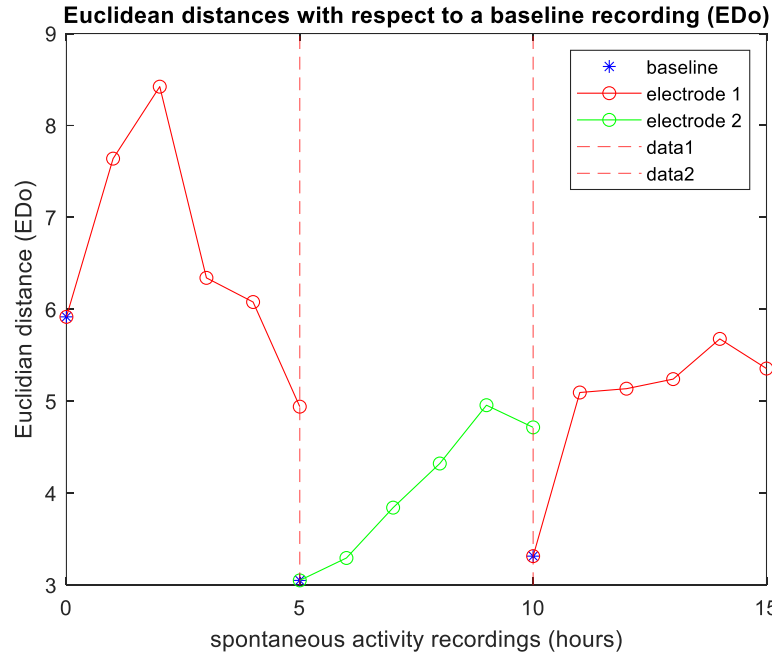
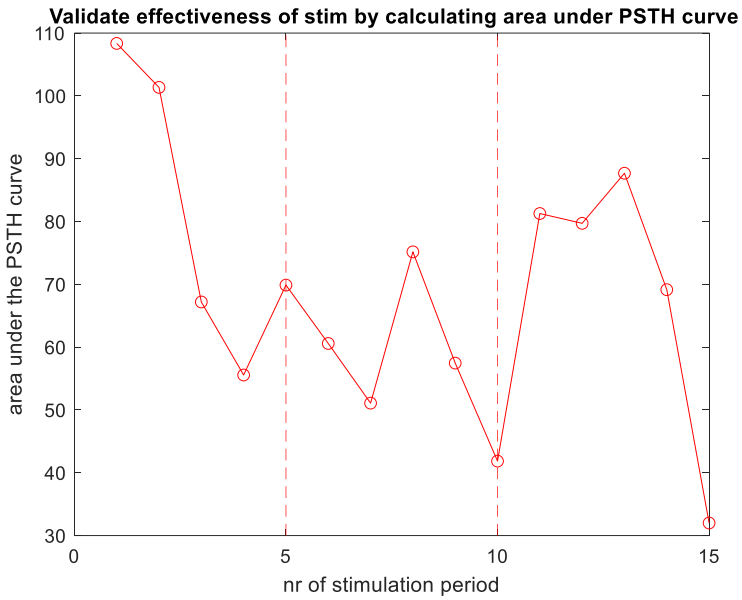
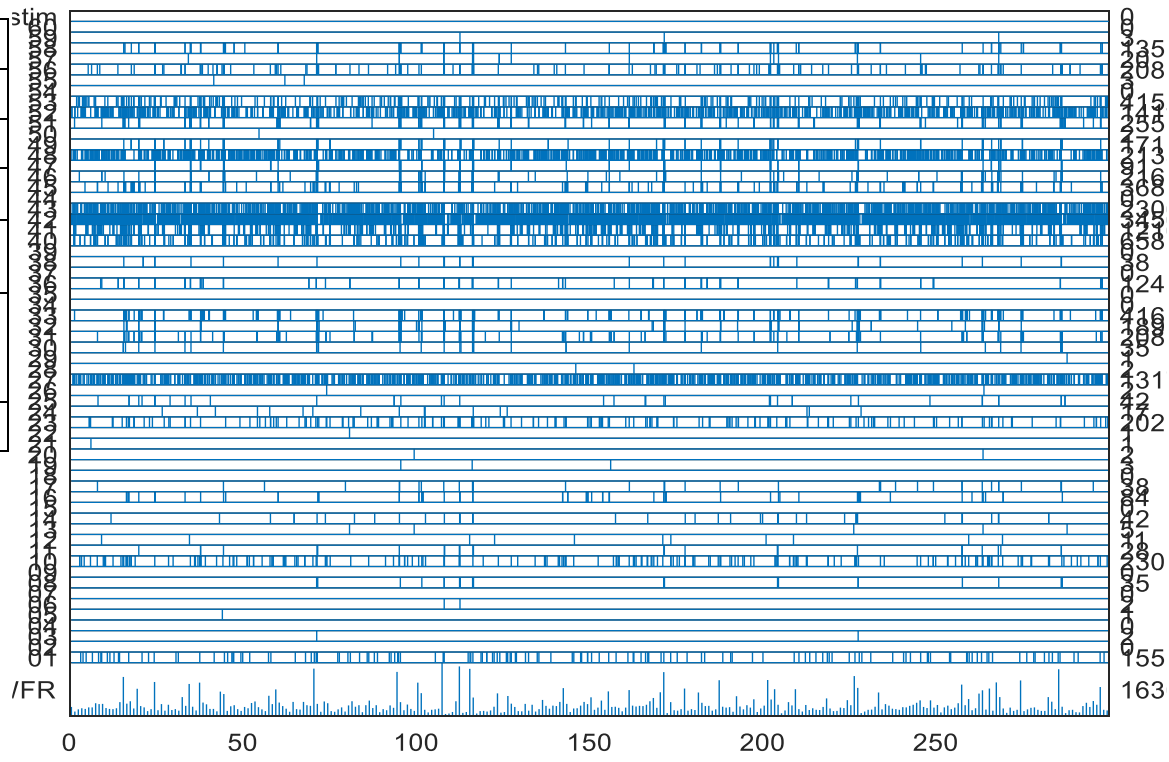
Experiment date	07/02/22
MEA nr	24851
Plating date	13/01/22
Amplitude (μ A)	36
Grounded electrodes	8
Artifacts removed from baseline (%)	43,21%
Active electrodes	18



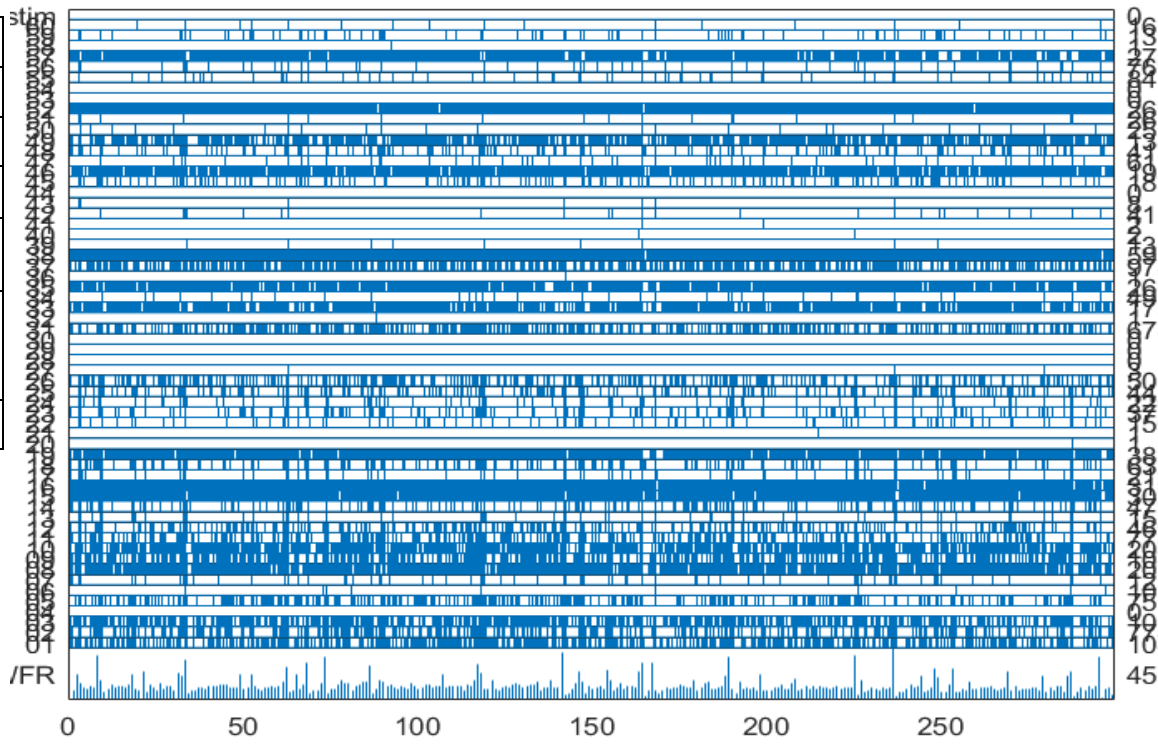
Experiment date	22/02/22
MEA nr	40319
Plating date	27/01/22
Amplitude (μA)	24
Grounded electrodes	6
Artifacts removed from baseline (%)	64,86%
Active electrodes	20



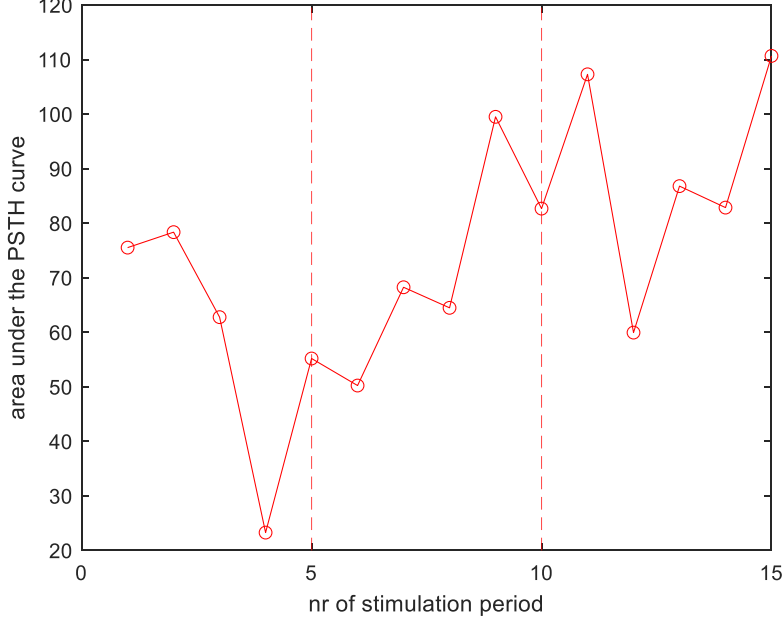
Experiment date	01/03/22
MEA nr	38897
Plating date	09/02/22
Amplitude (μA)	24
Grounded electrodes	11
Artifacts removed from baseline (%)	30,24%
Active electrodes	20



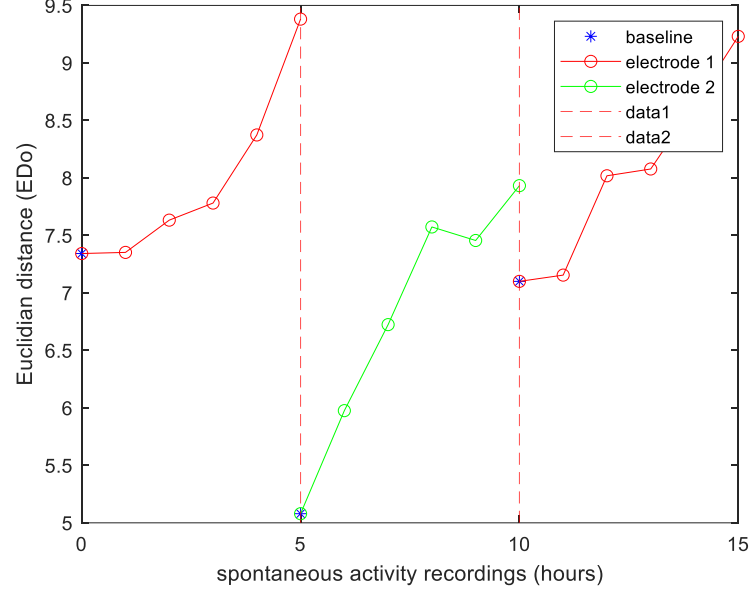
Experiment date	02/03/22
MEA nr	40459
Plating date	09/02/22
Amplitude (μA)	24
Grounded electrodes	6
Artifacts removed from baseline (%)	43,19%
Active electrodes	27



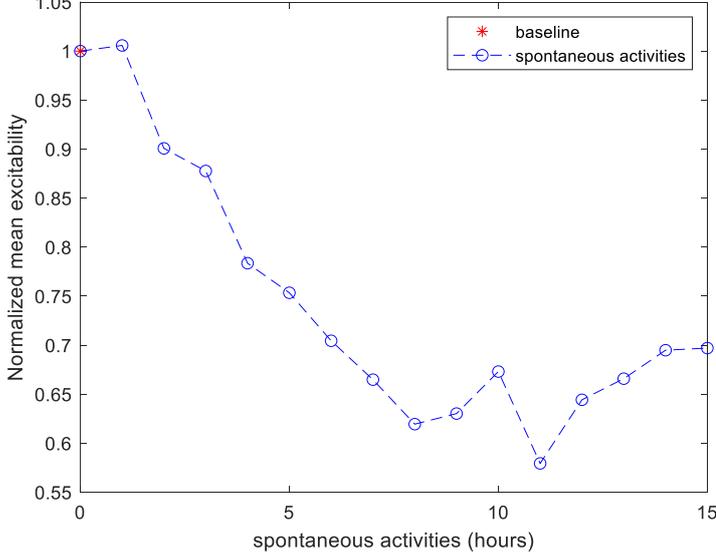
Validate effectiveness of stim by calculating area under PSTH curve



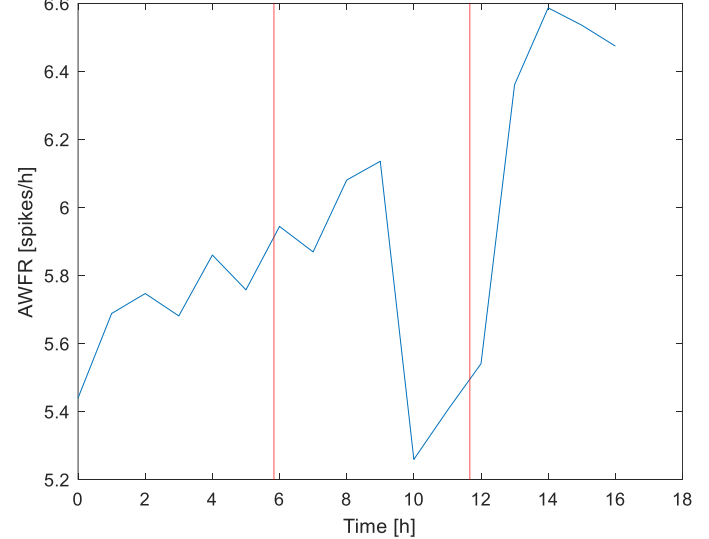
Euclidean distances with respect to a baseline recording (EDo)



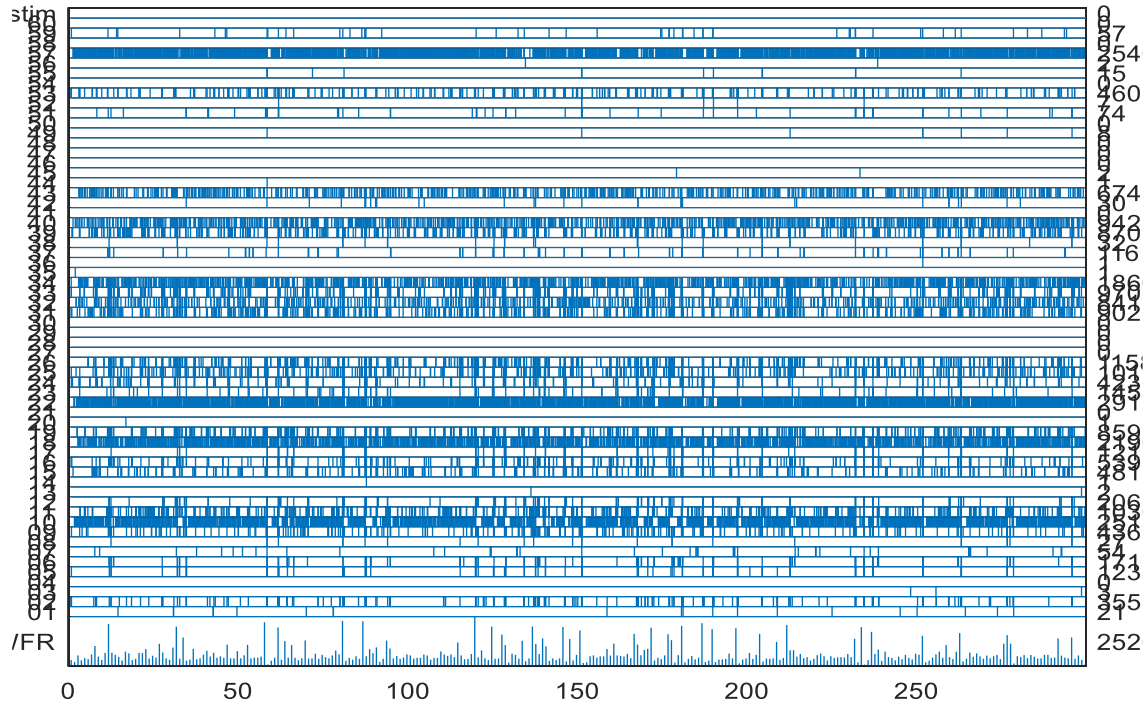
Normalized mean excitability for every spontaneous activity



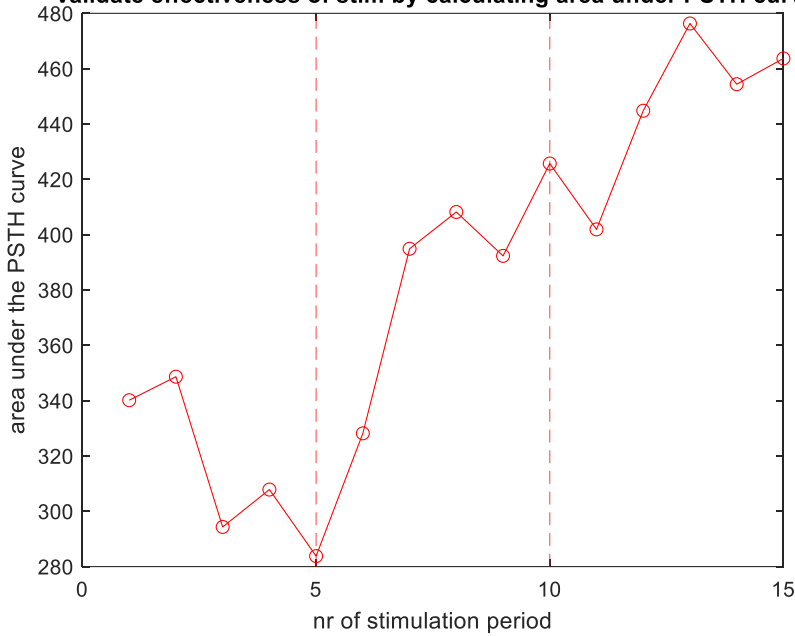
Array wide firing rate - time



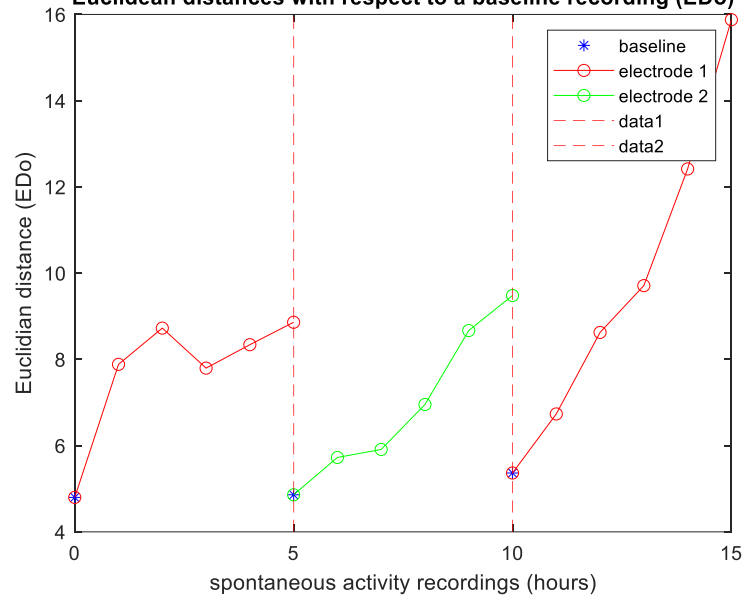
Experiment date	04/03/22
MEA nr	38857
Plating date	09/02/22
Amplitude (μA)	24
Grounded electrodes	11
Artifacts removed from baseline (%)	36,97%
Active electrodes	23



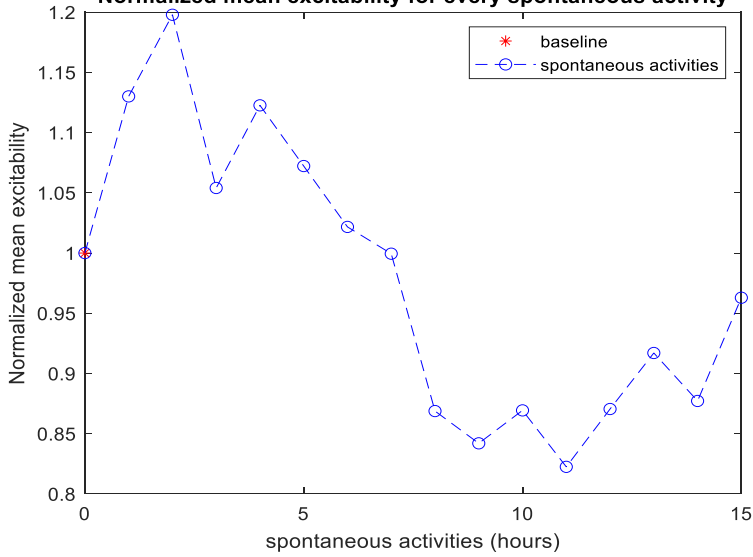
Validate effectiveness of stim by calculating area under PSTH curve



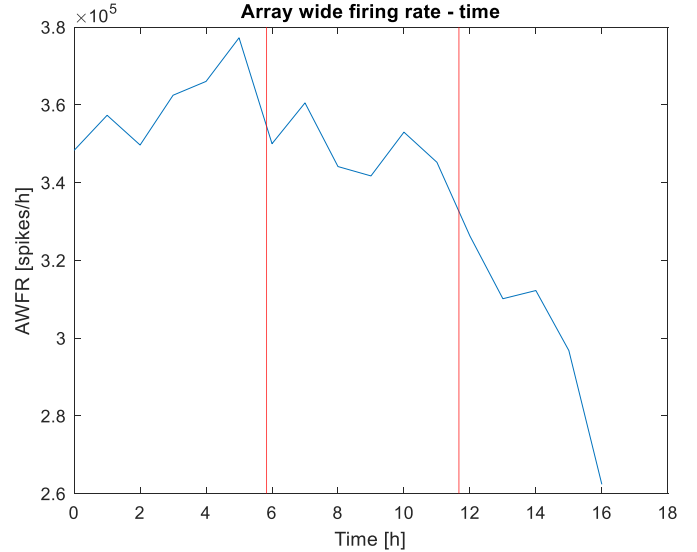
Euclidean distances with respect to a baseline recording (EDo)



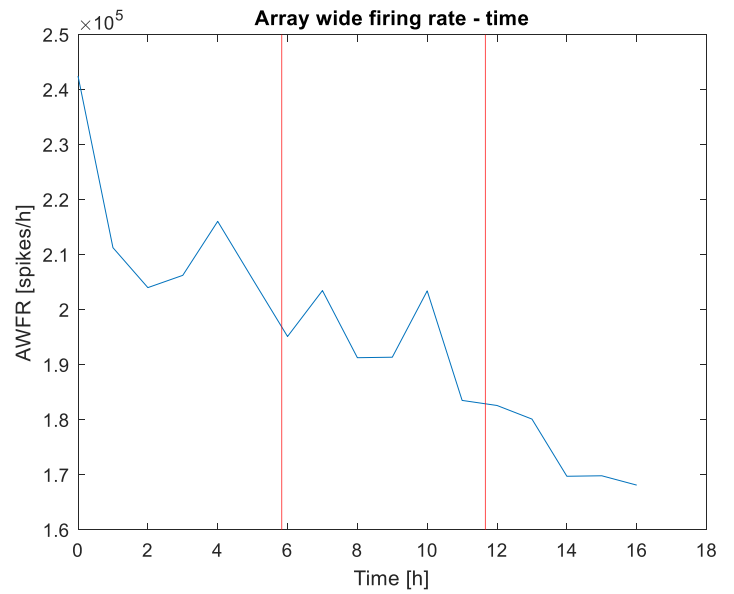
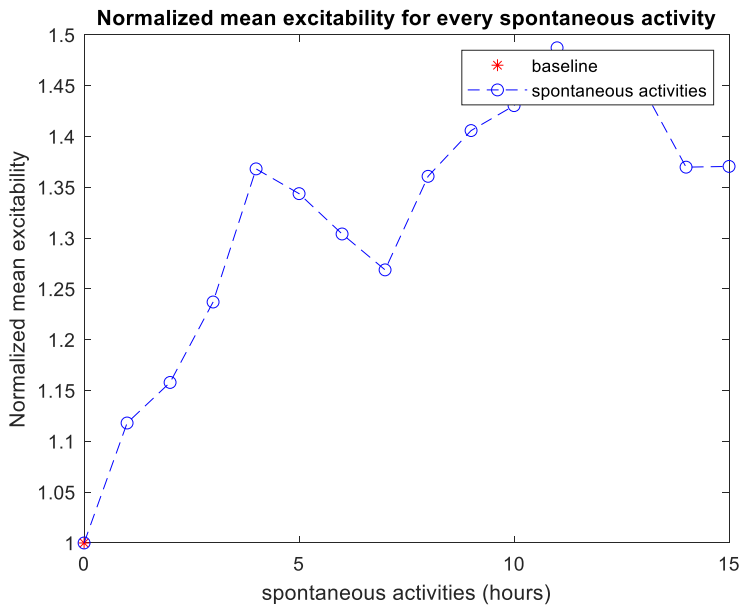
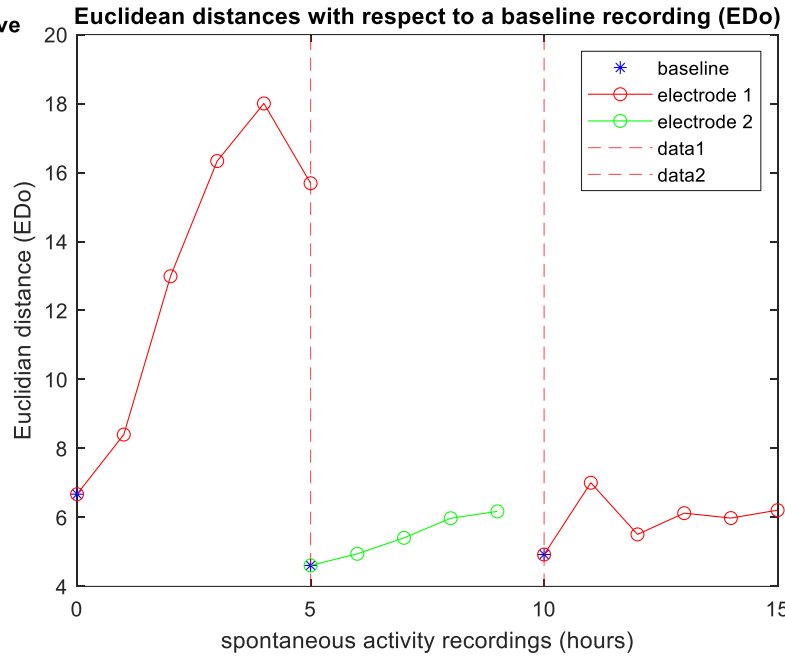
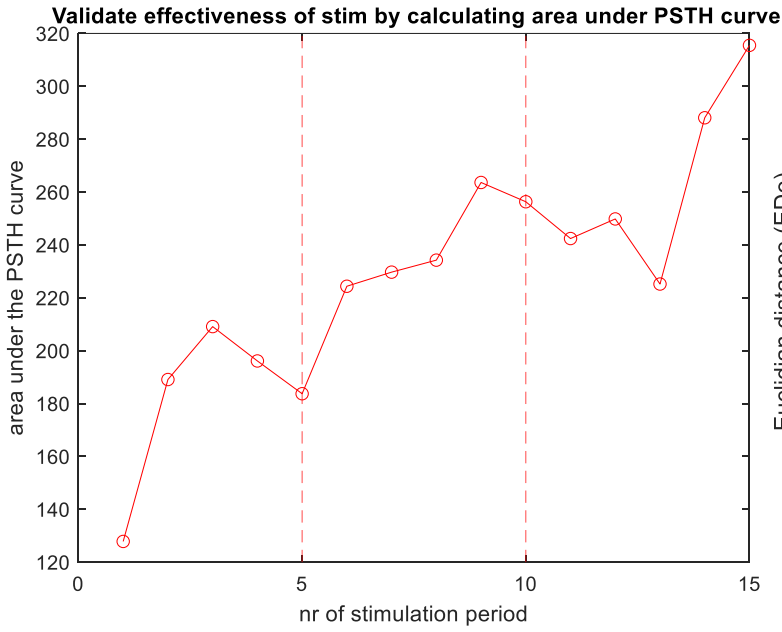
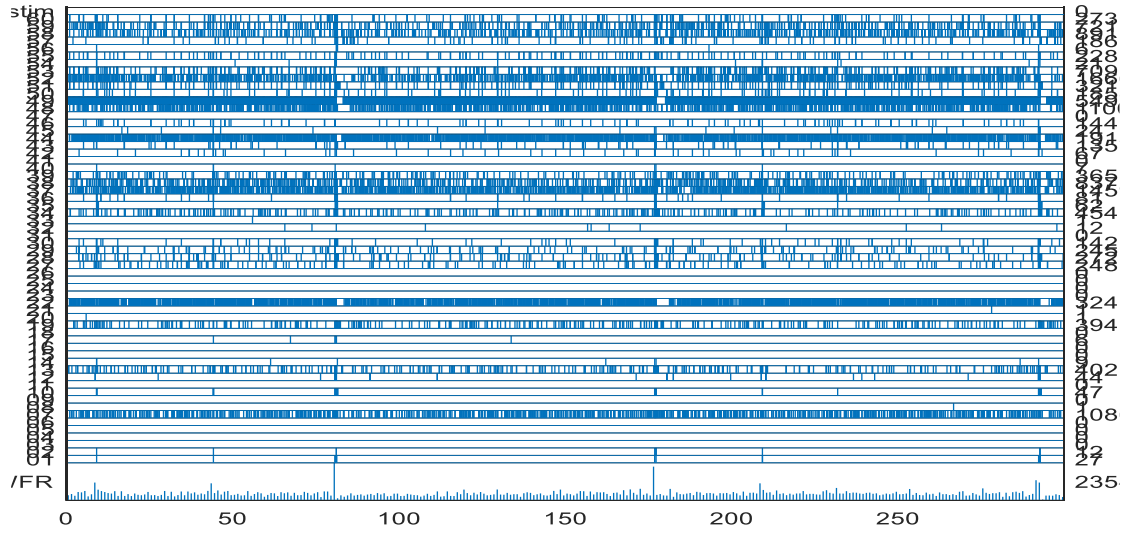
Normalized mean excitability for every spontaneous activity



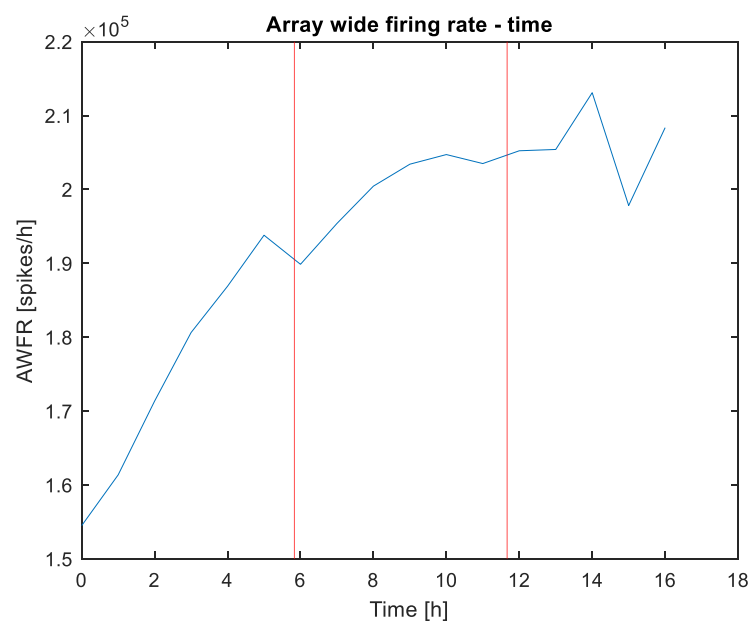
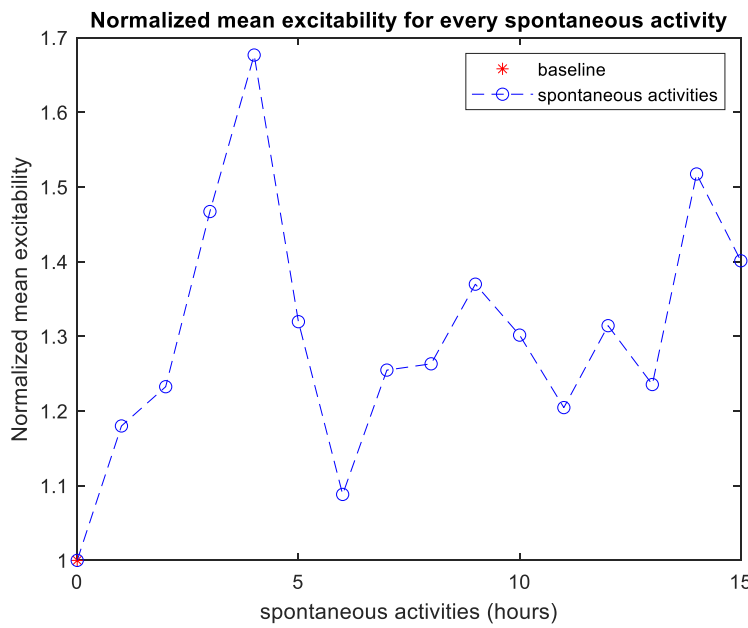
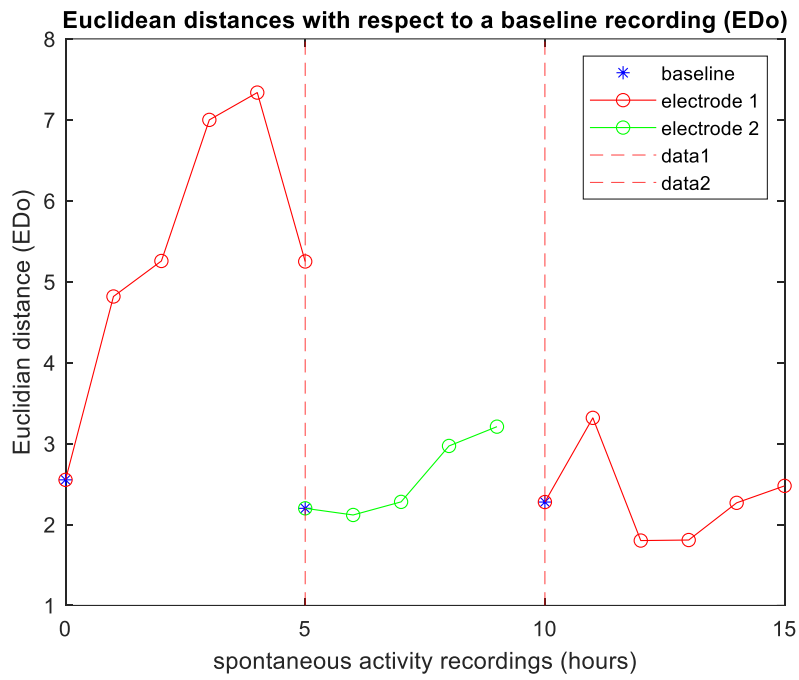
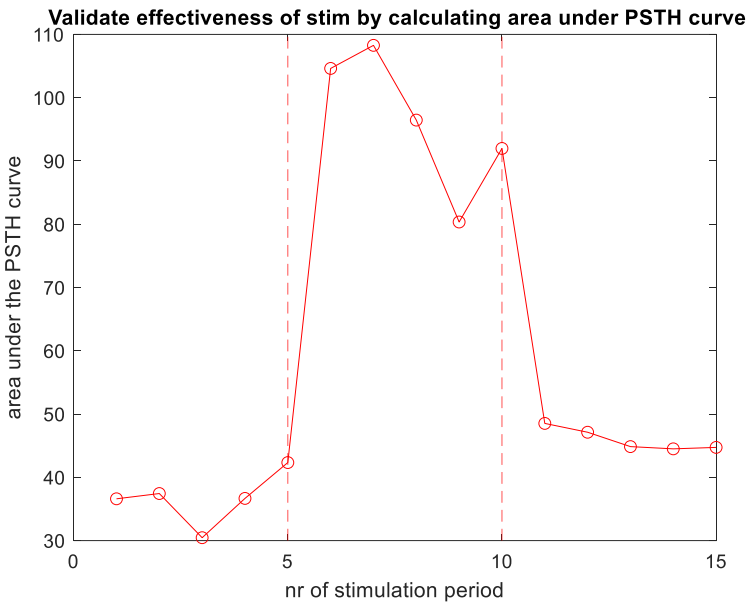
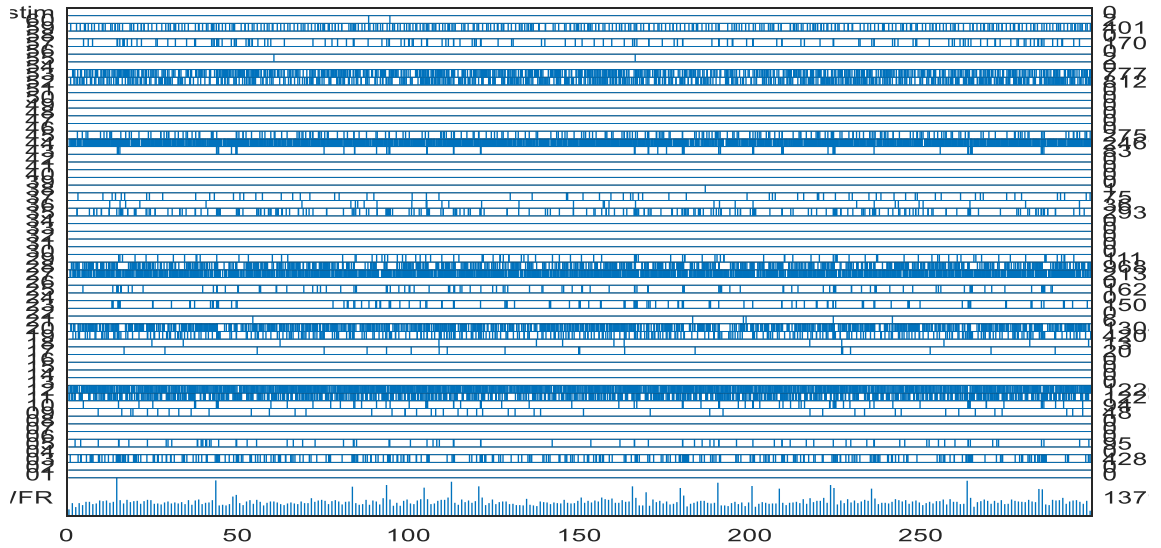
Array wide firing rate - time



Experiment date	21/06/22
MEA nr	40314
Plating date	02/06/22
Amplitude (μA)	24
Grounded electrodes	0
Artifacts removed from baseline (%)	16,59%
Active electrodes	24



Experiment date	23/06/22
MEA nr	38898
Plating date	02/06/22
Amplitude (μA)	32
Grounded electrodes	0
Artifacts removed from baseline (%)	20,57%
Active electrodes	18



A.3 Background input memory experiments

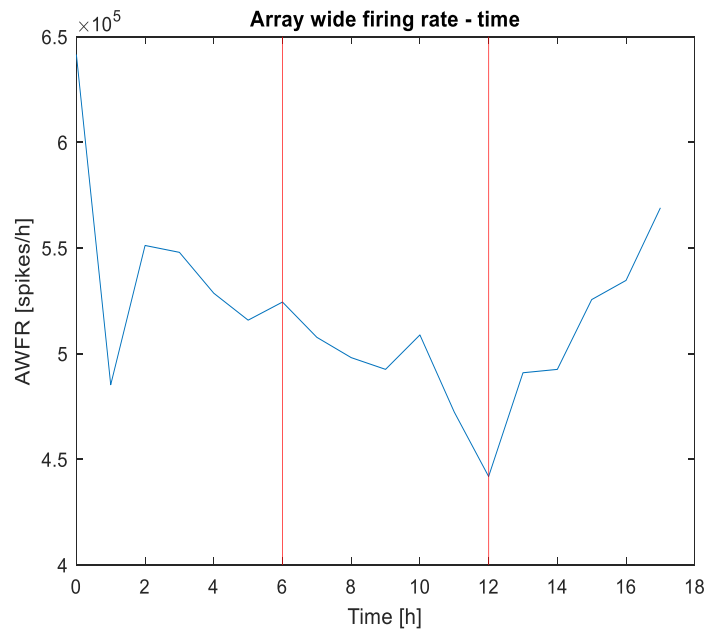
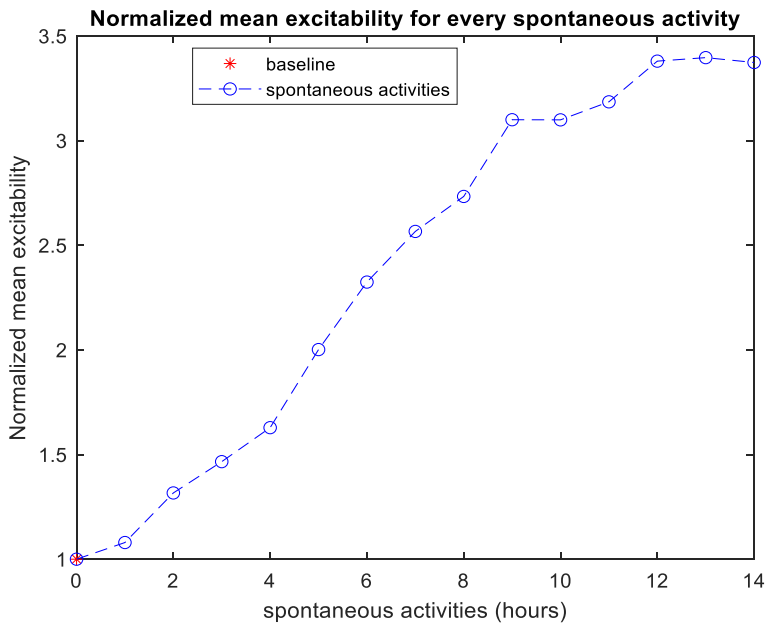
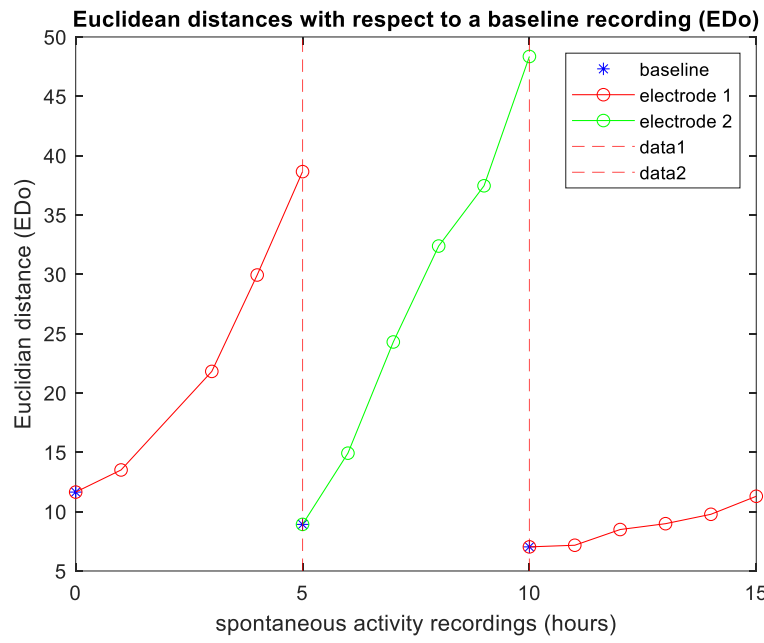
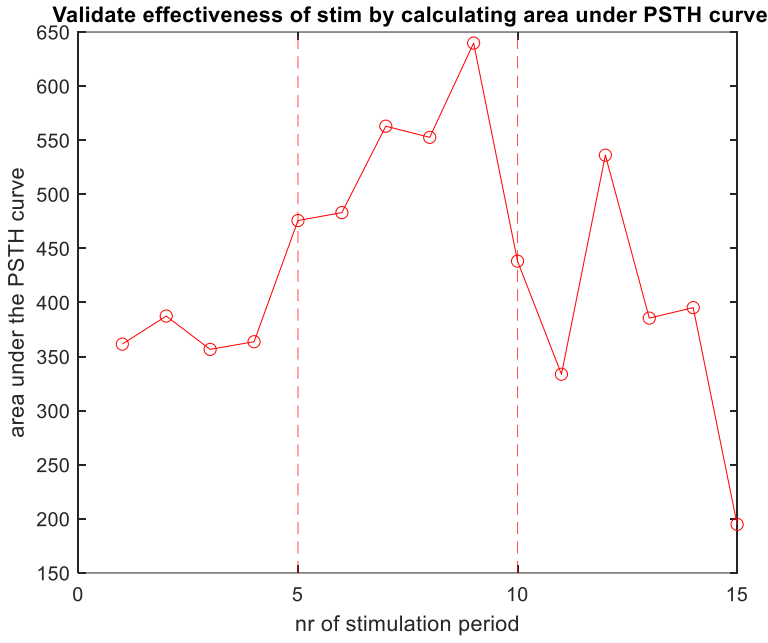
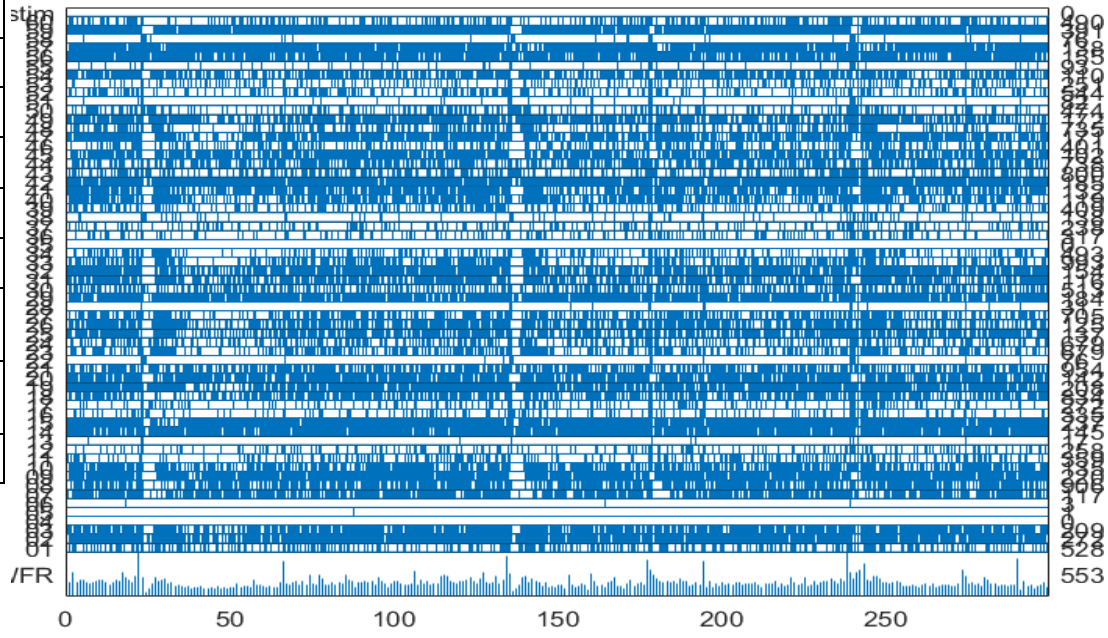
In each of these experiments we illustrate:

- A raster plot
- The area under the curve (AUC) of the mean post-stimulus time histogram (PSTH) which quantifies the effectiveness of electrical stimulation. If $AUC < 0$ the graph is depicted with a red border and this experiment is excluded.
- The Euclidean distance between baselines and spontaneous activity recordings (EDo) which quantifies connectivity changes in the network.
- The array-wide firing rate. This metric was not used in the main report illustrates the number of spikes detected from all the electrodes at any time of the experiment. If the detected spikes are $< 2^{15}$ then experiment is not included and the graph is illustrated with a red outline.
- Finally, we show a normalized graph of SPR strengths which serve as an estimate of network excitability during spontaneous activity recordings. This graph is only shown if the experiment was not meeting any of the exclusion criteria stated in section 2.3.

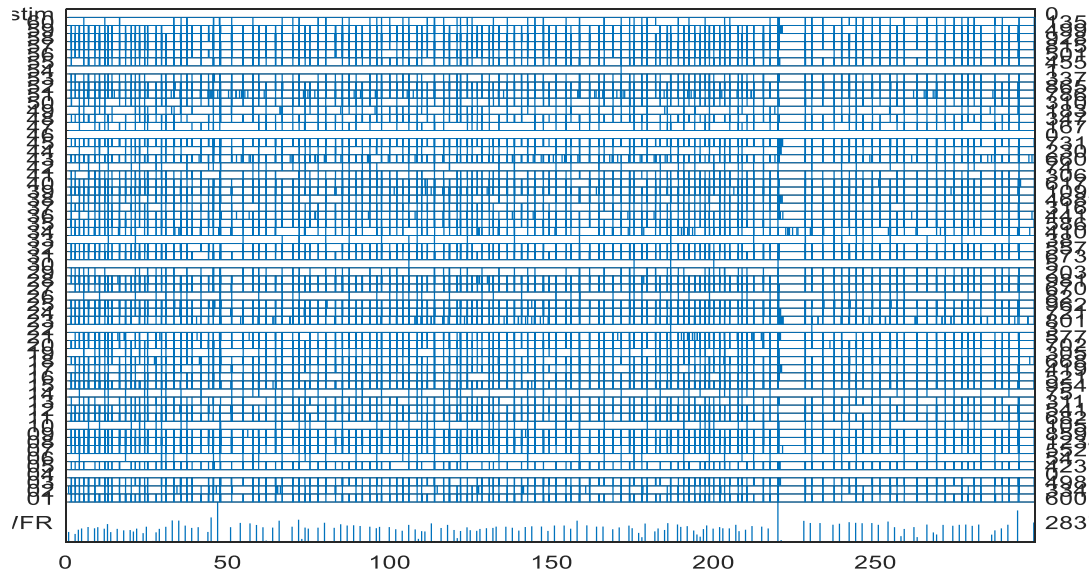
Table A.3 - Overview of background input memory experiments

Experiment date	MEA nr.	DIV	Electrical pulse amplitude (μA)	Pulse width (ms)	Light intensity (%)	Active electrodes >15	Nr. of spikes > 2^{15}	Response to electrical stim
30/05/2022	40315	18	12	100	50	42	YES	YES
31/05/2022	40464	19	24	100	50	47	YES	YES
01/06/2022	40317	20	24	100	50	55	YES	YES
02/06/2022	40318	21	12	100	50	40	YES	YES
03/06/2022	38900	22	12	100	50	47	YES	YES
08/06/2022	37070	26	36	100	50	34	YES	YES
20/06/2022	40313	18	24	100	50	14	YES	NO
22/06/2022	38899	20	24	100	50	30	YES	YES
24/06/2022	40459	22	24	100	50	31	YES	YES

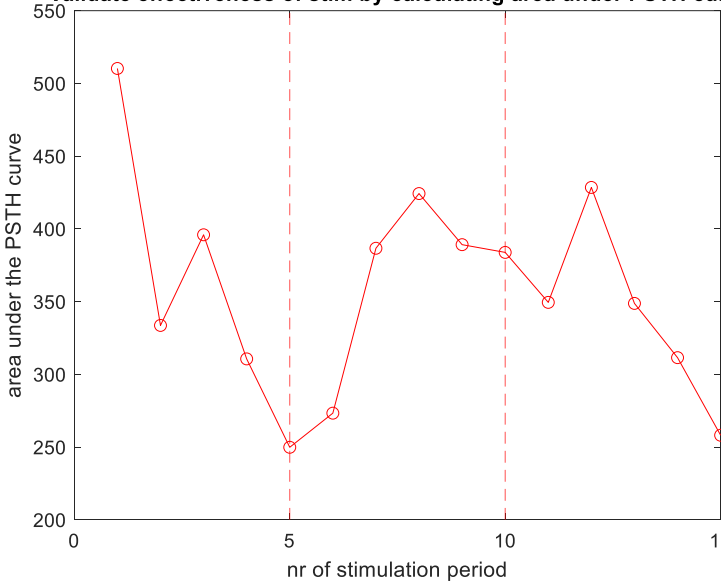
Experiment date	30/05/22
MEA nr	40315
Plating date	12/05/22
Amplitude (μA)	12
Pulse duration (ms)	100
Intensity %	50
Grounded electrodes	2
Artifacts removed from baseline (%)	17,93%
Active electrodes	42



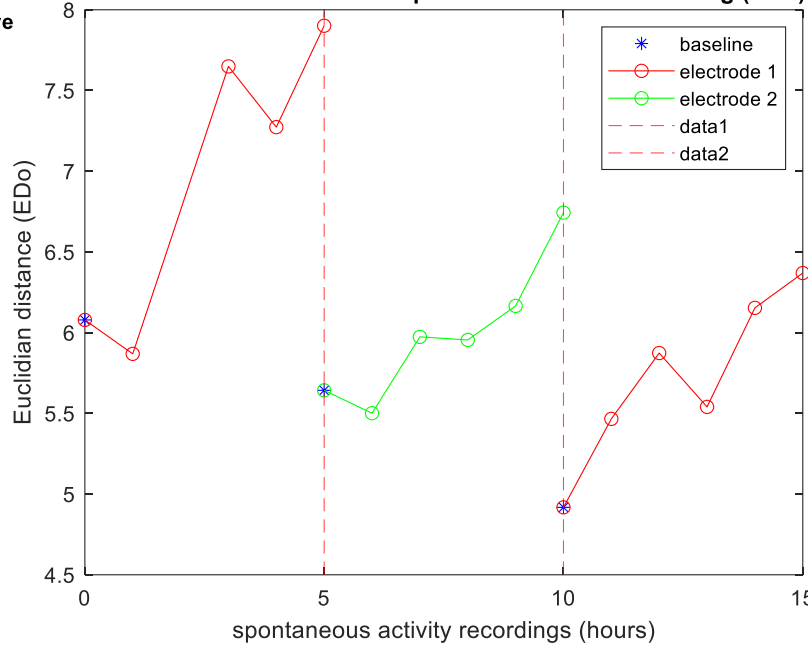
Experiment date	31/05/22
MEA nr	40464
Plating date	12/05/22
Amplitude (μA)	24
Pulse duration (ms)	100
Intensity %	50%
Grounded electrodes	0
Artifacts removed from baseline (%)	35,44%
Active electrodes	47



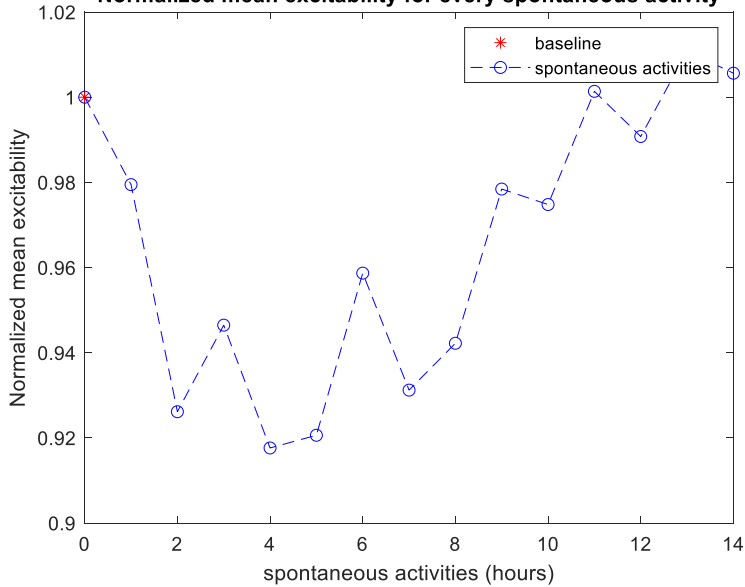
Validate effectiveness of stim by calculating area under PSTH curve



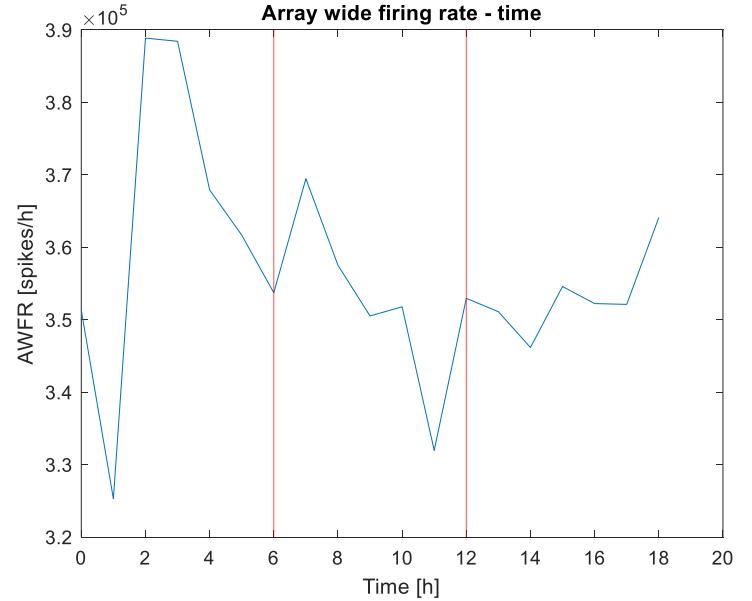
Euclidean distances with respect to a baseline recording (EDo)



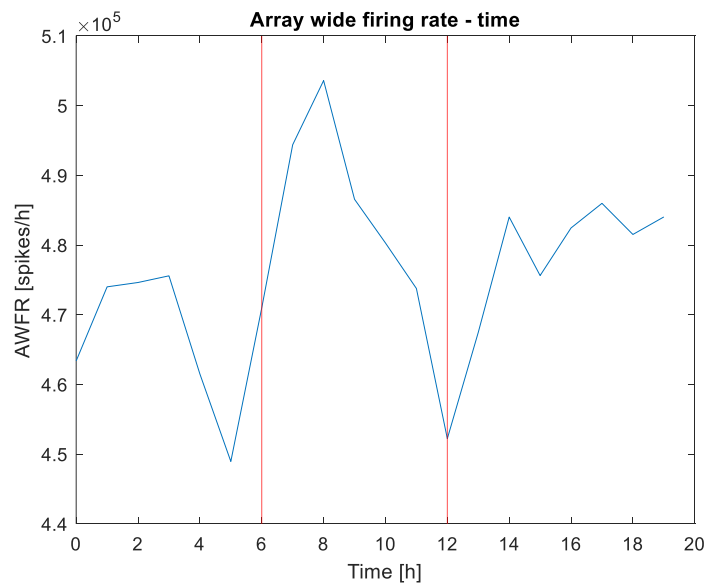
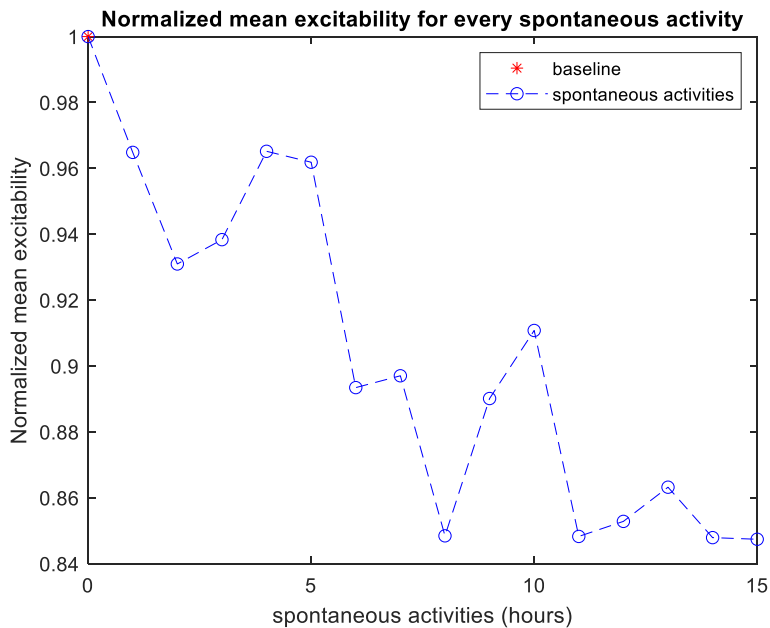
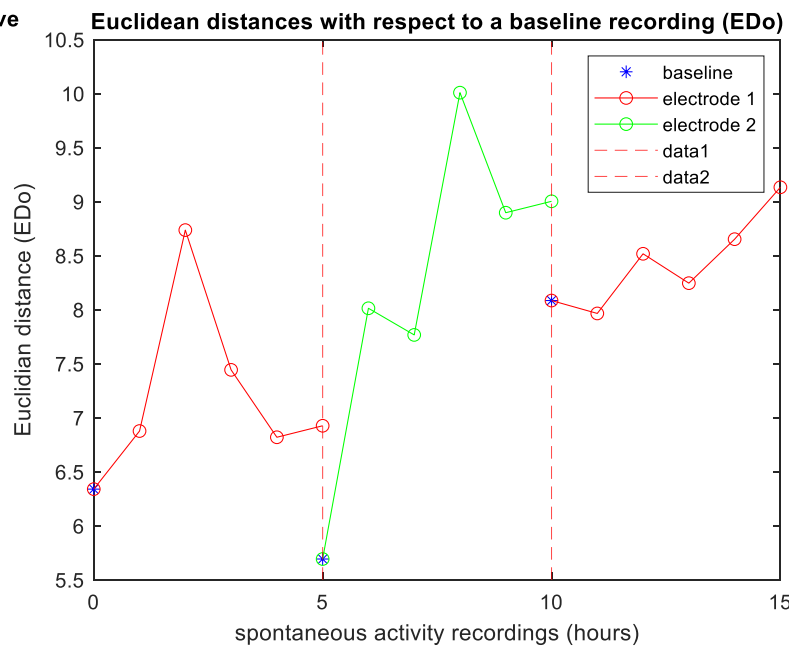
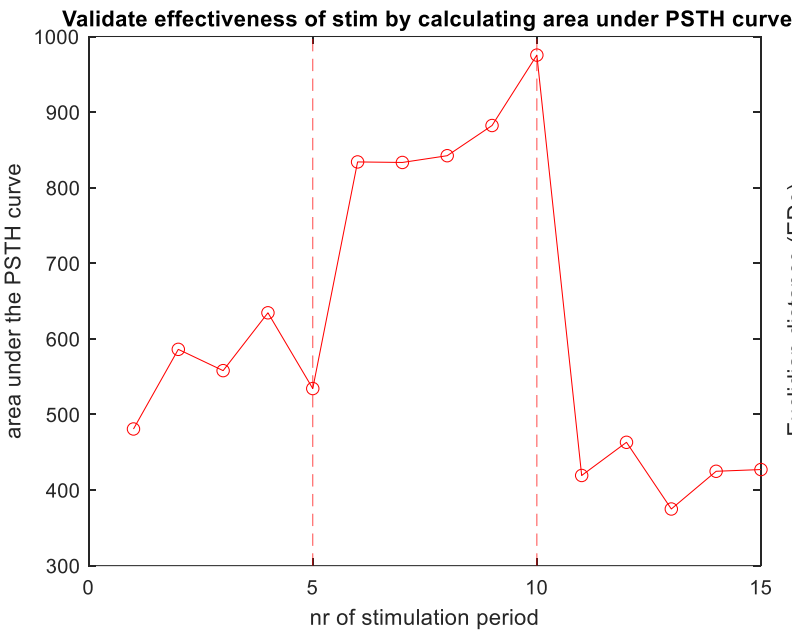
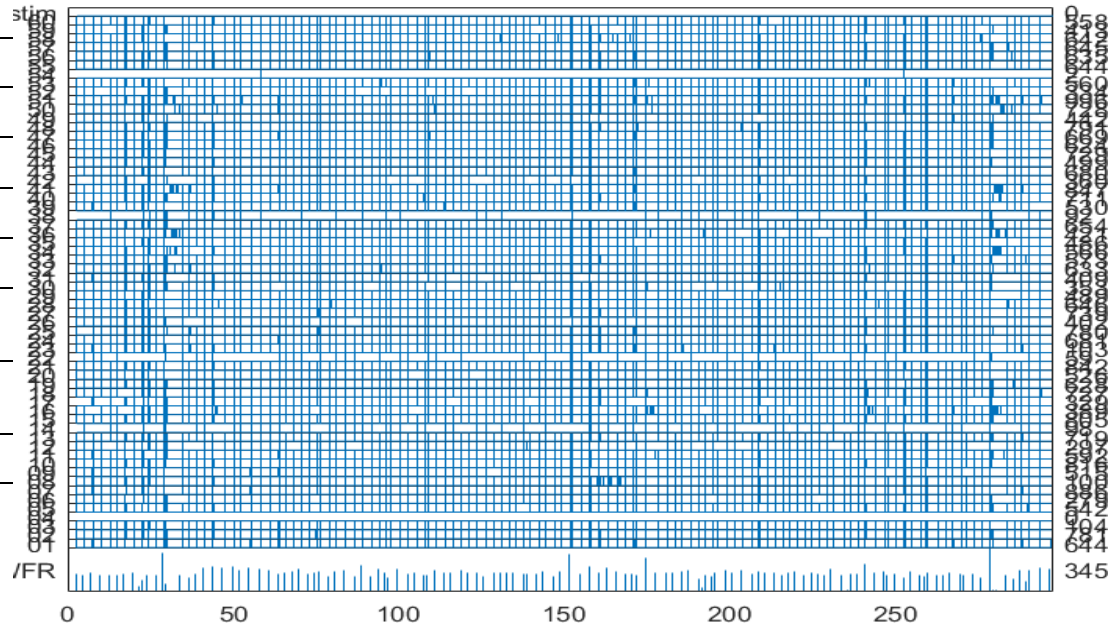
Normalized mean excitability for every spontaneous activity



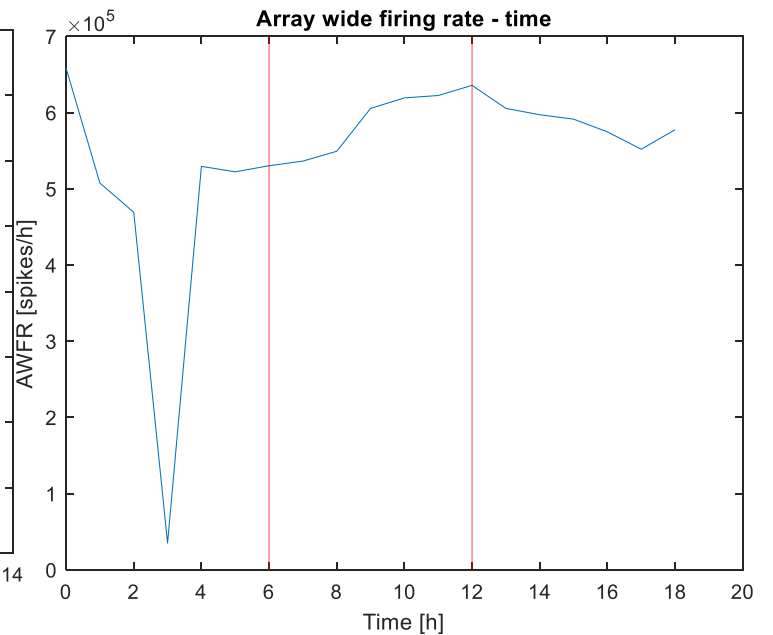
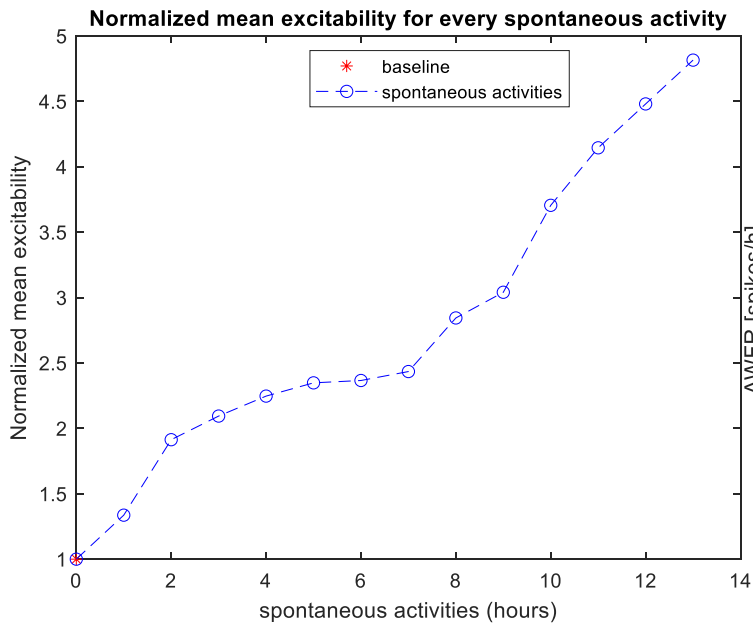
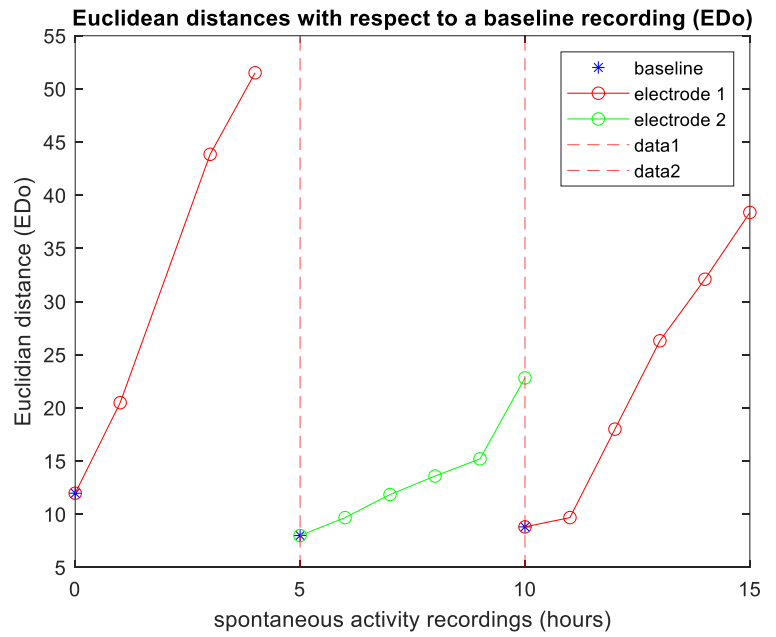
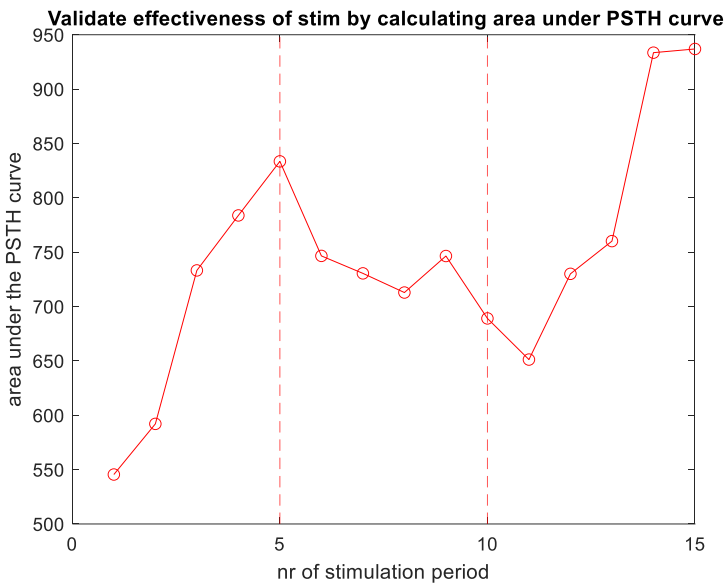
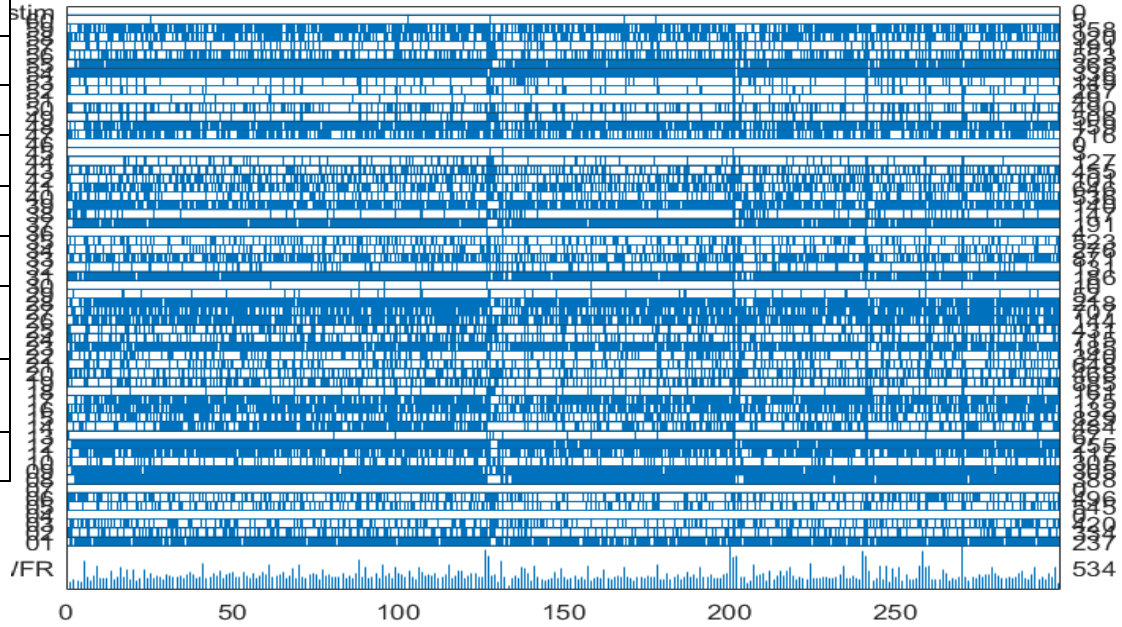
Array wide firing rate - time



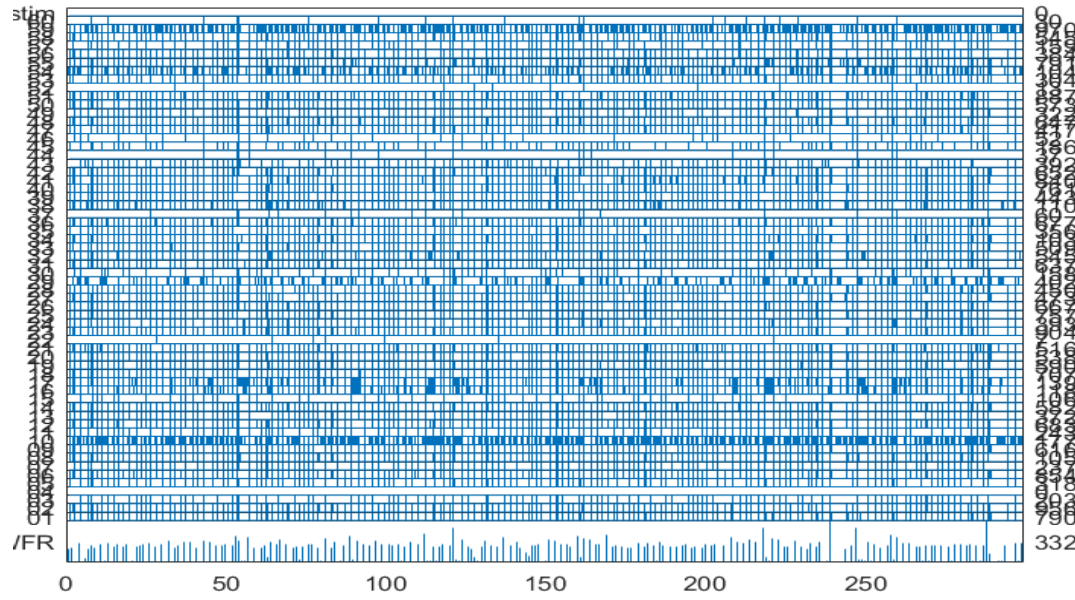
Experiment date	01/06/22
MEA nr	40317
Plating date	12/05/22
Amplitude (μA)	24
Pulse duration (ms)	100
Intensity %	50%
Grounded electrodes	0
Artifacts removed from baseline (%)	33,82%
Active electrodes	55



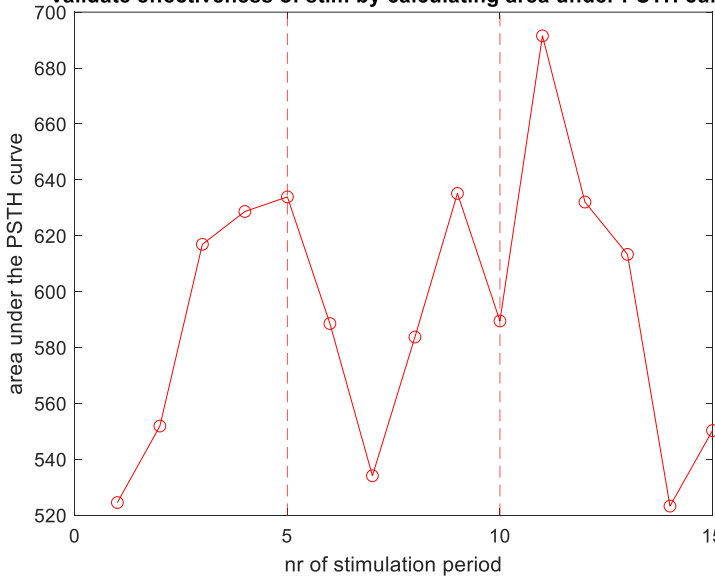
Experiment date	02/06/22
MEA nr	40318
Plating date	12/05/22
Amplitude (μA)	12
Pulse duration (ms)	100
Intensity %	50%
Grounded electrodes	1
Artifacts removed from baseline (%)	-
Active electrodes	40



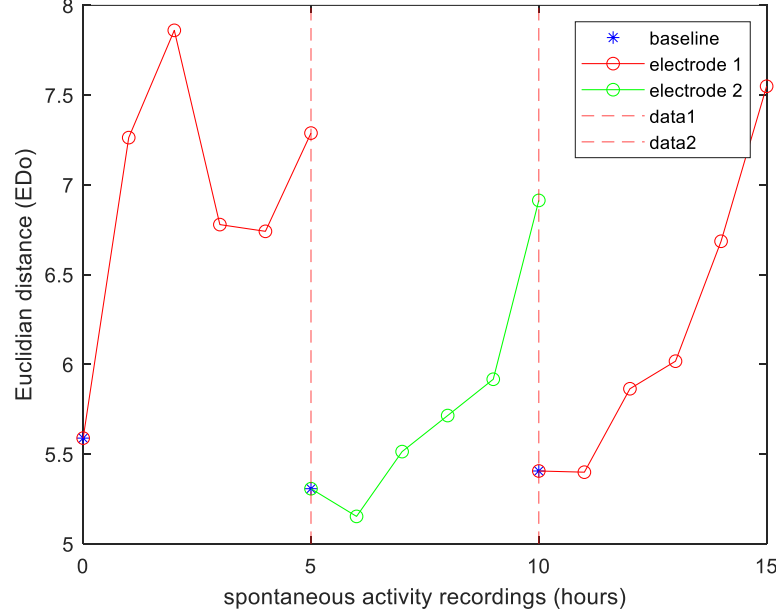
Experiment date	03/06/22
MEA nr	38900
Plating date	12/05/22
Amplitude (μA)	12
Pulse duration (ms)	100
Intensity %	50%
Grounded electrodes	0
Artifacts removed from baseline (%)	28,72%
Active electrodes	47



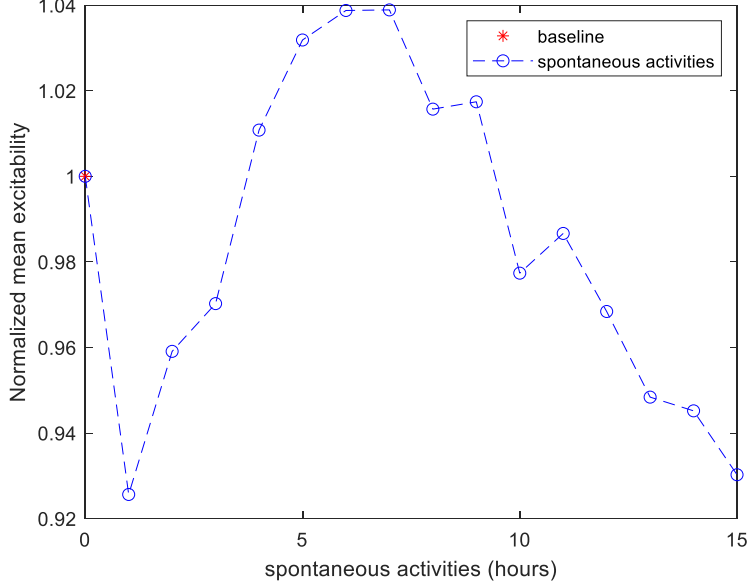
Validate effectiveness of stim by calculating area under PSTH curve



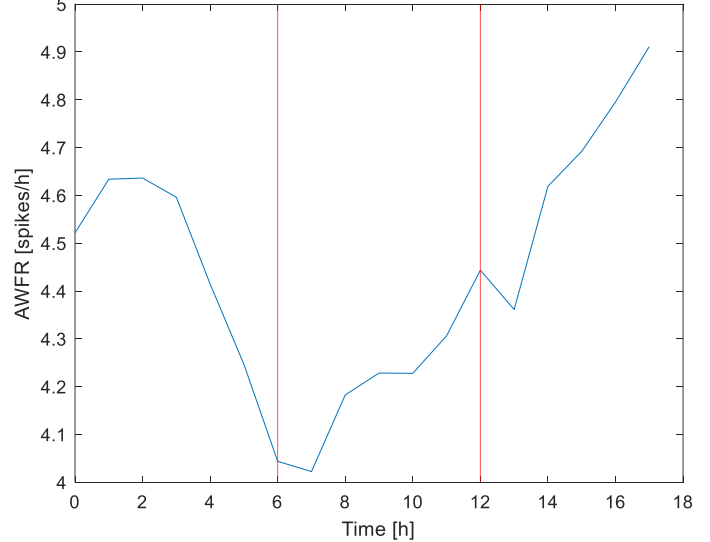
Euclidean distances with respect to a baseline recording (EDo)



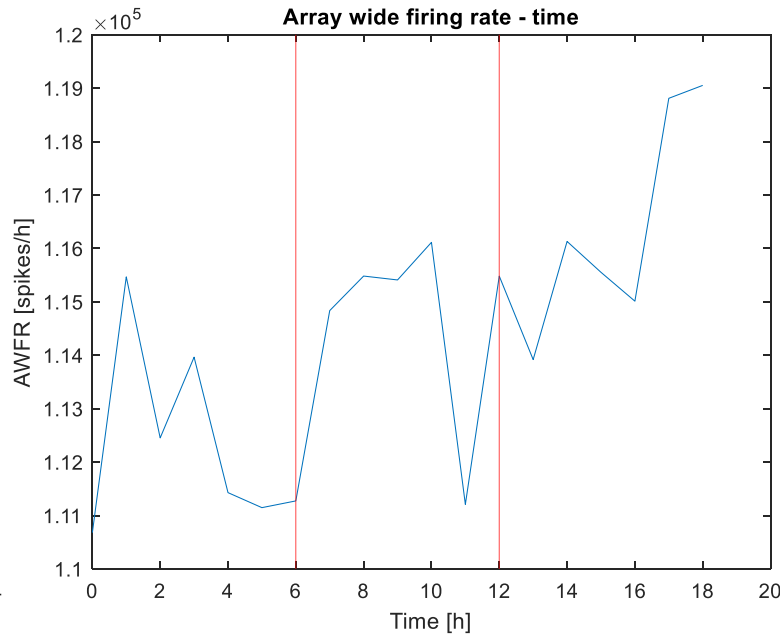
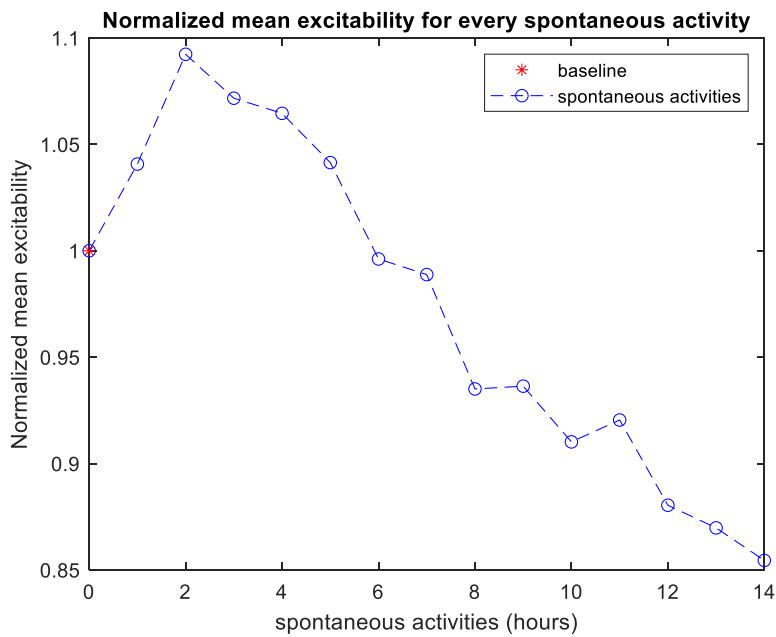
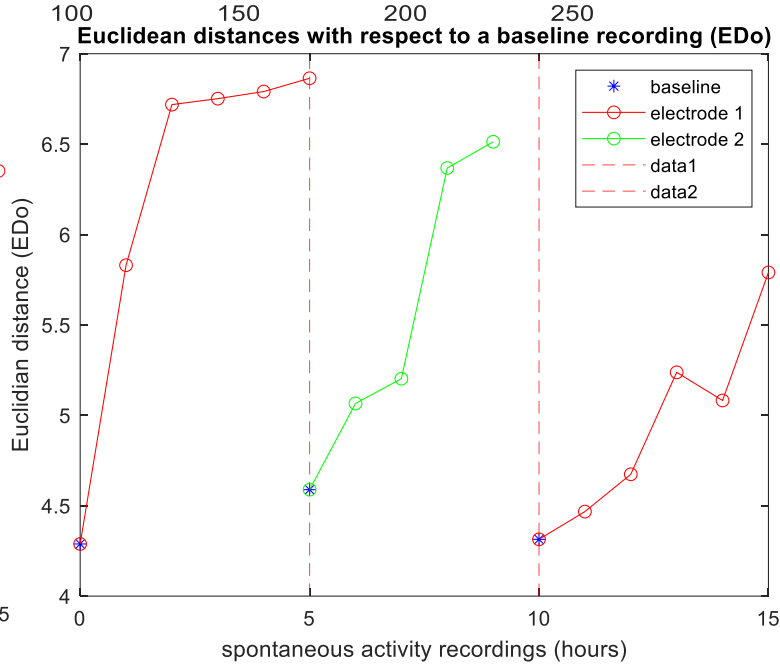
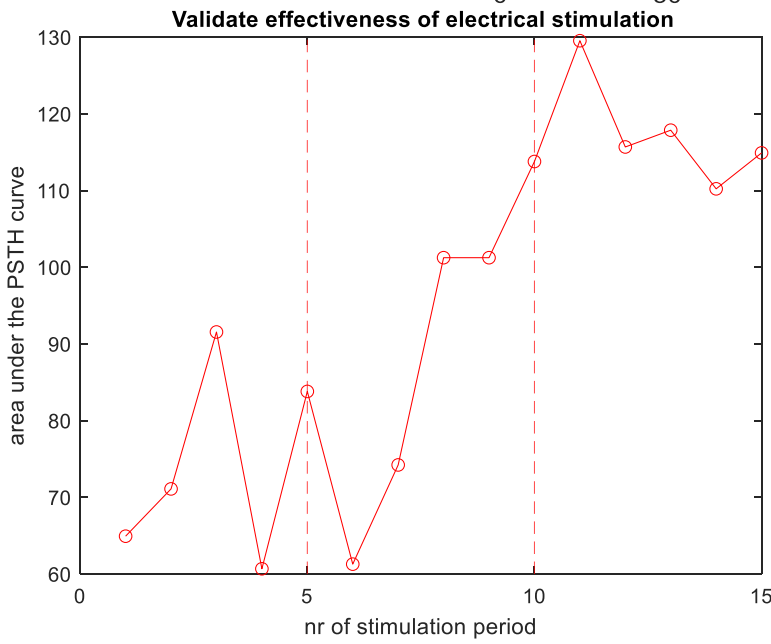
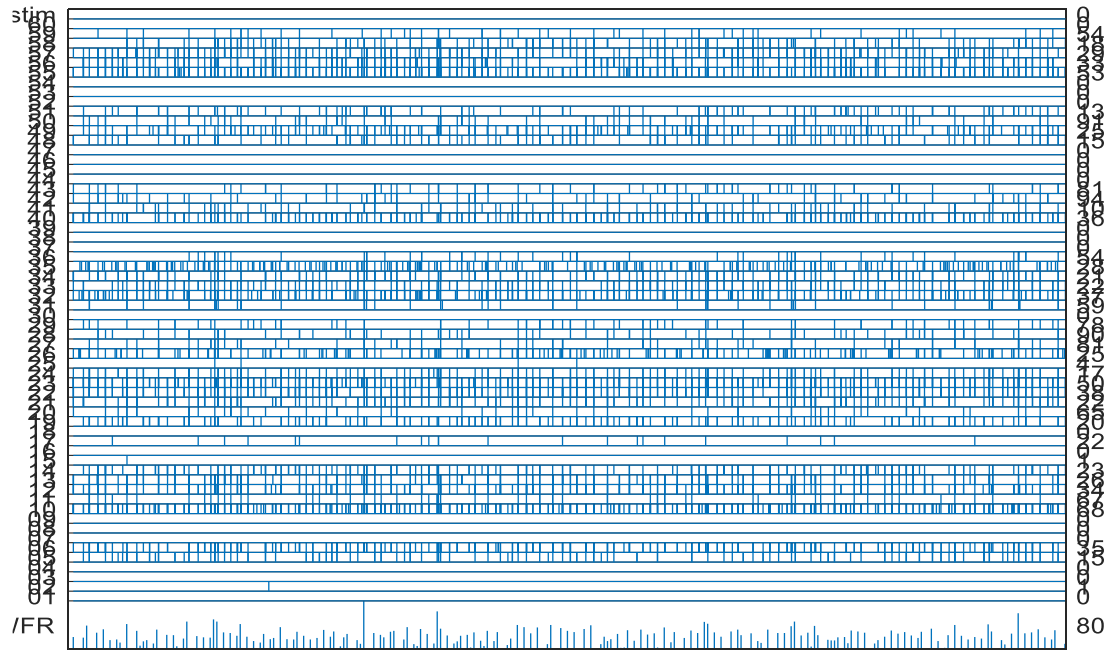
Normalized mean excitability for every spontaneous activity



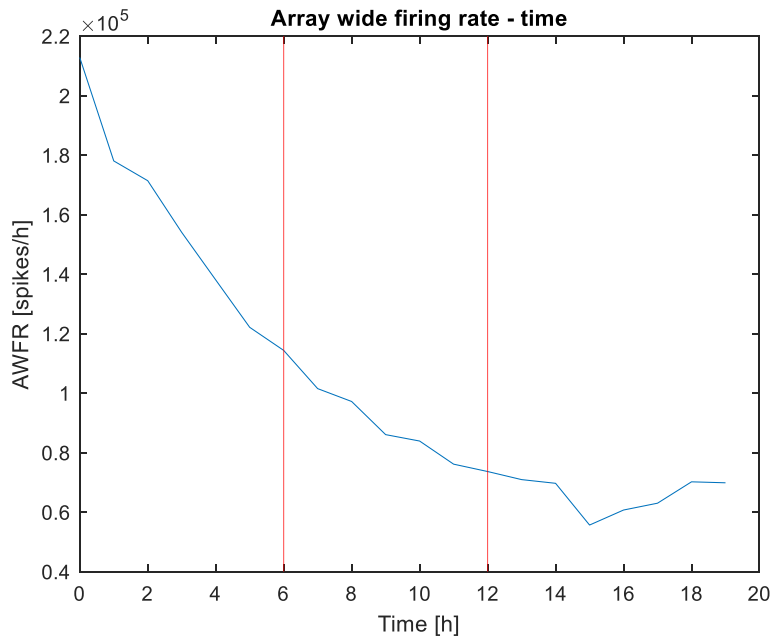
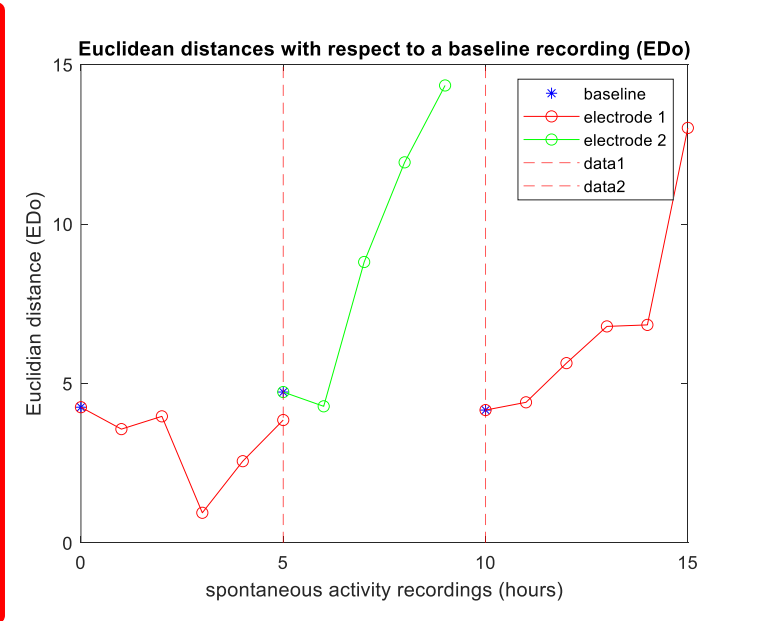
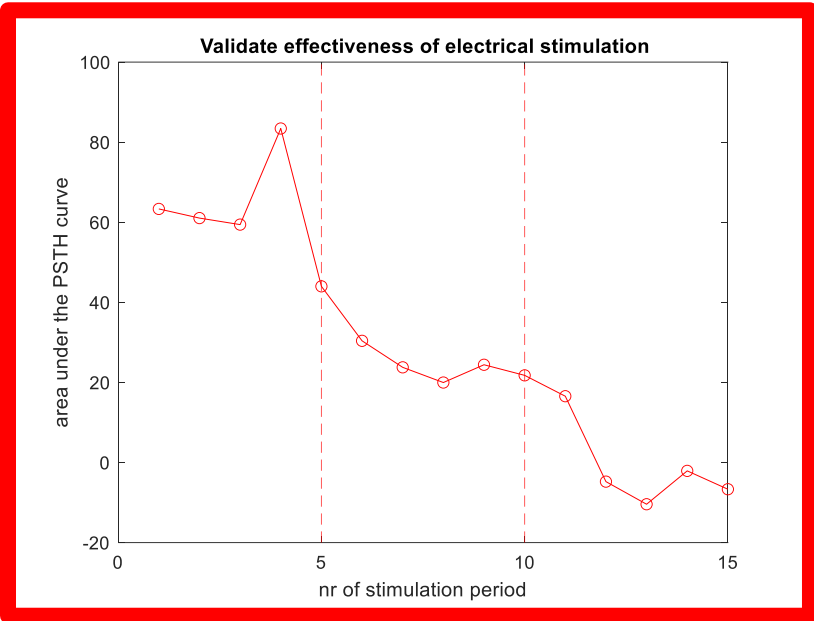
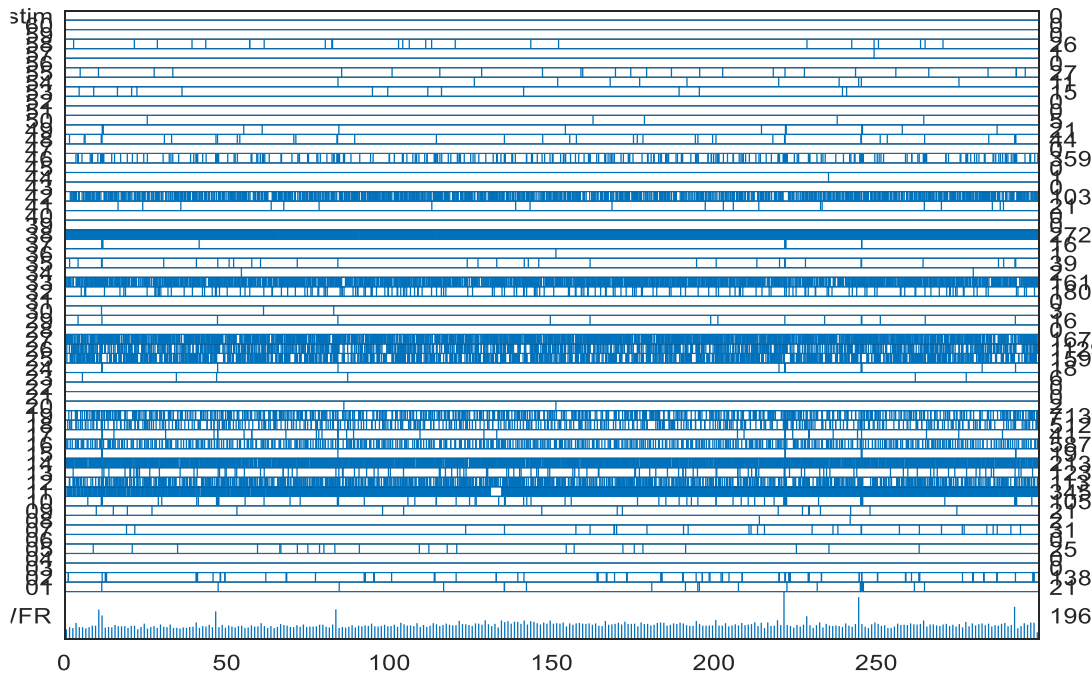
Array wide firing rate - time



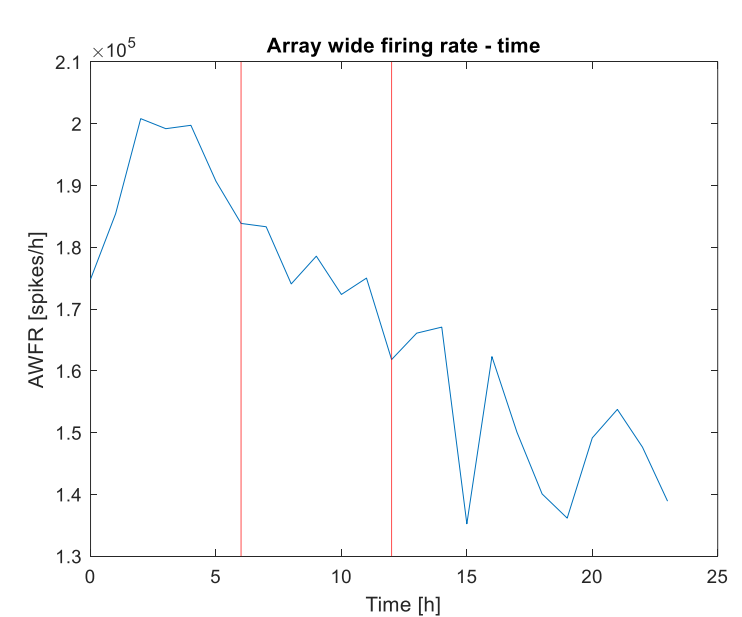
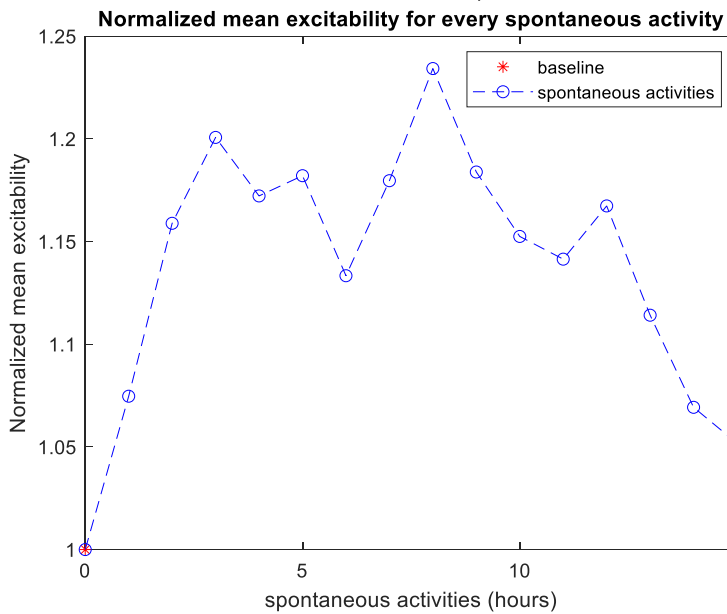
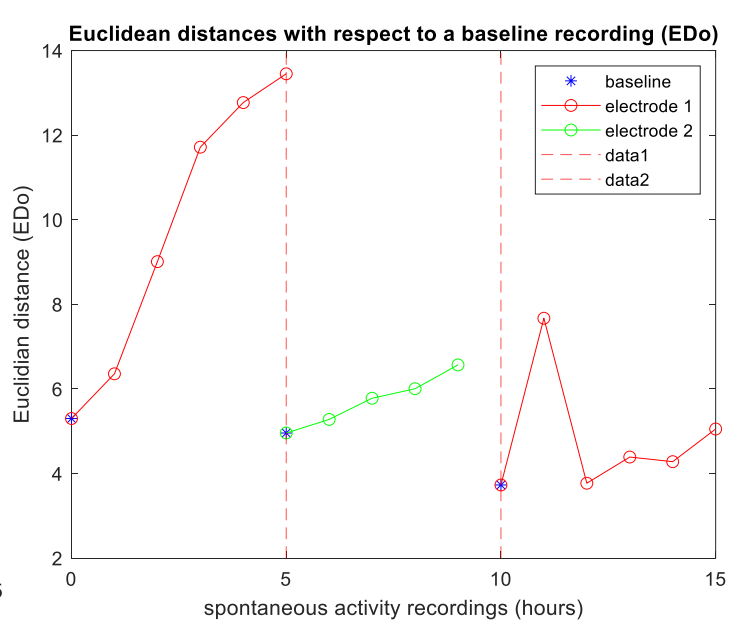
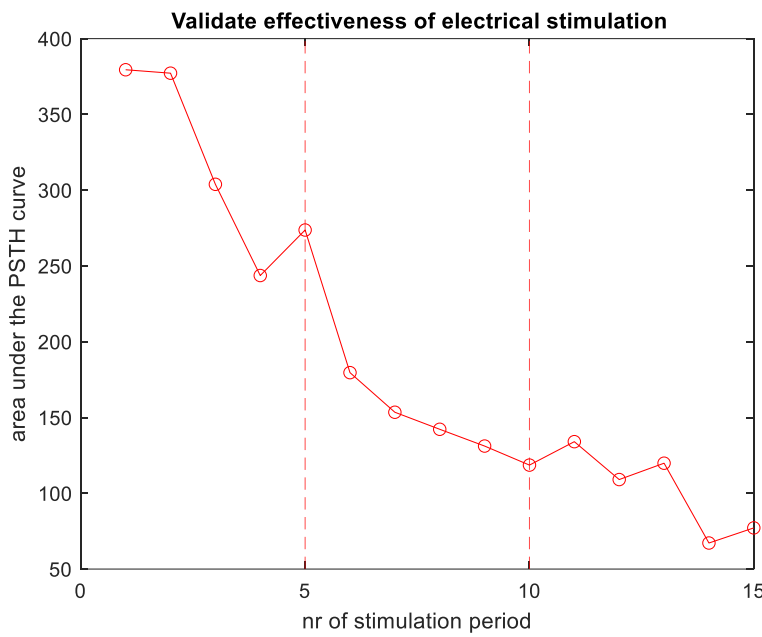
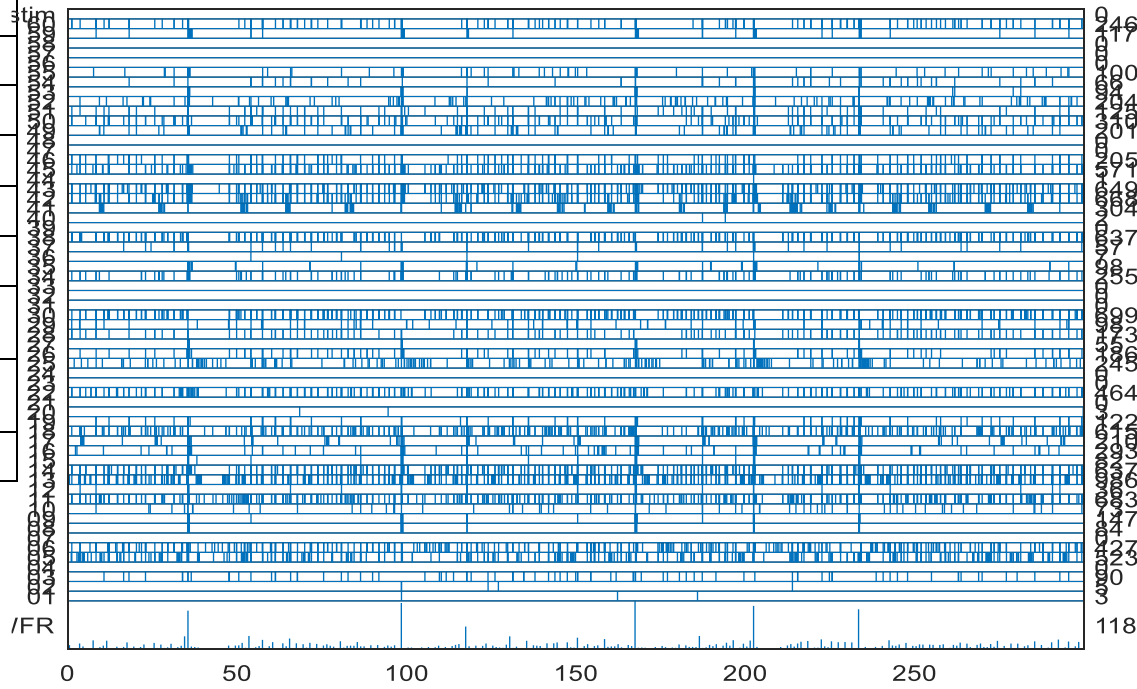
Experiment date	08/06/22
MEA nr	37070
Plating date	02/06/22
Amplitude (μA)	36
Pulse duration (ms)	100
Intensity %	50%
Grounded electrodes	0
Artifacts removed from baseline (%)	-
Active electrodes	34



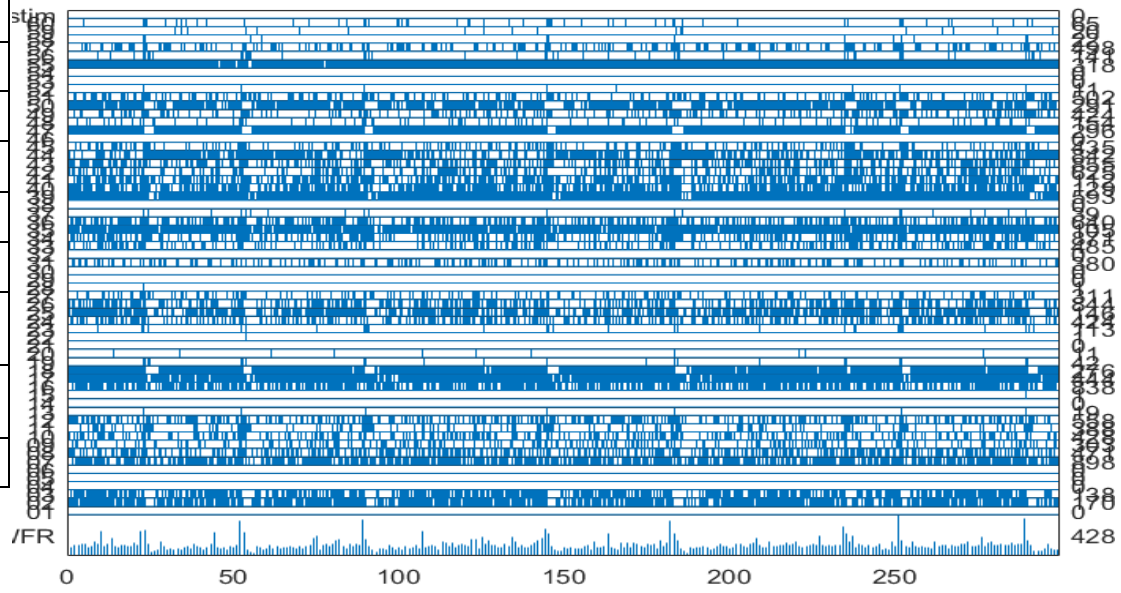
Experiment date	20/06/22
MEA nr	40313
Plating date	02/06/22
Amplitude (μ A)	24
Pulse duration (ms)	100
Intensity %	50%
Grounded electrodes	6
Artifacts removed from baseline (%)	10,62%
Active electrodes	14



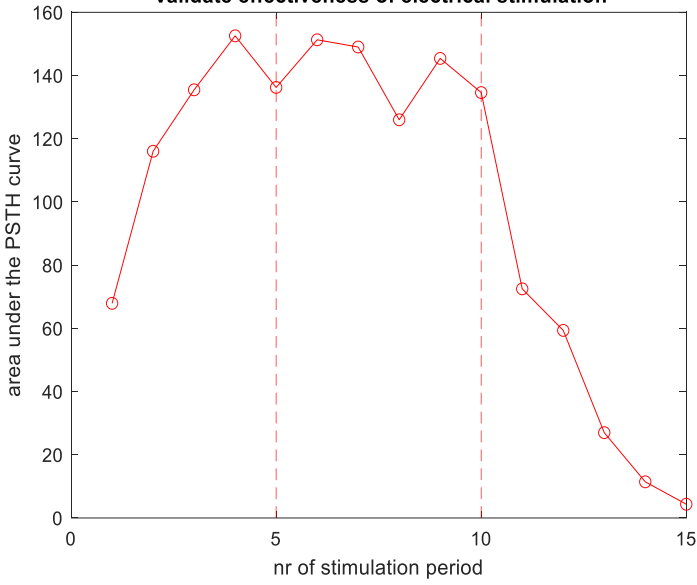
Experiment date	22/06/22
MEA nr	38899
Plating date	02/06/22
Amplitude (μA)	24
Pulse duration (ms)	100
Intensity %	50%
Grounded electrodes	2
Artifacts removed from baseline (%)	26,03%
Active electrodes	30



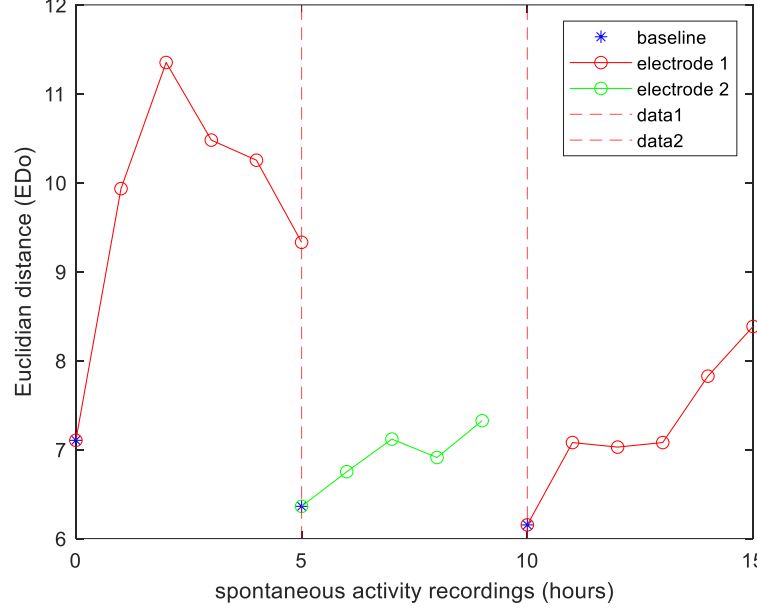
Experiment date	24/06/22
MEA nr	40459
Plating date	02/06/22
Amplitude (μA)	24
Pulse duration (ms)	100
Intensity %	50%
Grounded electrodes	0
Artifacts removed from baseline (%)	18,26%
Active electrodes	31



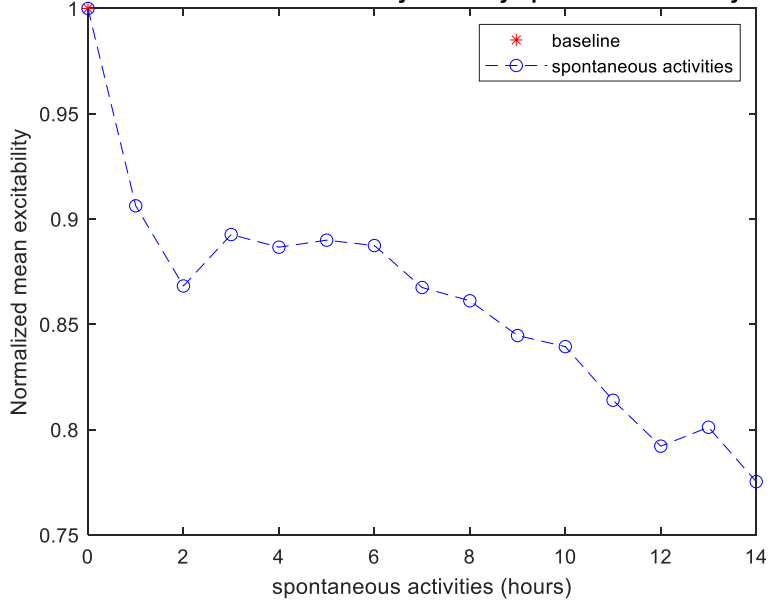
Validate effectiveness of electrical stimulation



Euclidean distances with respect to a baseline recording (EDo)



Normalized mean excitability for every spontaneous activity



Array wide firing rate - time

